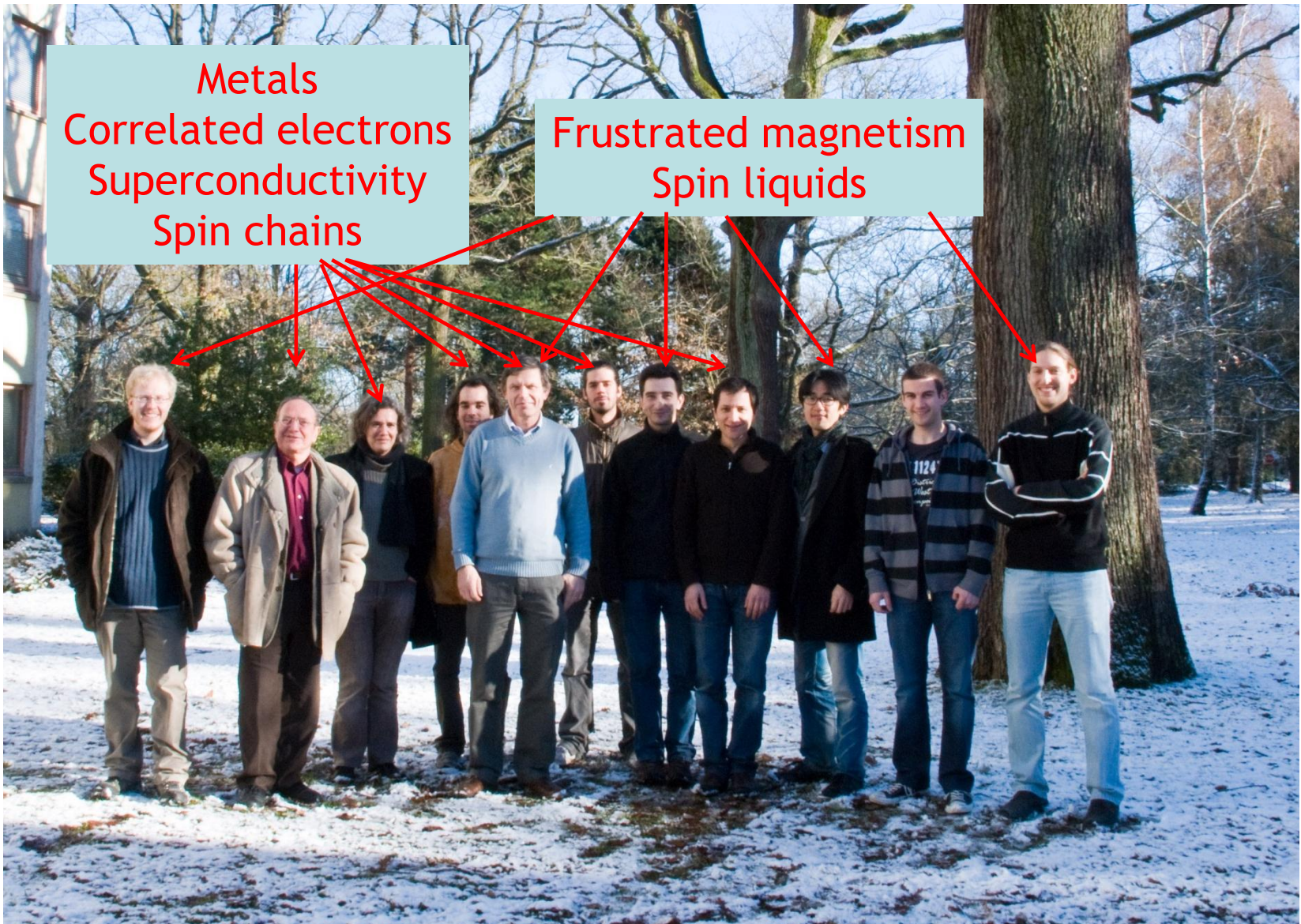


# NMR, ESR, Mössbauer ( $\mu$ SR)

(for solid-state physics  $\oplus$  magnetism)



# NMR, ESR, Mössbauer ( $\mu$ SR)

(for solid- state physics  $\oplus$  magnetism)

P. Mendels

Lab. Physique des solides  
Univ. Paris-Sud Orsay

- All probes are resonant bulk, **local** probes: **integrate over q**, similar formalism
- Difference through
  - (i) the coupling to the environment
  - (ii) the time window, the field range
  - (iii) sensitivity and pulsed versus continuum



UNIVERSITÉ  
PARIS-SUD 11



AGENCE NATIONALE DE LA RECHERCHE

ANR

LPS  
ORSAY



Zeeman,  
Nobel Physics 1902



Rabi,  
Nobel Physics 1944

Nuclear spin  
Electronic spin



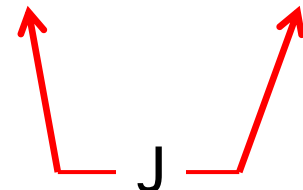
- Field induced splitting of the levels: transition  $v_{\text{res}} \sim H_0 + \delta H_{\text{local}}$
- Back to equilibrium: relaxation time probes low frequency fluctuations

- Hyperfine techniques: NMR, Mössbauer

The probe Hamiltonian is a weak perturbation of the electronic system; acts like a spy. ( $\mu$ SR also)

- ESR: acts on the electronic spin

More involved treatment



- In practice

- ✓ Sweep the frequency at a fixed external field
- ✓ Sweep the field at a constant frequency

$\chi''$

- Outline: Principles and selected examples

NMR, Mössbauer and ESR

*Note: Highest similarity is between NMR and  $\mu$ SR, see D. Andreica*

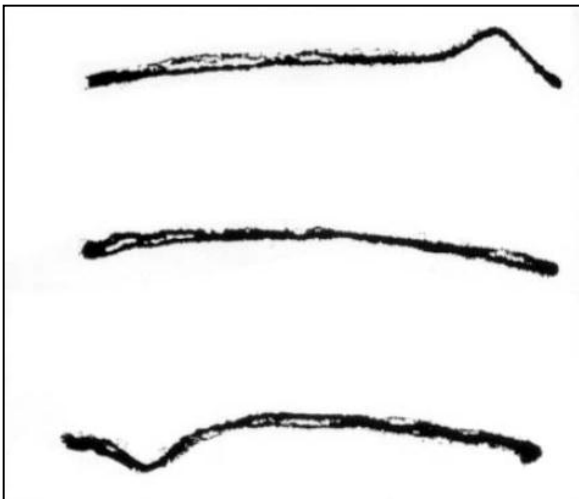
Many thanks to:

J. Bobroff (NMR, Orsay); P. Bonville (Mössbauer, CEA Saclay);  
D. Arcon and A. Zorko (ESR, Ljubljana)  
(Some slides also borrowed from Carretta, Murad, Takigawa)

# Framework of the presentation

- Basics: energy levels, coupling Hamiltonian
- What do we look at ~ what we see in papers ?
- Selected examples

# NMR: milestones (1)



Bloch & Purcell,  
Nobel Physique 1952



Ernst,  
Nobel Chemistry 1991      Wuthrich,  
Nobel Chemistry 2002



Lauterbur & Mansfeld,  
Nobel Medecine 2003

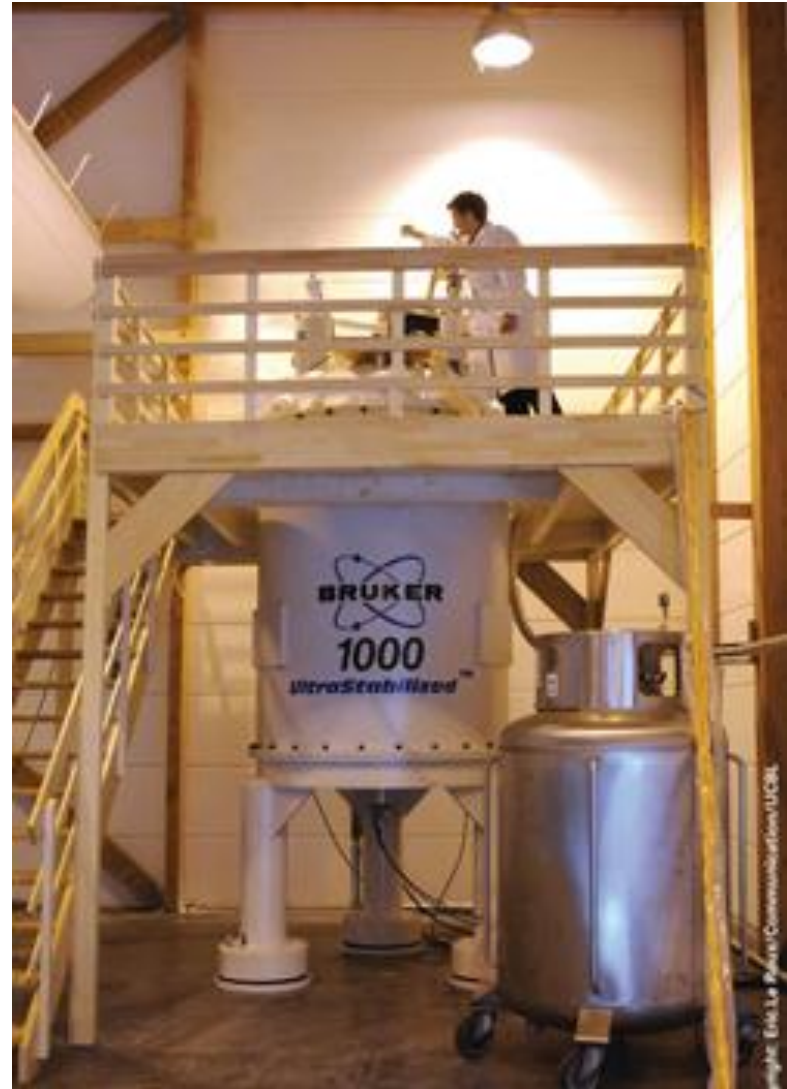
# NMR: milestones (2)



# NMR for chemistry



7 Tesla



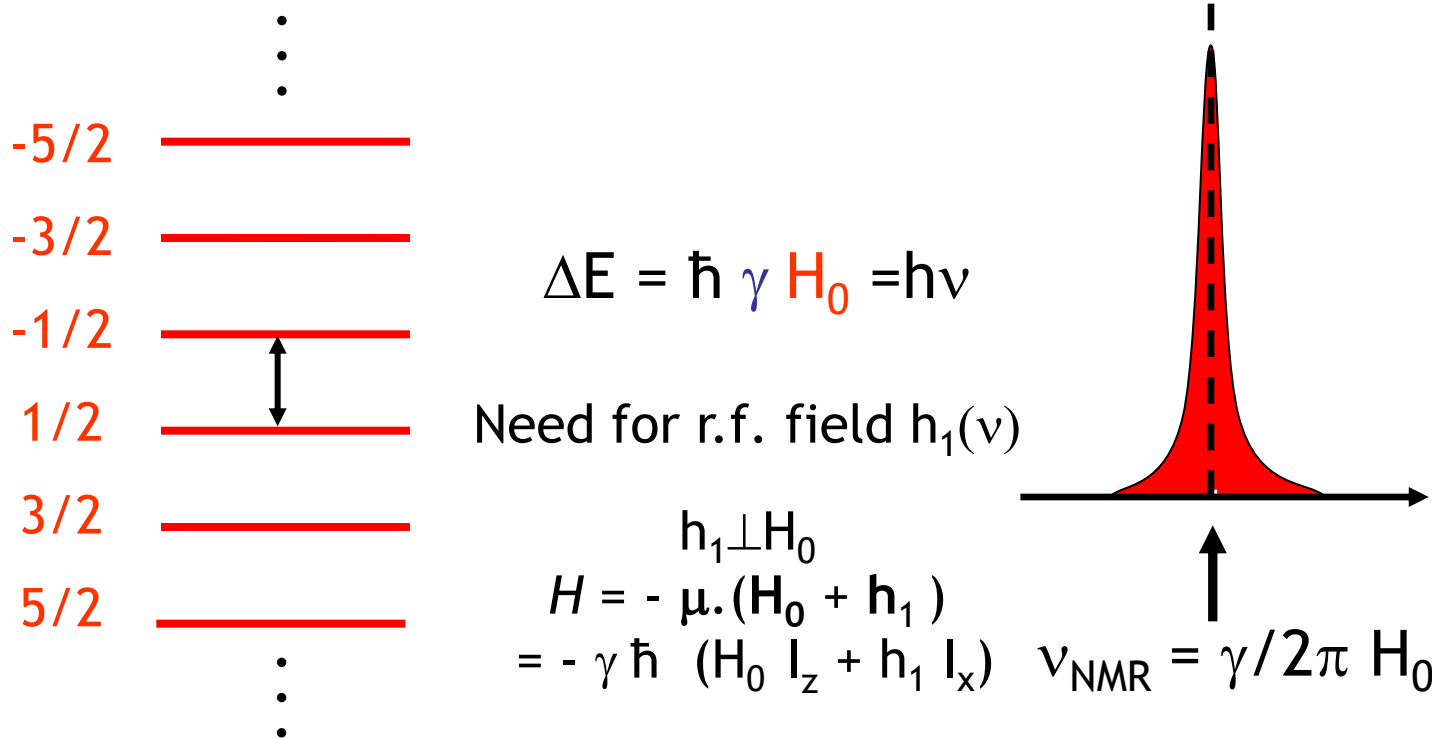
23 Tesla

# NMR basic principles (1)

Nuclear spin  $I$  in a magnetic field  $H_0$

Zeeman effect :  $H = - \mu \cdot H_0 = - \gamma \hbar H_0 I_z$

Energy levels  $E = - m \gamma \hbar H_0$ ,  $m=-I, -I+1 \dots I-1, I$



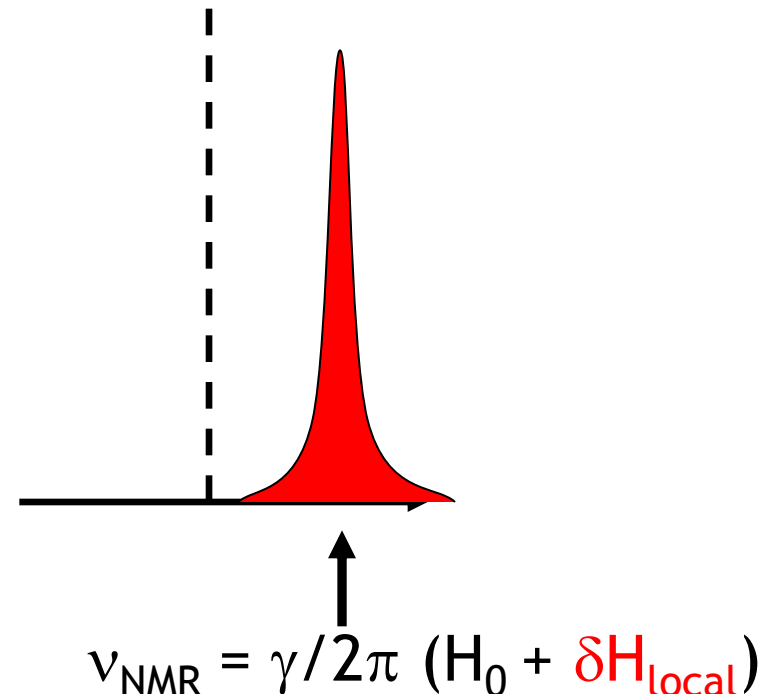
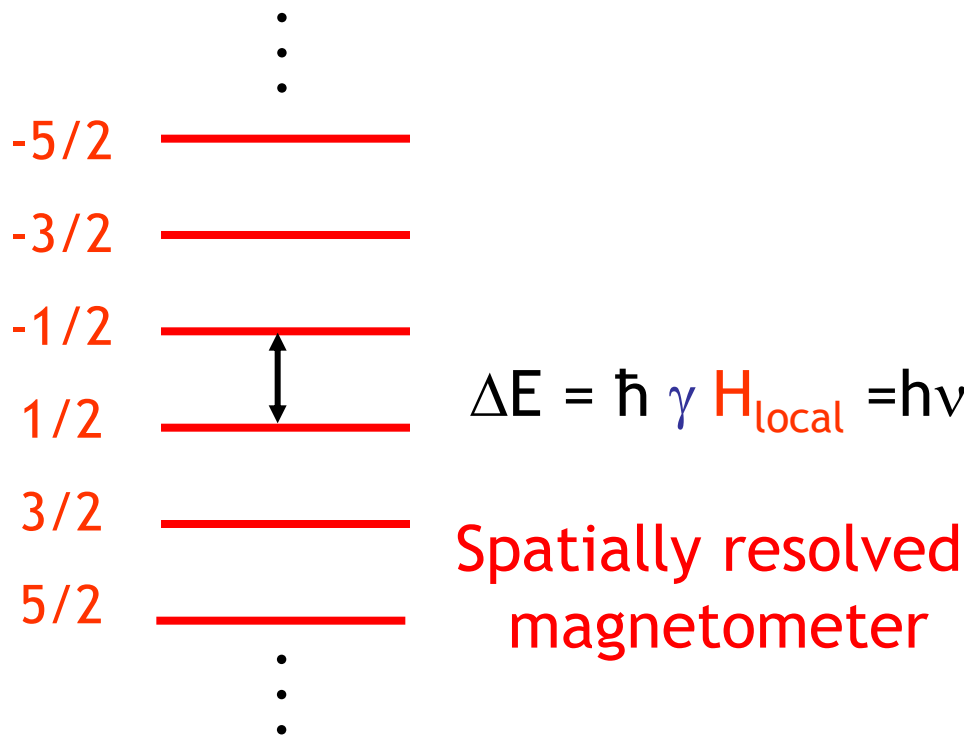
ZFNMR: impossible...not common, also NQR

# NMR basic principles (2)

Nuclear spin  $I$  in a magnetic field  $H_0 \oplus$  r.f. field  $h_1$

Zeeman effect :  $H = -\mu \cdot H_0 = -\gamma \hbar H_0 I_z$

Energy levels  $E = -m \gamma \hbar H_0$ ,  $m=-I, -I+1 \dots I-1, I$



ZFNMR: impossible...not common, also NQR

# Which nuclei ?

Nuclear magnetic moment  $\vec{M} = \gamma \hbar \vec{I}$

## Common NMR Active Nuclei

Isotope	Spin $I$	%age abundance	$\gamma$ MHz/T
$^1\text{H}$	1/2	99.985	42.575
$^2\text{H}$	1	0.015	6.53
$^{13}\text{C}$	1/2	1.108	10.71
$^{14}\text{N}$	1	99.63	3.078
$^{15}\text{N}$	1/2	0.37	4.32
$^{17}\text{O}$	5/2	0.037	5.77
$^{19}\text{F}$	1/2	100	40.08
$^{23}\text{Na}$	3/2	100	11.27
$^{31}\text{P}$	1/2	100	17.25

1 - 40 MHz / Tesla

Resonance are in the FM (radiofrequency) range!

# Which nuclei ?

*eNMR*

NMR Periodic Table

Group	I	II	IIIa	IVa	Va	VIa	VIIa	VIIIa	VIIIb	VIIIc	IB	IIB	III	IV	V	VI	VII	VIII	
Period																			
1	1 <u>H</u>																	2 <u>He</u>	
2	3 <u>Li</u>	4 <u>Be</u>												5 <u>B</u>	6 <u>C</u>	7 <u>N</u>	8 <u>O</u>	9 <u>F</u>	10 <u>Ne</u>
3	11 <u>Na</u>	12 <u>Mg</u>												13 <u>Al</u>	14 <u>Si</u>	15 <u>P</u>	16 <u>S</u>	17 <u>Cl</u>	18 Ar
4	19 <u>K</u>	20 <u>Ca</u>		21 <u>Sc</u>	22 <u>Ti</u>	23 <u>V</u>	24 <u>Cr</u>	25 <u>Mn</u>	26 <u>Fe</u>	27 <u>Co</u>	28 <u>Ni</u>	29 <u>Cu</u>	30 <u>Zn</u>	31 <u>Ga</u>	32 <u>Ge</u>	33 <u>As</u>	34 <u>Se</u>	35 <u>Br</u>	36 <u>Kr</u>
5	37 <u>Rb</u>	38 <u>Sr</u>		39 <u>Y</u>	40 <u>Zr</u>	41 <u>Nb</u>	42 <u>Mo</u>	43 Tc	44 <u>Ru</u>	45 <u>Rh</u>	46 Pd	47 <u>Ag</u>	48 <u>Cd</u>	49 <u>In</u>	50 <u>Sn</u>	51 <u>Sb</u>	52 <u>Te</u>	53 <u>I</u>	54 <u>Xe</u>
6	55 <u>Cs</u>	56 <u>Ba</u>	*	71 <u>Lu</u>	72 <u>Hf</u>	73 <u>Ta</u>	74 <u>W</u>	75 <u>Re</u>	76 <u>Os</u>	77 <u>Ir</u>	78 <u>Pt</u>	79 <u>Au</u>	80 <u>Hg</u>	81 <u>Tl</u>	82 <u>Pb</u>	83 <u>Bi</u>	84 Po	85 At	86 Rn
7	87 Fr	88 Ra	**	103 Lr	104 Unq	105 Unp	106 Unh	107 Uns	108 Uno	109 Mt	110 Uun	111 Uuu	112 Uub	113 Uut	114 Uuq	115 Uup	116 Uuh	117 Uus	118 Uuo
*Lanthanides		*	57 <u>La</u>	58 <u>Ce</u>	59 <u>Pr</u>	60 <u>Nd</u>	61 Pm	62 <u>Sm</u>	63 <u>Eu</u>	64 <u>Gd</u>	65 <u>Tb</u>	66 <u>Dy</u>	67 <u>Ho</u>	68 <u>Er</u>	69 <u>Tm</u>	70 <u>Yb</u>			
**Actinides		**	89 Ac	90 Th	91 Pa	92 <u>U</u>	93 Np	94 Pu	95 Am	96 Cm	97 Bk	98 Cf	99 Es	100 Fm	101 Md	102 No			

Nuclear Spins  $1/2$   $1$   $3/2$   $5/2$   $7/2$   $9/2$

Many resident nuclei ... sensitivity, detection pbs...

# NMR basics (3): the chemistry side

*With NMR we study the time evolution of nuclear magnetization, driven by the hyperfine interactions...*

$$\mathcal{H} = \mathcal{H}_Z + \mathcal{H}_{n-n} + \mathcal{H}_{n-e} + \mathcal{H}_{EFG}$$

$$\mathcal{H}_Z = -\gamma\hbar \sum_i I_z^i H_0 .$$

$$\mathcal{H}_{n-n} = \sum_{j < k} \frac{\hbar^2 \gamma^2}{r^3} \left( A + B + C + D + E + F \right)_{jk}$$

Screening of  $H_0$  by electrons

⊕

modification of orbitals by the applied field

Chemical shift ~ ppm - 1000 ppm

A very useful tool to determine the chemical bonding

# NMR basics (3): the chemistry side

*With NMR we study the time evolution of nuclear magnetization, driven by the hyperfine interactions...*

$$\mathcal{H} = \mathcal{H}_Z + \mathcal{H}_{n-n} + \mathcal{H}_{n-e} + \mathcal{H}_{EFG}$$

$$\mathcal{H}_Z = -\gamma\hbar \sum_i I_z^i H_0 .$$

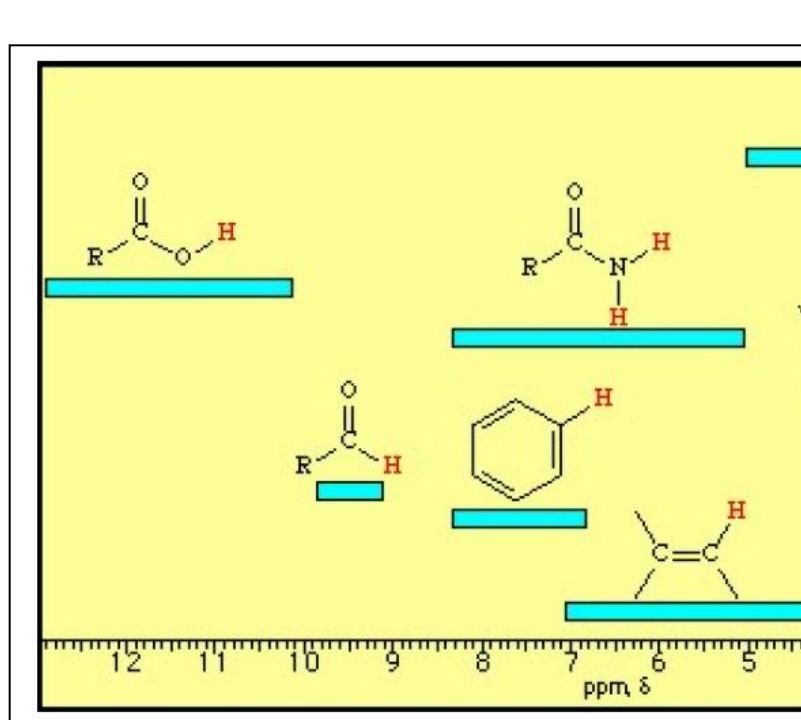
$$\mathcal{H}_{n-n} = \sum_{j < k} \frac{\hbar^2 \gamma^2}{r^3} \left( A + B + C + D + E + F \right)_{jk}$$

Indirect interaction between nuclear moments  
(electrons)

Fine structure

A very useful tool to determine the chemical bonding

# Chemical shift (ppm)



## Gasoline Application

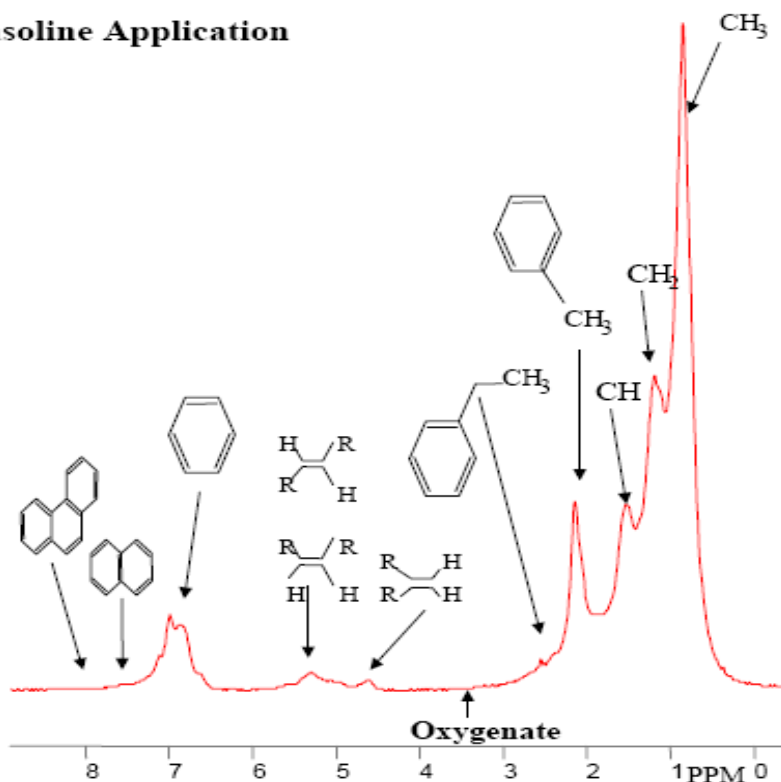


Figure 3: H-Types Observed in a Gasoline  $^1\text{H}$  NMR Spectrum

# NMR basics (4): the nuclear Hamiltonian for solids

*With NMR we study the time evolution of nuclear magnetization, driven by the hyperfine interactions...*

$$\mathcal{H} = \mathcal{H}_Z + \mathcal{H}_{n-n} + \mathcal{H}_{n-e} + \mathcal{H}_{EFG}$$

$$\mathcal{H}_Z = -\gamma\hbar \sum_i I_z^i H_0 .$$

$$\mathcal{H}_{n-n} = \sum_{j < k} \frac{\hbar^2 \gamma^2}{r^3} \left( A + B + C + D + E + F \right)_{jk}$$

$$\mathcal{H}_{n-e} = -\gamma\hbar \sum_{i,k} \mathbf{I}_i \tilde{A}_{ik} \mathbf{S}_k$$

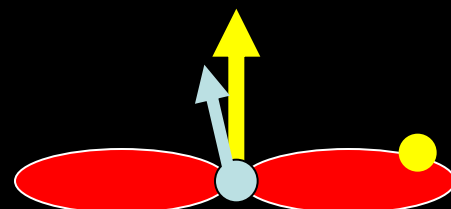
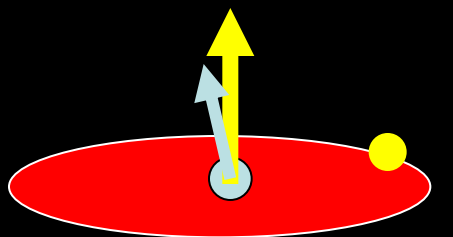
$$\mathcal{H}_{EFG} = \sum_i \frac{e^2 Q V_{ZZ}}{4I(2I-1)} \left( 3(I_z^i)^2 - I(I+1) + \frac{\eta}{2} [(I_+^i)^2 + (I_-^i)^2] \right)$$

A very involved Hamiltonian...coupling to electronic moments and surrounding charges

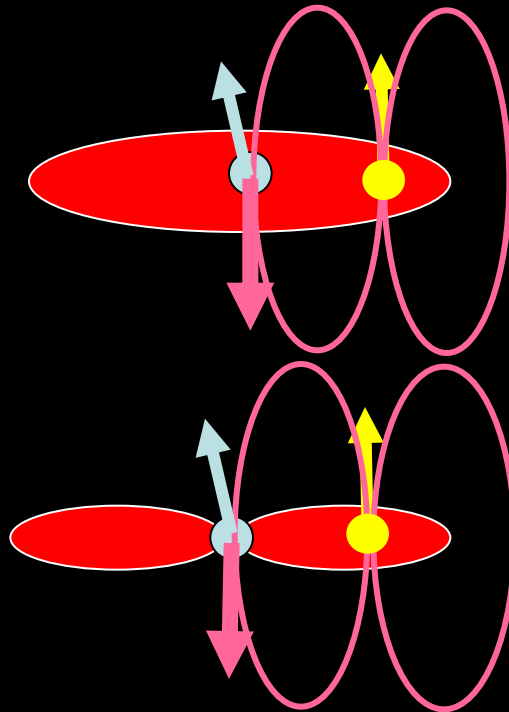
# Nucleus - electron coupling

$$H_{hf} = -\hbar^2 \gamma_e \gamma_n \frac{\vec{I} \cdot \vec{l}}{r^3} + \hbar^2 \gamma_e \gamma_n \left[ \frac{\vec{I} \cdot \vec{s}}{r^3} - 3 \frac{(\vec{I} \cdot \vec{r})(\vec{s} \cdot \vec{r})}{r^5} \right] - \hbar^2 \gamma_e \gamma_n \frac{8\pi}{3} \vec{I} \cdot \vec{s} \delta(r)$$

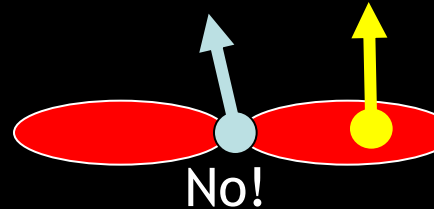
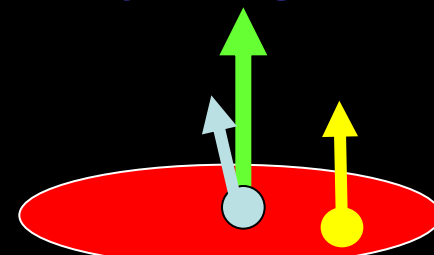
Orbital effect  
*weak - anisotropic*



Dipolar effect from  
An unpaired spin  
*weak - anisotropic*



Contact contribution from an  
unpaired spin on a s orbital  
*Very strong - Isotropic*



# NMR basics (5): nucleus-electron coupling (hyperfine interaction)

$$\mathcal{H}_{hf} = -\hbar^2 \gamma_e \gamma_n \frac{\vec{I} \cdot \vec{l}}{r^3} + \hbar^2 \gamma_e \gamma_n \left[ \frac{\vec{I} \cdot \vec{s}}{r^3} - 3 \frac{(\vec{I} \cdot \vec{r})(\vec{s} \cdot \vec{r})}{r^5} \right] - \hbar^2 \gamma_e \gamma_n \frac{8\pi}{3} \vec{I} \cdot \vec{s} \delta(r)$$

Orbital effect

Spin-dipolar effect  
from an unpaired spin s

Contact contribution from an  
unpaired spin on a s orbital

$$\nu^i = \frac{\gamma}{2\pi} H_0 + \frac{\gamma}{2\pi} H_{hf}^{orb} + \frac{\gamma}{2\pi} H_{hf}^{dip} + \frac{\gamma}{2\pi} H_{hf}^{contact}$$

$$\nu^{i=x,y,z} = \frac{\gamma}{2\pi} (1 + K_{orb}^i + K_{dip}^i + K_{contact} + K_{core-polarization})$$

Gyromagnetic ratio:  
depends on the nucleus

Orbital shift

Spin shift

# NMR basics (5): nucleus-electron coupling (hyperfine interaction)

$$\mathcal{H}_{hf} = -\hbar^2 \gamma_e \gamma_n \frac{\vec{I} \cdot \vec{l}}{r^3} + \hbar^2 \gamma_e \gamma_n \left[ \frac{\vec{I} \cdot \vec{s}}{r^3} - 3 \frac{(\vec{I} \cdot \vec{r})(\vec{s} \cdot \vec{r})}{r^5} \right] - \hbar^2 \gamma_e \gamma_n \frac{8\pi}{3} \vec{I} \cdot \vec{s} \delta(r)$$

Orbital effect

Spin-dipolar effect  
from an unpaired spin s

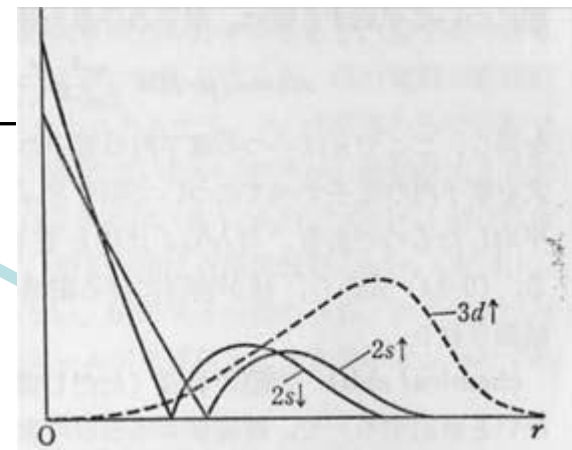
Contact contribution from an  
unpaired spin on a s orbital

$$\nu^i = \frac{\gamma}{2\pi} H_0 + \frac{\gamma}{2\pi} H_{hf}^{orb} + \frac{\gamma}{2\pi} H_{hf}^{dip} + \frac{\gamma}{2\pi} H_{hf}^{contact}$$

$$\nu^{i=x,y,z} = \frac{\gamma}{2\pi} (1 + K_{orb}^i + K_{dip}^i + K_{contact} +$$

Gyromagnetic ratio:  
depends on the nucleus

Orbital shift



# Orbital shift

$$H = -\hbar^2 \gamma_{e^-} \gamma_{nucleus} \frac{\mathbf{I} \cdot \mathbf{L}}{r^3}$$

## Orbital shift

- Filled shells
- Unpaired electrons

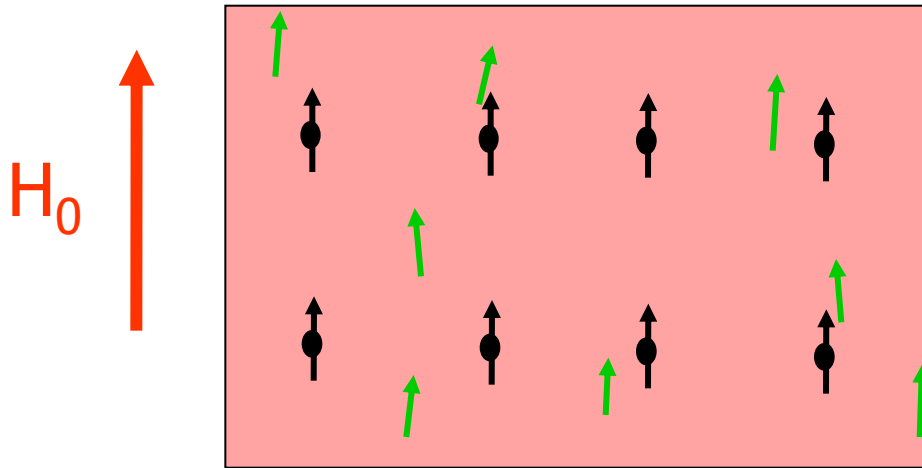
## Main features

- T-independent
- Tensor: linear response in field, orientation dependent

## Information

- Nature of orbitals (e.g. spin state for 3d elements)
- → Orbital susceptibility

# Spin shift



$$M = \chi H_0$$

$$H_{loc} = H_0 + \alpha \chi_{loc} H_0$$

The spin shift yields the local susceptibility near the nucleus: « atomic » resolved susceptibility susceptibility

$$H = A_{hf} \vec{I} \cdot \vec{s}$$
$$K_{spin} = A_{hf} \frac{1}{\hbar^2 \gamma_n \gamma_e} \chi_{electron}$$

Knight shift = Spin shift for metals

# Spin shift

$$H = A_{hf} \vec{I} \cdot \vec{s}$$

## Spin shift

- Unpaired electrons

## Main features

- T-dependent
- Isotropic coupling but susceptibility can be anisotropic

## Information

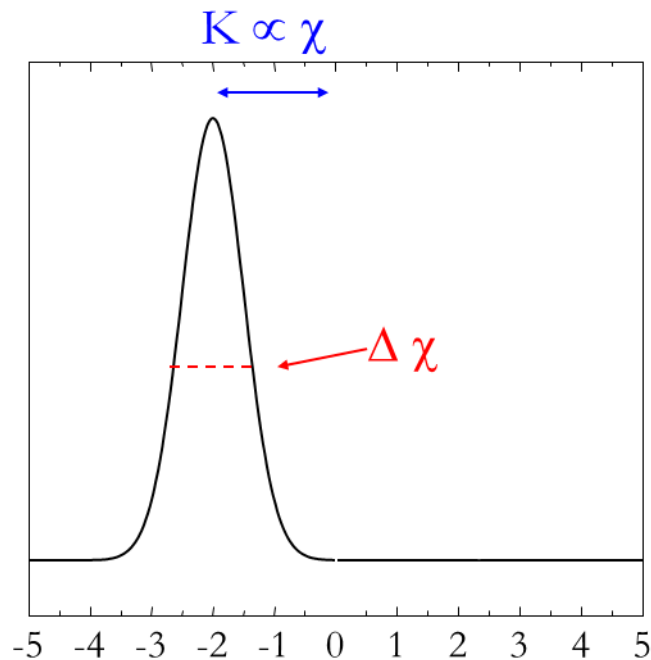
- Measures the local susceptibility
- → histogram of local environments
- → site selective

Knight shift = Spin shift for metals

# Spin shift

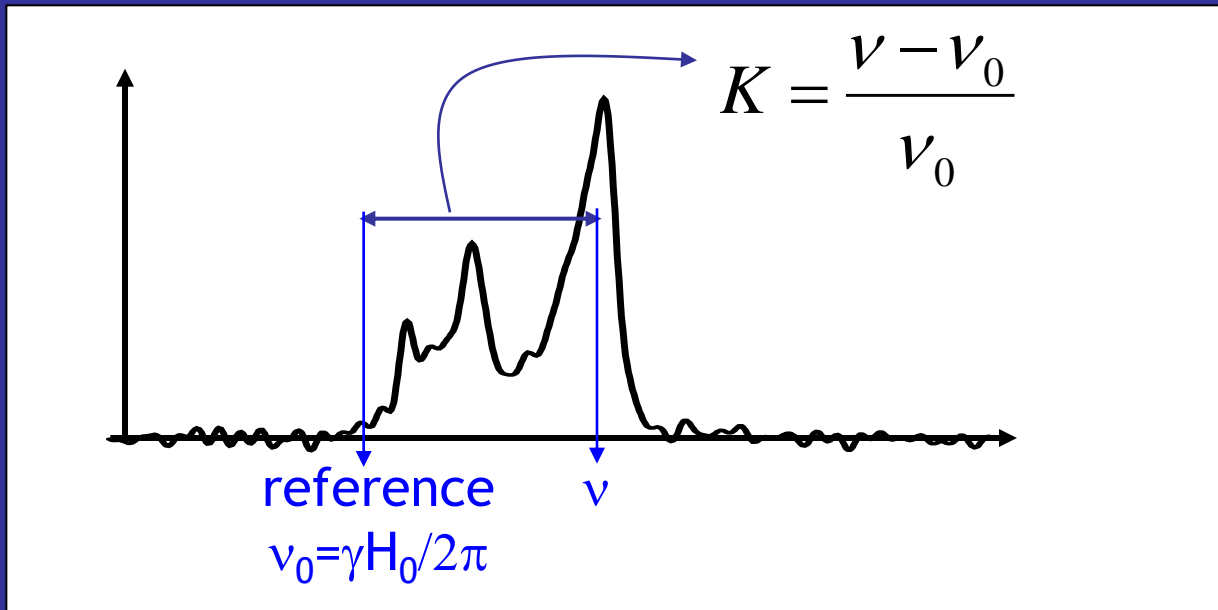
$$H = A_{hf} \vec{I} \cdot \vec{s}$$

Line shift  $\mathbf{K}$  :  
susceptibility  $\chi_{\text{frustr}}$



Linewidth  $\Delta H$  :  
spatially inhomogeneous  
susceptibility (dilution)

# Electron-nucleus interaction



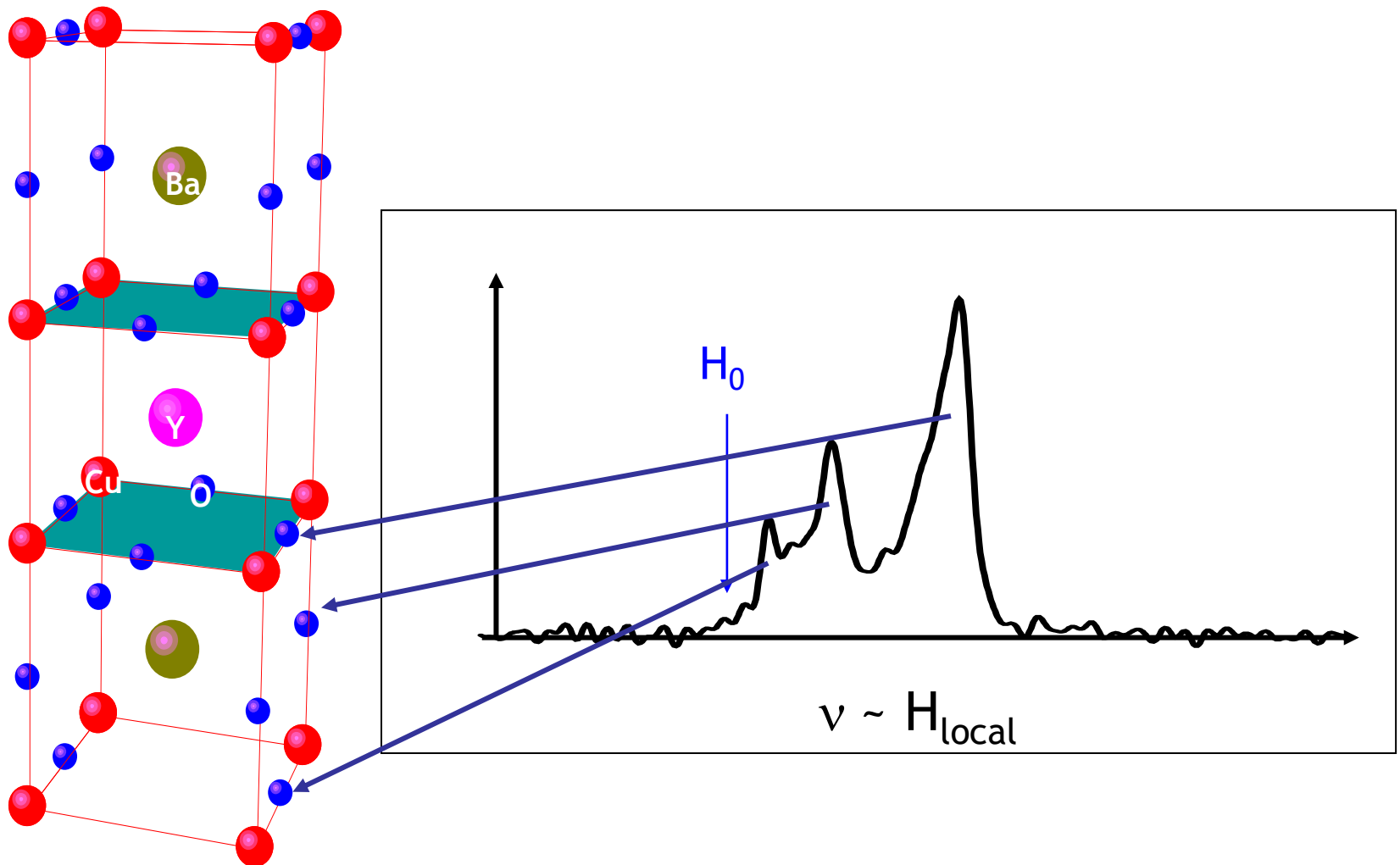
$$\nu^{i=x,y,z} = \frac{\gamma}{2\pi} (1 + K_{orb}^i + K_{dip}^i + K_{contact} + K_{core polarization})$$

Gyromagnetic ratio

Orbital or  
chemical shift

Magnetic  
(« Knight ») shifts »

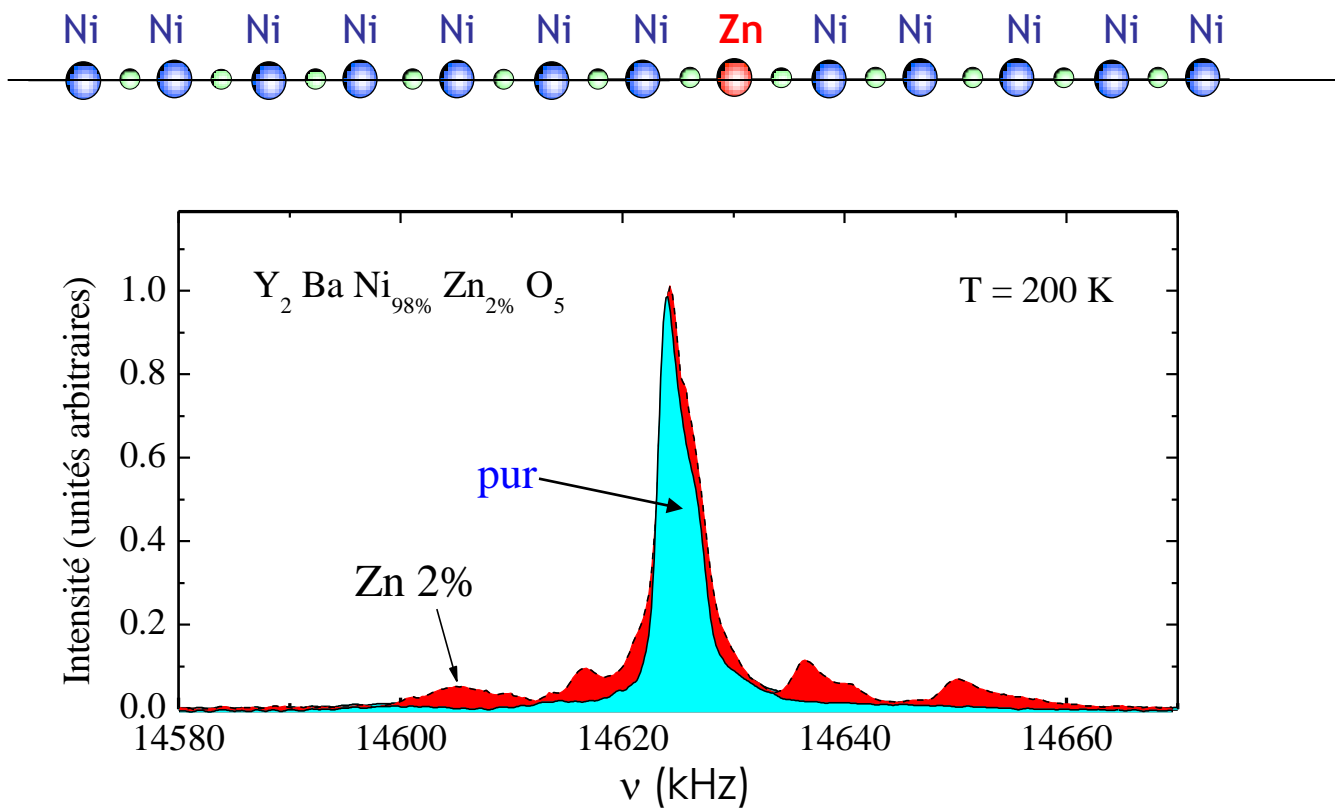
# nucleus-electron coupling: Y BaCuO



# Spin shift

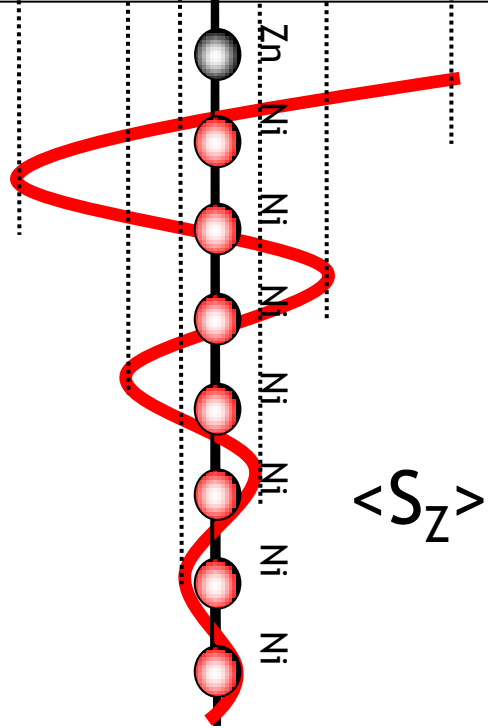
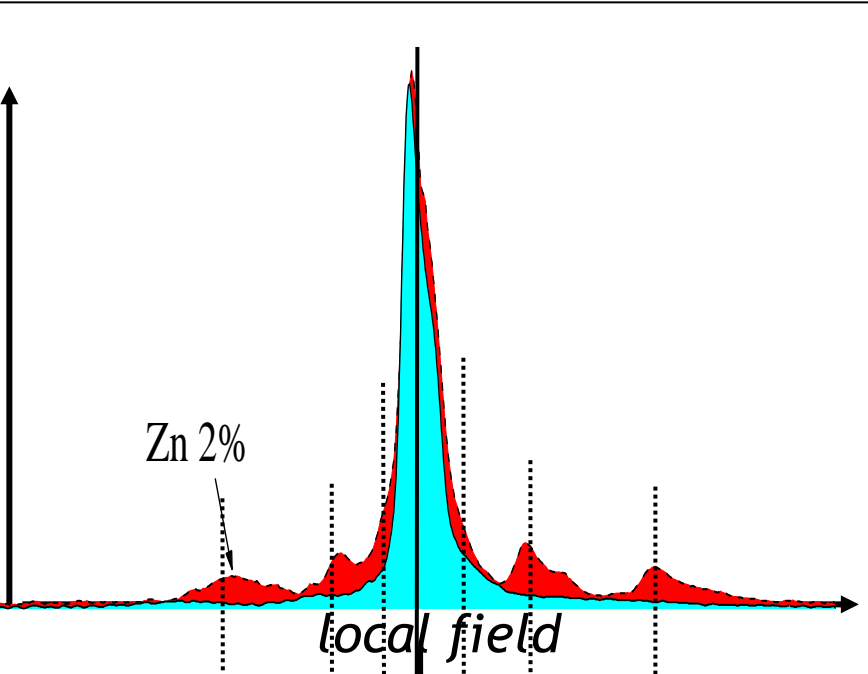
$K_{\text{spin}}$  yields a histogram of  $\chi$  values, not a sum

One impurity in a Haldane chain,  $\text{YBa}_2\text{NiO}_5$  ( $S=1$ ) with Zn impurities on Ni site

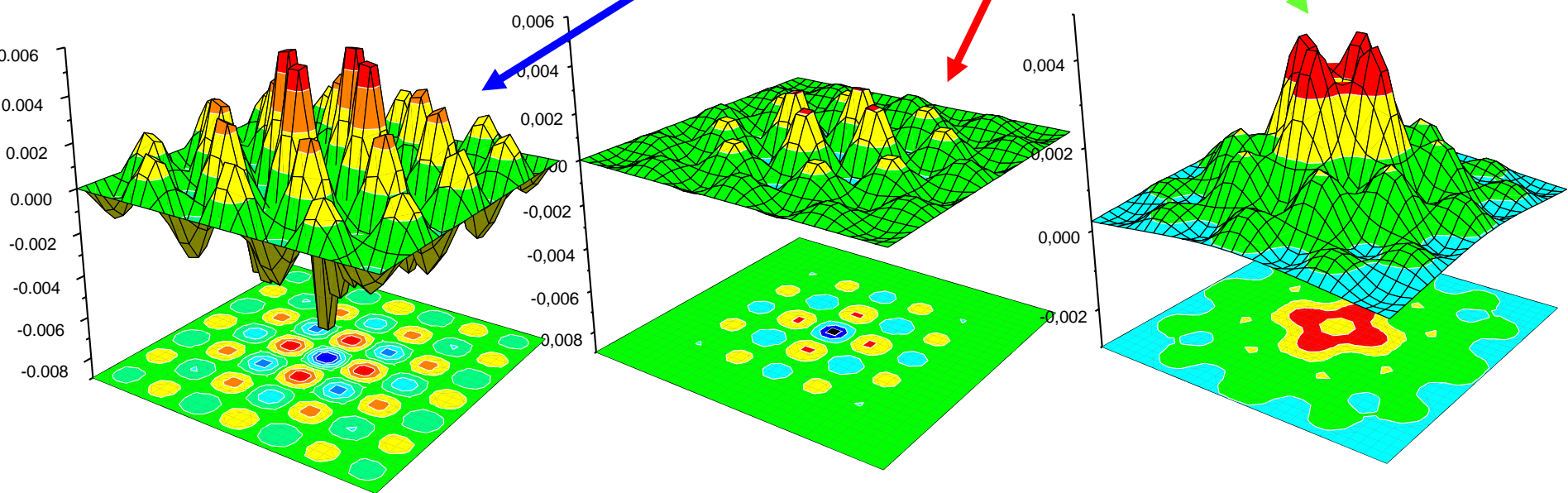
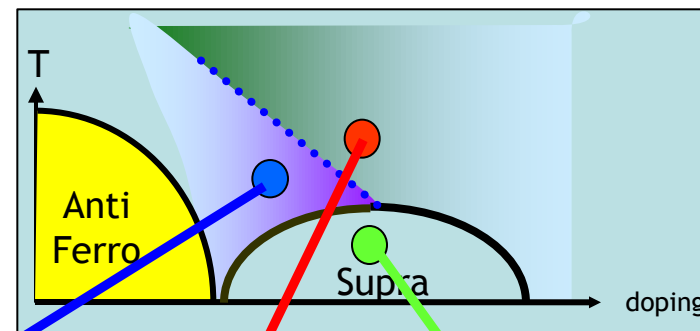
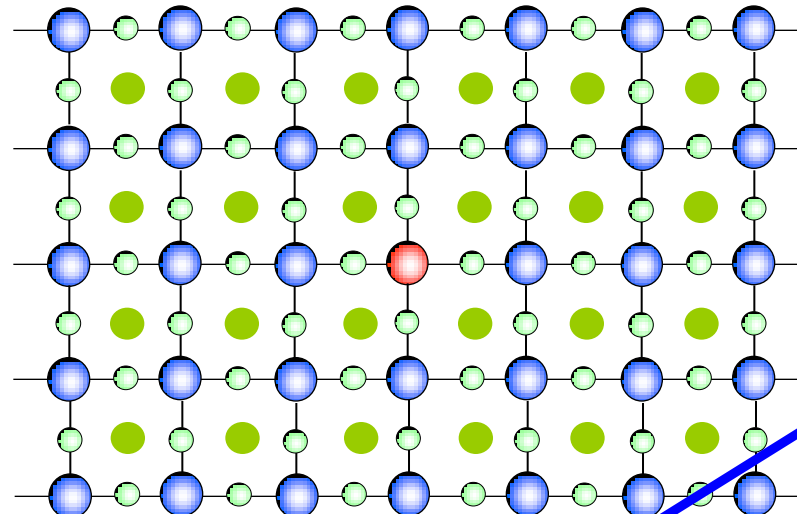


Tedoldi *et al.*, PRL 99; Das *et al.* PRB 04

Spatially resolved probe of susceptibility  $\chi$



# Measurement of local susceptibility



Perturb to reveal: selectivity of the coupling in NMR

# NMR basics (6): nucleus-charges coupling

*With NMR we study the time evolution of nuclear magnetization, driven by the hyperfine interactions...*

$$\mathcal{H} = \mathcal{H}_Z + \mathcal{H}_{n-n} + \mathcal{H}_{n-e} + \mathcal{H}_{EFG}$$

$$\mathcal{H}_Z = -\gamma\hbar \sum_i I_z^i H_0 .$$

$$\mathcal{H}_{n-n} = \sum_{j < k} \frac{\hbar^2 \gamma^2}{r^3} \left( A + B + C + D + E + F \right)_{jk}$$

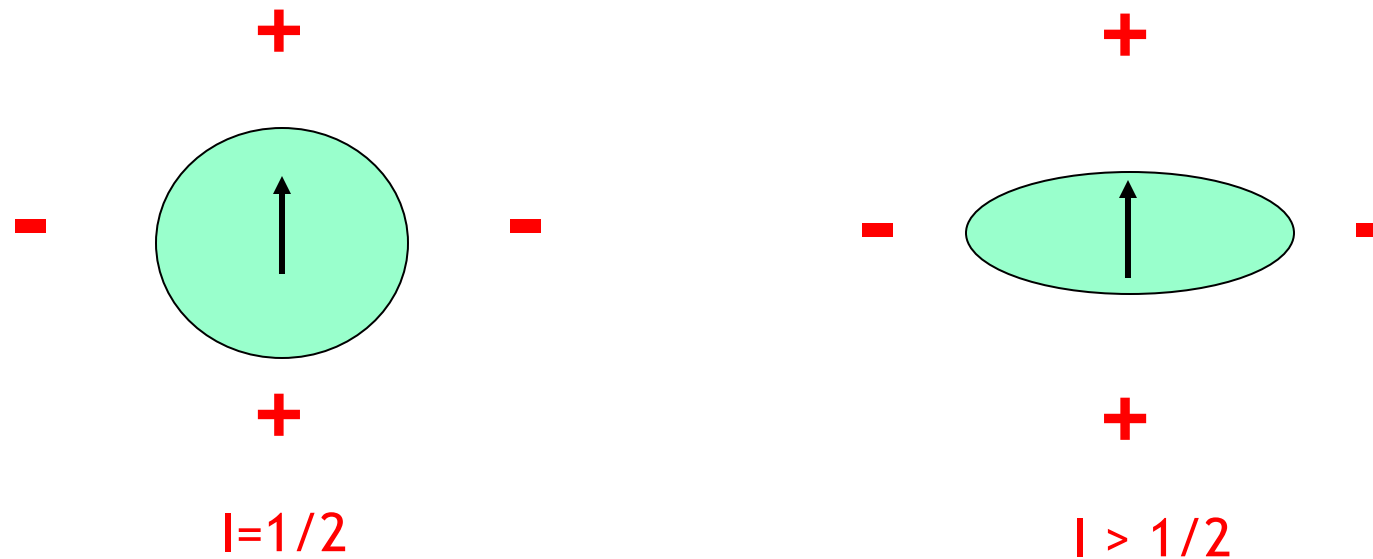
$$\mathcal{H}_{n-e} = -\gamma\hbar \sum_{i,k} \mathbf{I}_i \tilde{A}_{ik} \mathbf{S}_k$$

$$\mathcal{H}_{EFG} = \sum_i \frac{e^2 Q V_{ZZ}}{4I(2I-1)} \left( 3(I_z^i)^2 - I(I+1) + \frac{\eta}{2} [(I_+^i)^2 + (I_-^i)^2] \right)$$

A very involved Hamiltonian...quite rewarding

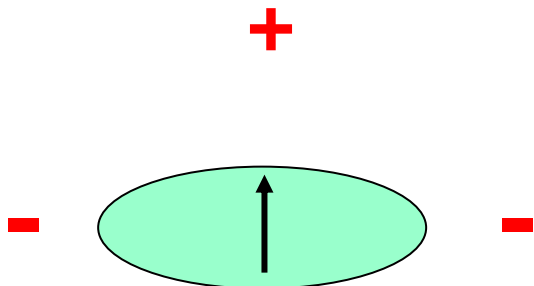
# NMR basics (6): quadrupole interaction

If  $I > 1/2$ , nuclear spin  $I$  is sensitive to any Electric Field Gradient from the lattice (non-sphericity of the nucleus)



$$\mathcal{H}_{EFG} = \sum_i \frac{e^2 Q V_{ZZ}}{4I(2I-1)} \left( 3(I_z^i)^2 - I(I+1) + \frac{\eta}{2} [(I_+^i)^2 + (I_-^i)^2] \right)$$

# NMR basics (6): quadrupole interaction



$$V(r) = V(0) + \left. \sum_{i=3\_directions} x_i \frac{\partial V}{\partial x_i} \right)_{r=0} + \frac{1}{2} \left. \sum_{i=3\_directions} x_i x_j \frac{\partial^2 V}{\partial x_i \partial x_j} \right)_{r=0} + \dots$$

cst

0 since center  
of mass and  
charge  
coincides

+

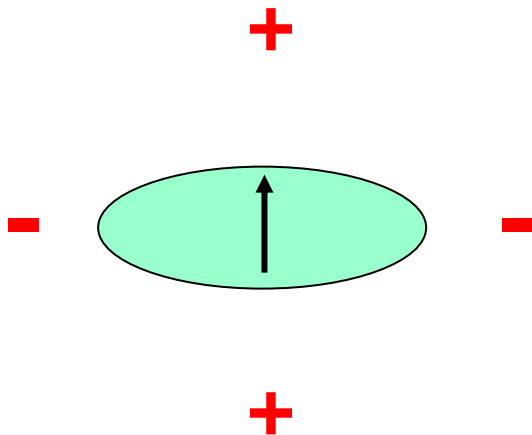
Quadrupole  
term

We express it in principal  
axes where  $V$  is diagonal :

Quadrupolar moment of the nucleus

$$eQ = \frac{1}{2} \int (3z^2 - r^2) \rho d^3 R$$

# NMR basics (6): quadrupole interaction



$$V(r) = V(0) + \left. \sum_{i=3\_directions} x_i \frac{\partial V}{\partial x_i} \right)_{r=0} + \frac{1}{2} \left. \sum_{i=3\_directions} x_i x_j \frac{\partial^2 V}{\partial x_i \partial x_j} \right)_{r=0} + \dots$$

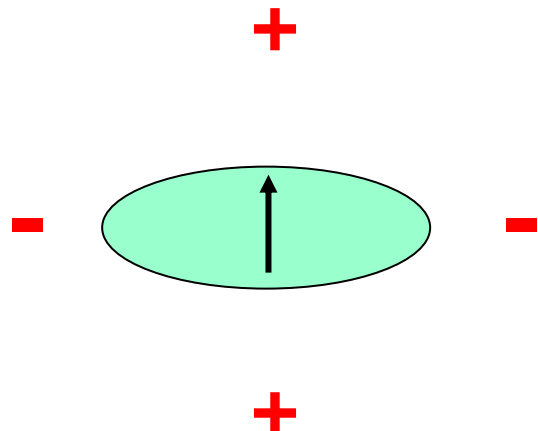
$$H_Q = \int \rho_n(\vec{r}) V(\vec{r}) d\vec{r}$$

Wigner-Eckart theorem

$$H_Q = \frac{eQ}{4I(2I-1)} \left\{ \left( \frac{\partial^2 V}{\partial x^2} - \frac{\partial^2 V}{\partial y^2} \right) (I_x^2 - I_y^2) + \frac{\partial^2 V}{\partial z^2} (3I_z^2 - I^2) \right\}$$

Quadrupolar moment of the nucleus       $eQ = \frac{1}{2} \int (3z^2 - r^2) \rho d^3 R$

# NMR basics (6): quadrupole interaction



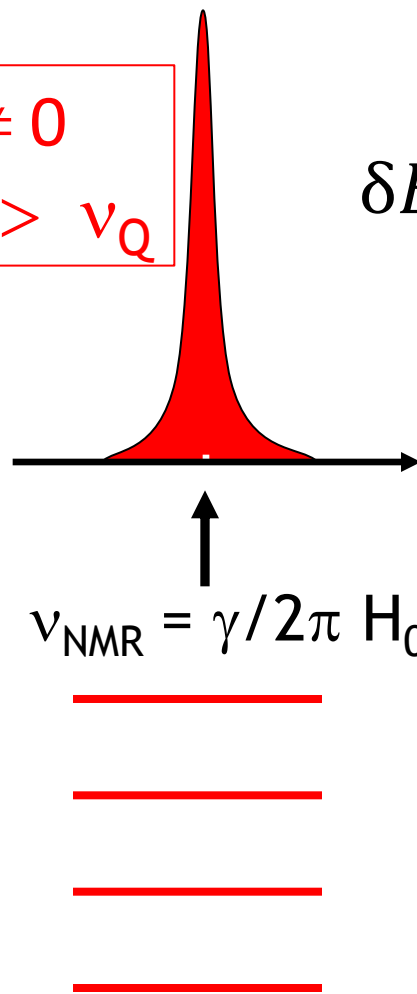
$$H_Q = \frac{eQ}{4I(2I-1)} \left\{ \left( \frac{\partial^2 V}{\partial x^2} - \frac{\partial^2 V}{\partial y^2} \right) (I_x^2 - I_y^2) + \frac{\partial^2 V}{\partial z^2} (3I_z^2 - I^2) \right\}$$

$$H_Q = \frac{e^2 q Q}{4I(2I-1)} \left\{ 3I_z^2 - I(I+1) + \frac{1}{2} \eta (I_x^2 - I_y^2) \right\}$$

$$eq = \frac{\partial^2 V}{\partial z^2}, \quad \eta = \frac{\left( \frac{\partial^2 V}{\partial x^2} - \frac{\partial^2 V}{\partial y^2} \right)}{\frac{\partial^2 V}{\partial z^2}}, \quad \left( \left| \frac{\partial^2 V}{\partial z^2} \right| > \left| \frac{\partial^2 V}{\partial y^2} \right| > \left| \frac{\partial^2 V}{\partial x^2} \right| \right)$$

# Quadrupole interaction: back to the spectrum

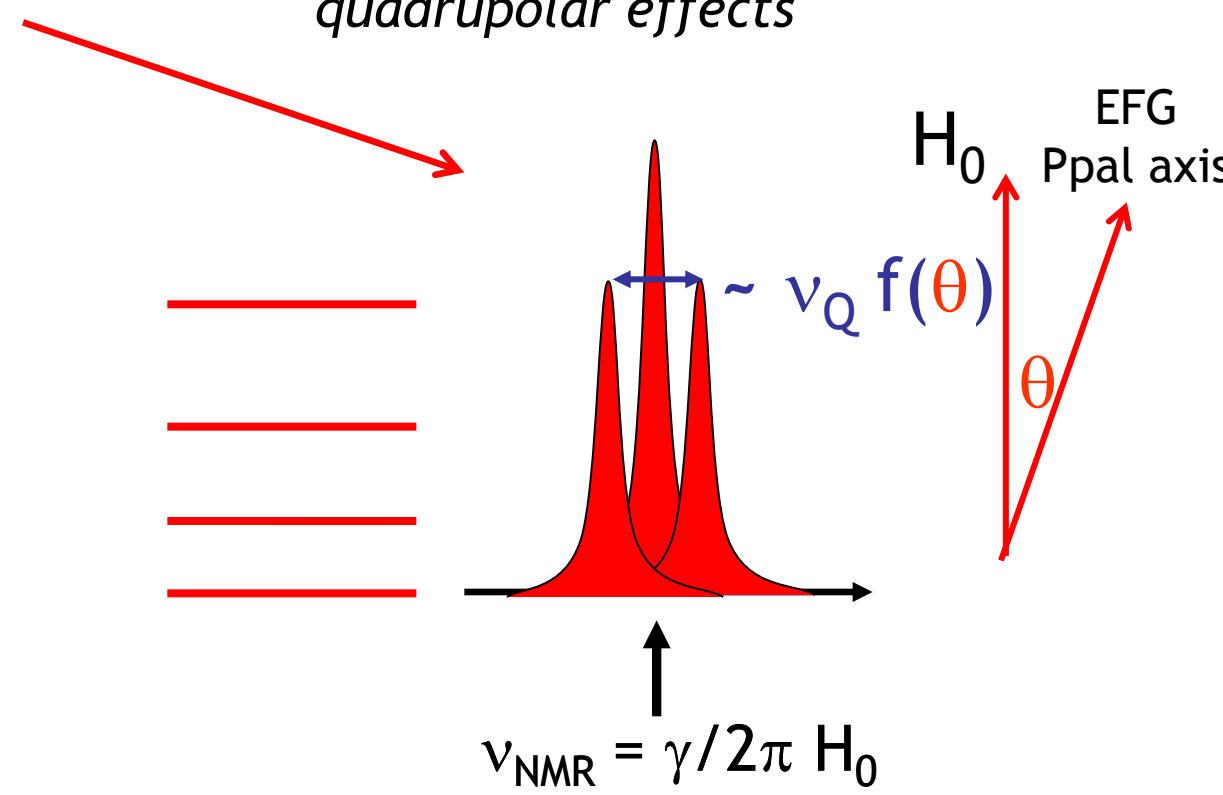
1-  $H_0 \neq 0$   
 $\nu_{\text{NMR}} \gg \nu_Q$



$\eta=0$ , axial sym. - 1<sup>st</sup> order

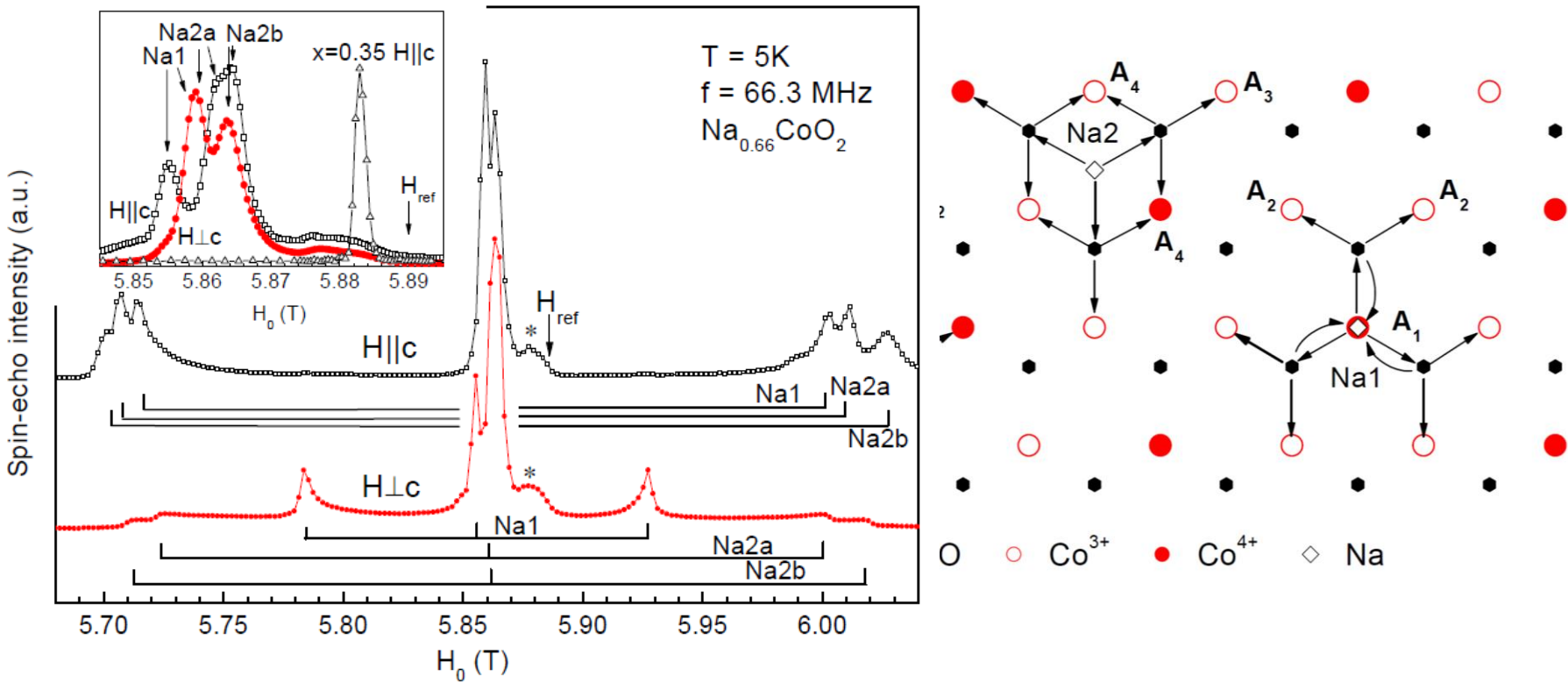
$$\delta E^{(1)} \sim \nu_Q (3 \cos^2 \theta - 1) [3m^2 - I(I+1)]$$

*Degeneracy of the transitions lifted by quadrupolar effects*



Quadrupolar nuclei: lifting the multiplicity of transitions on single crystals

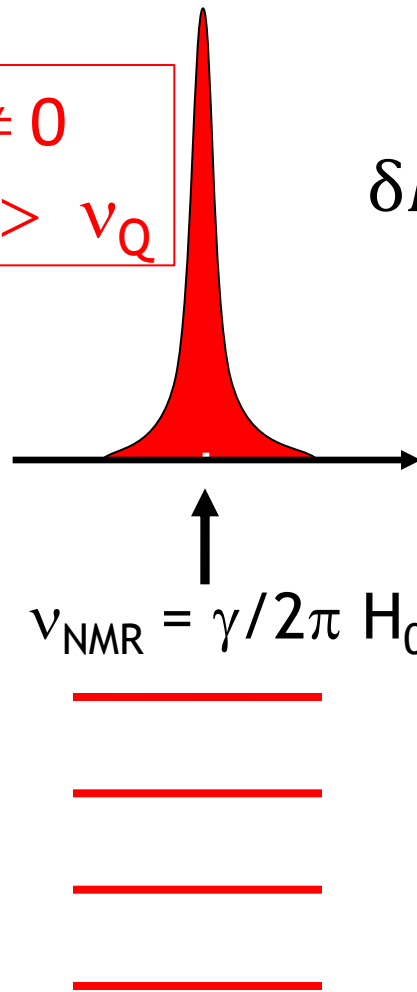
# Cobaltates $\text{Na}_{0.66}\text{CoO}_2$ : charge segregation



- Spectra taken in two field directions on oriented powders
- Different charge environments
- $\text{Na}^+$  is driving the charge state and physical properties

# Quadrupole interaction only: back to the spectrum

1-  $H_0 \neq 0$   
 $v_{\text{NMR}} \gg v_Q$

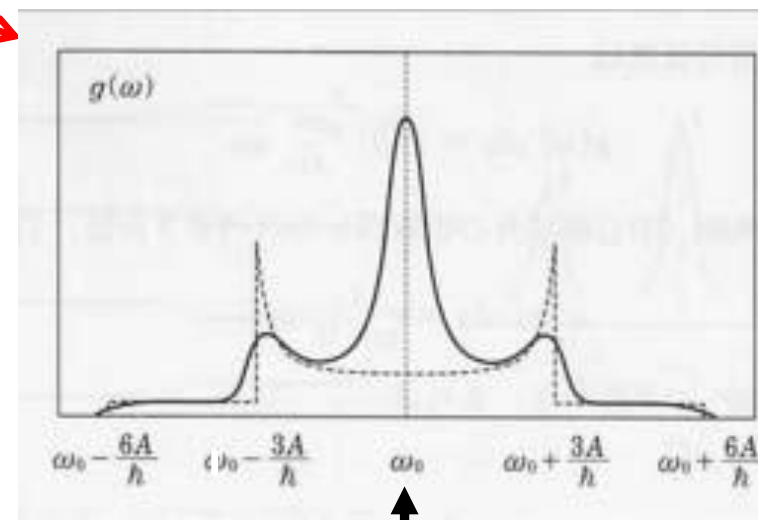


$I = 3/2$   
 $2I+1$  levels

$\eta=0$ , axial sym. - 1<sup>st</sup> order

$$\delta E^{(1)} \sim v_Q (3 \cos^2 \theta - 1) [3m^2 - I(I + 1)]$$

*Degeneracy of the transitions  
lifted by quadrupolar effects*

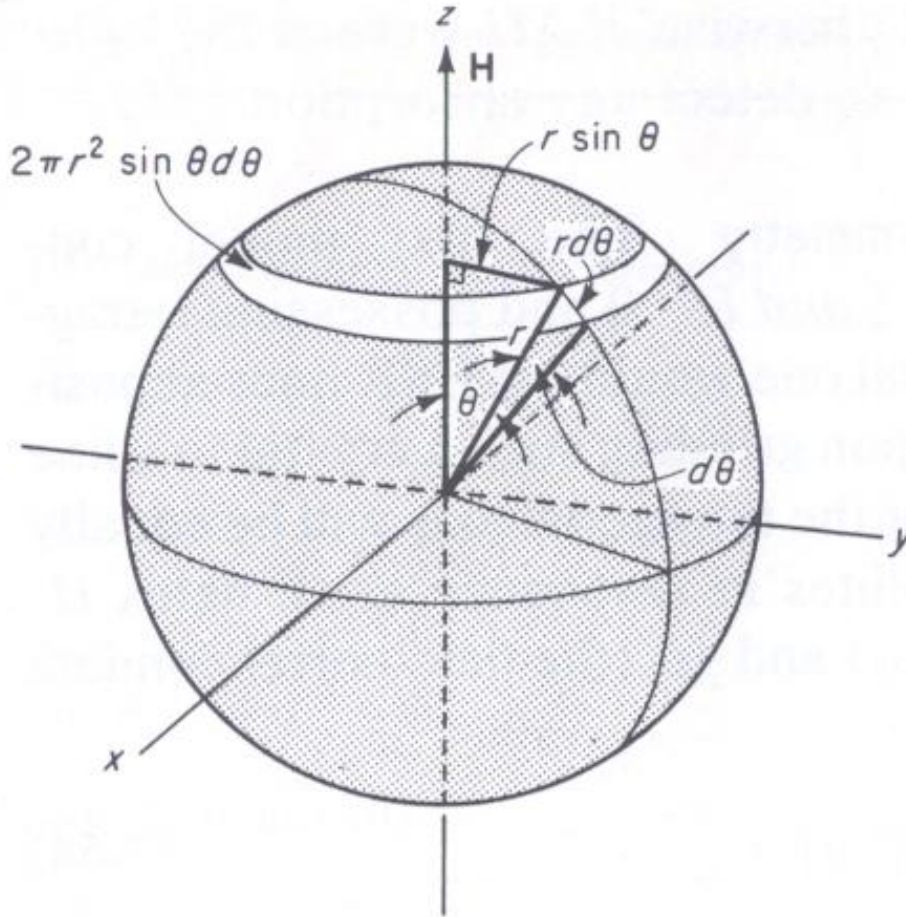


$v_{\text{NMR}} = \gamma/2\pi H_0$

Quadrupolar nuclei: distribution of angles → powder average

# Averaging on angles: EFG, hyperfine tensor

The EFG and hyperfine tensors may not have the same principal axis! One can manage, playing with isotopes, field ...



Single crystals are best. Fitting routines for powders ...

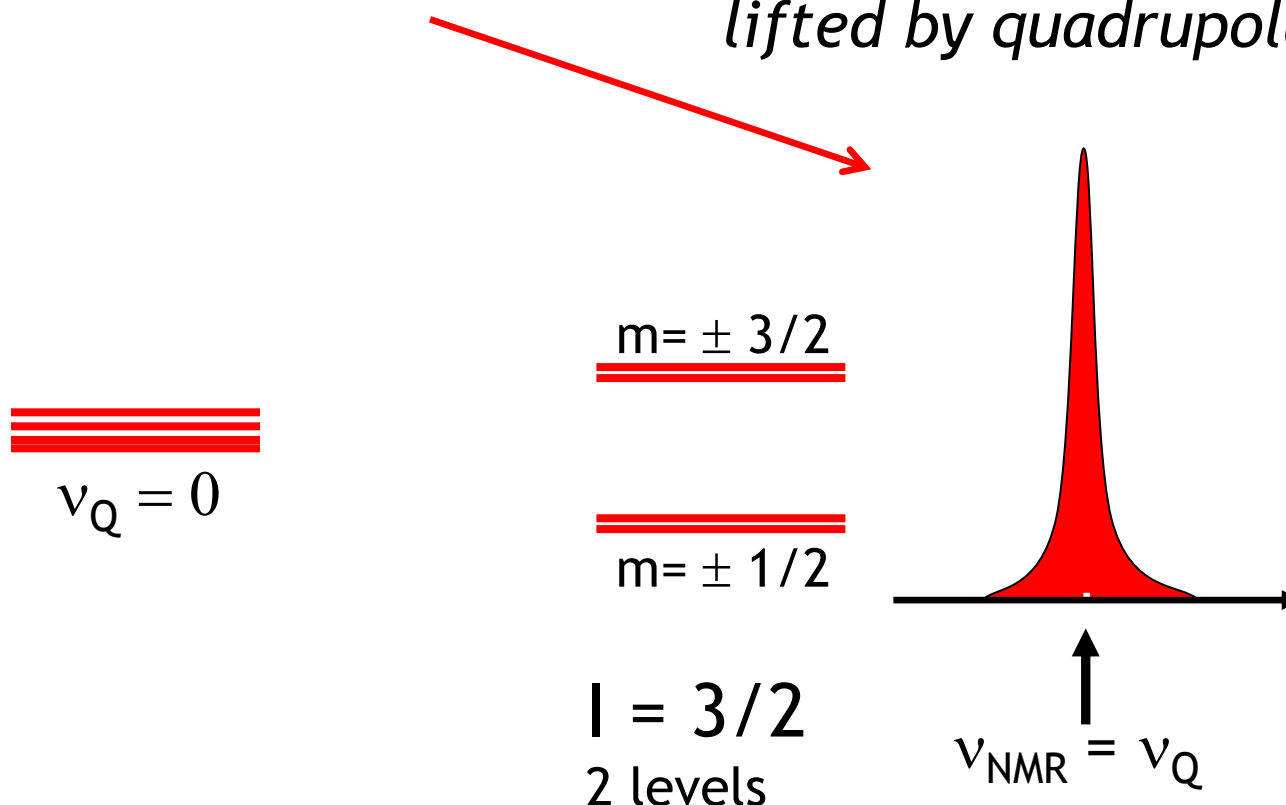
# Quadrupole interaction: NQR (6)

2- H = 0

$\eta=0$ , axial sym. - 1<sup>st</sup> order

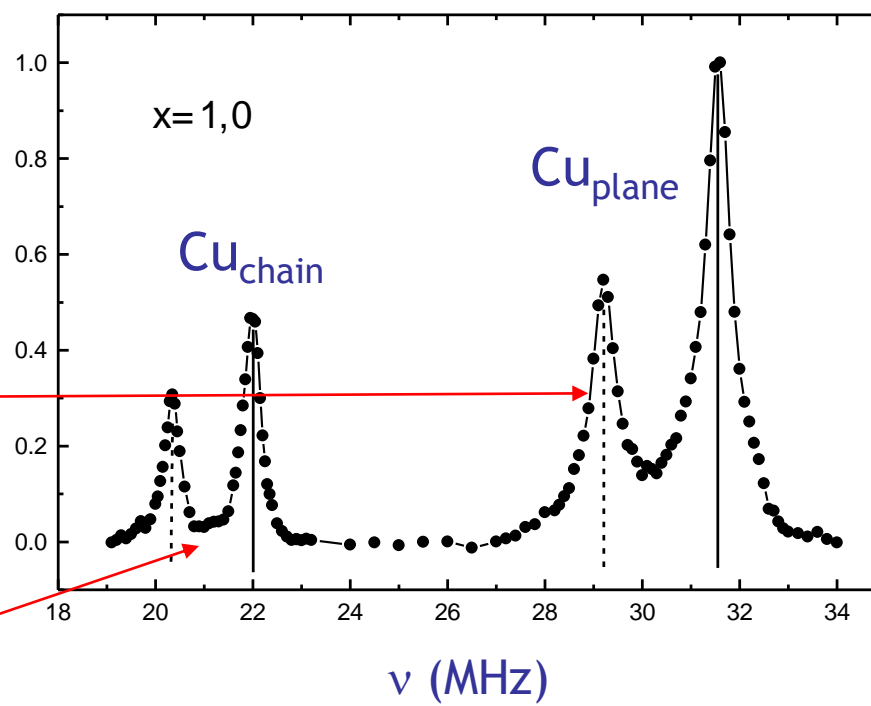
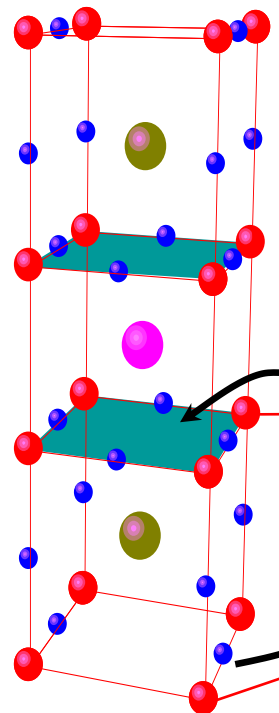
$$\delta E^{(1)} \sim v_Q / 6 [3m^2 - I(I+1)]$$

*Degeneracy of the transitions  
lifted by quadrupolar effects*



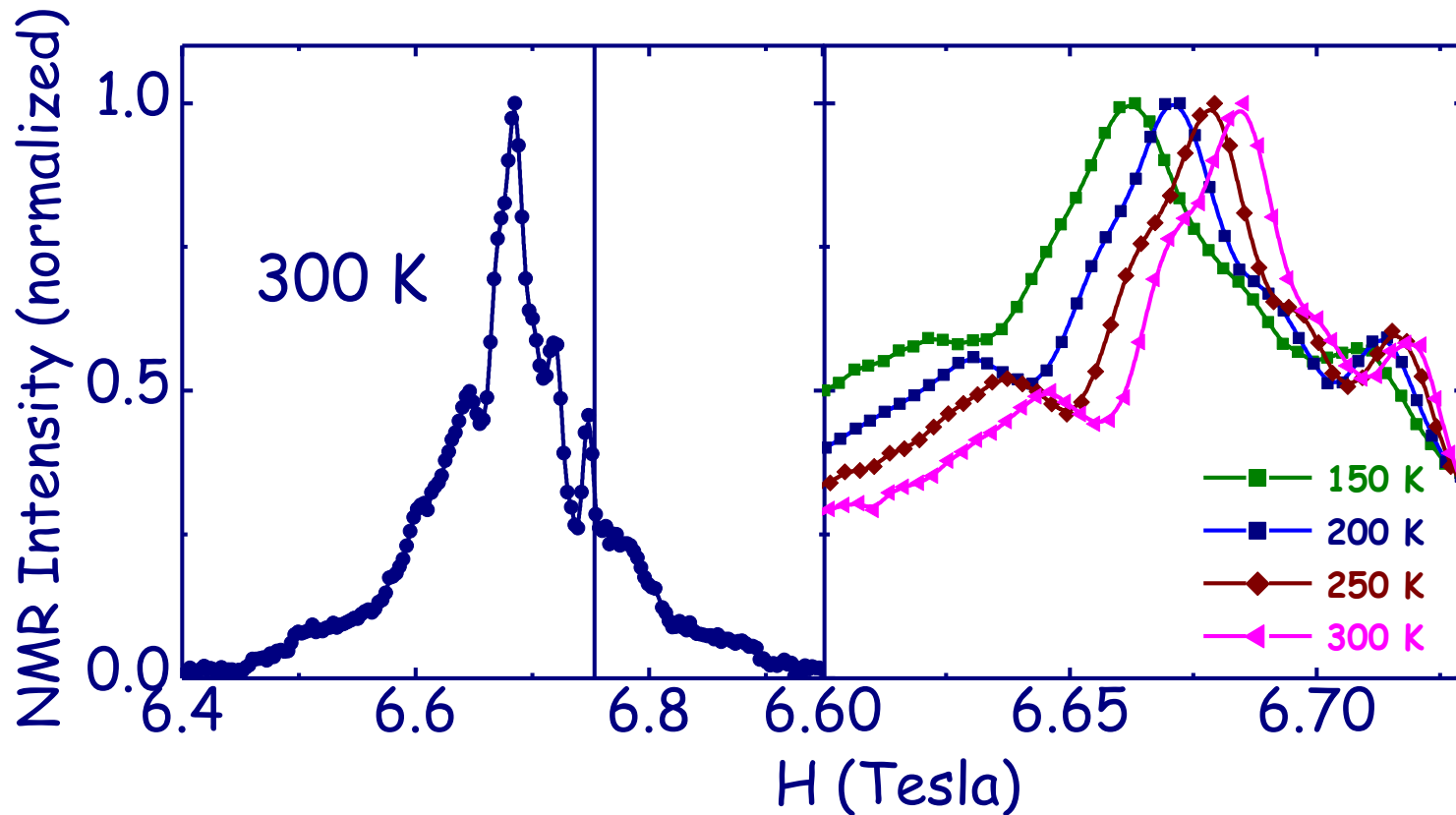
Quadrupolar resonance: powders = single crystals

# NQR of Cu in cuprates: 2 sites, 2 isotopes, $I = 3/2$



# One example of a difficult spectrum

If  $I > 1/2$ , nuclear spin  $I$  is sensitive to any Electric Field Gradient from the lattice



M.I.T., 2005

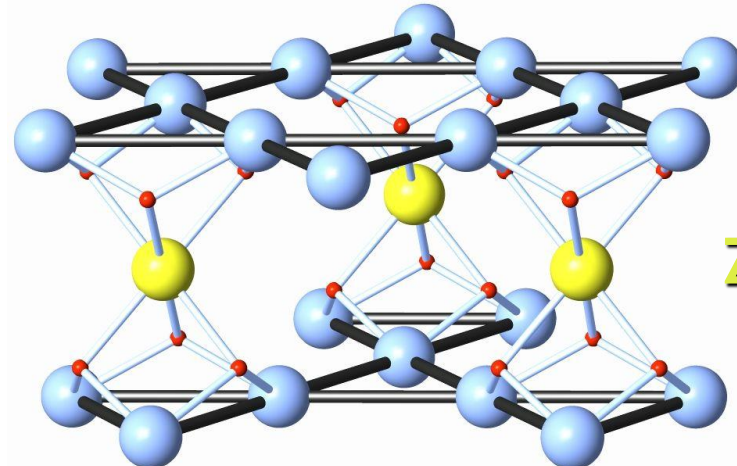
J|A|C|S  
COMMUNICATIONS

Published on Web 09/09/2005

## A Structurally Perfect $S = 1/2$ Kagomé Antiferromagnet

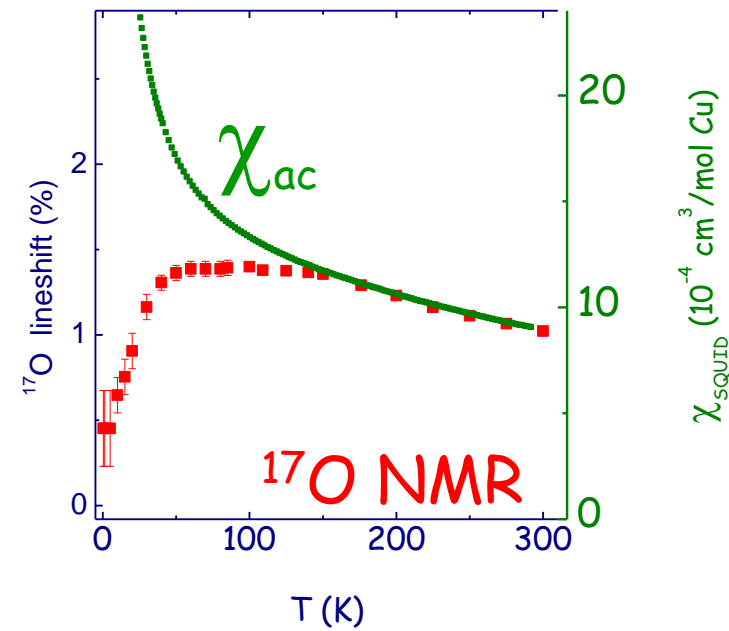
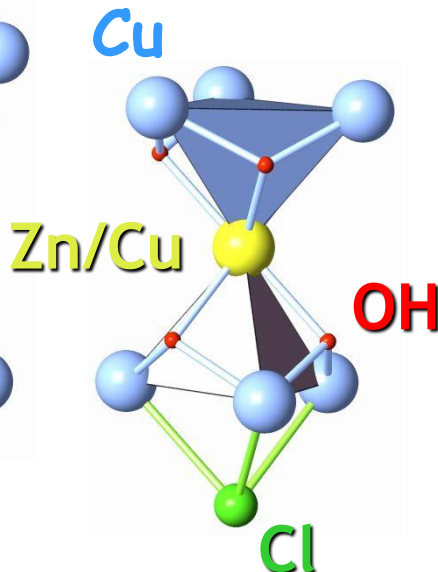
Matthew P. Shores, Emily A. Nytko, Bart M. Bartlett, and Daniel G. Nocera\*

Department of Chemistry, 6-335, Massachusetts Institute of Technology, 77 Massachusetts Avenue,  
Cambridge, Massachusetts 02139-4307



Herbertsmithite  
 $ZnCu_3(OH)_6Cl_2$

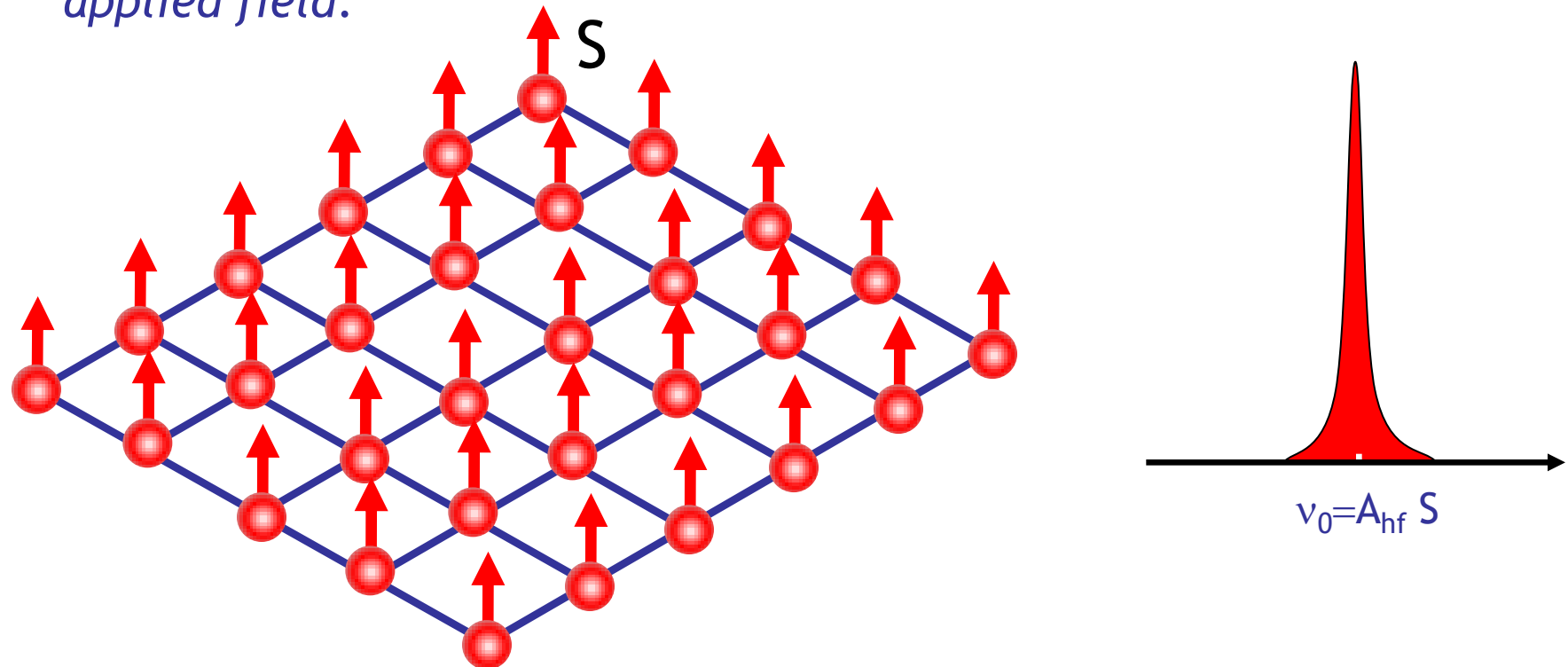
$Cu^{2+}$ ,  $S=1/2$



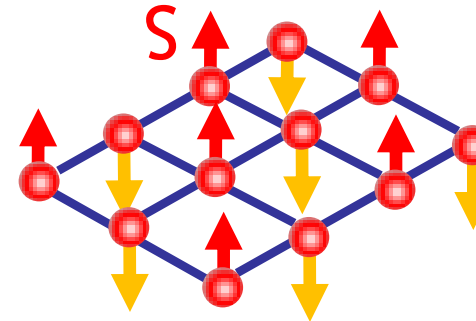
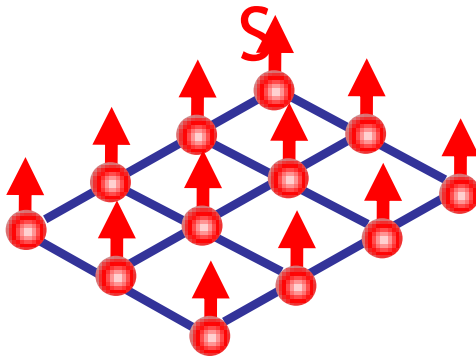
A. Olariu et al., Phys. Rev. Lett (2008)

# Magnetic ordering

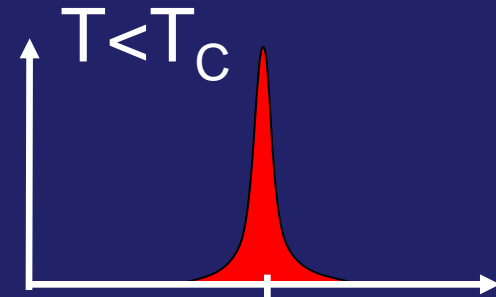
- for a ferromagnet : « enhancement factor »: collective response from electronic spins; associated with the existence of a magnetization
- very strong local fields : in the paramagnetic phase, need of a field  $H_0$  so that  $\langle S \rangle \neq 0$ ; in an ordered phase  $H \sim A_{hf} \langle S \rangle$ ,  $\langle S \rangle \neq 0$
- ZERO FIELD NMR : if hyperfine field is strong enough, *no need of an applied field*:



# Magnetic ordering

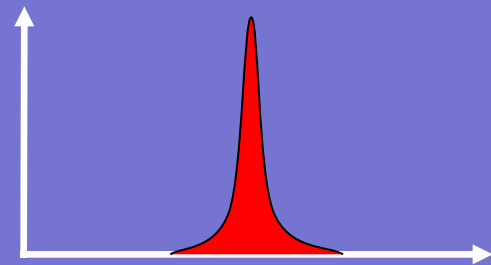


Zero Field  $H_0=0$



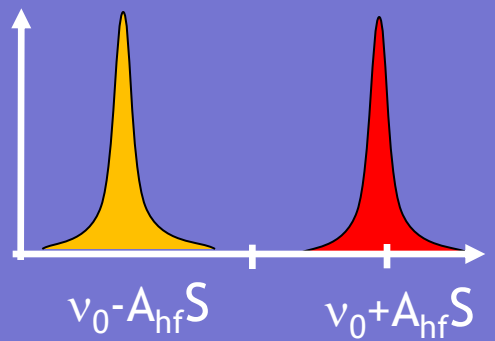
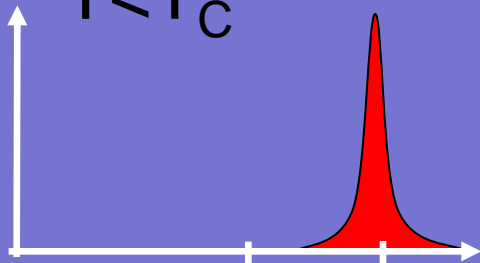
NMR under an applied field  $H_0$

$T > T_C$

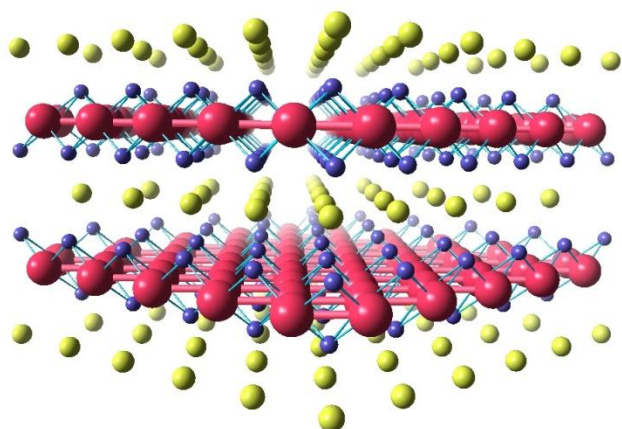


$$v_0 = v_0(1+K)$$

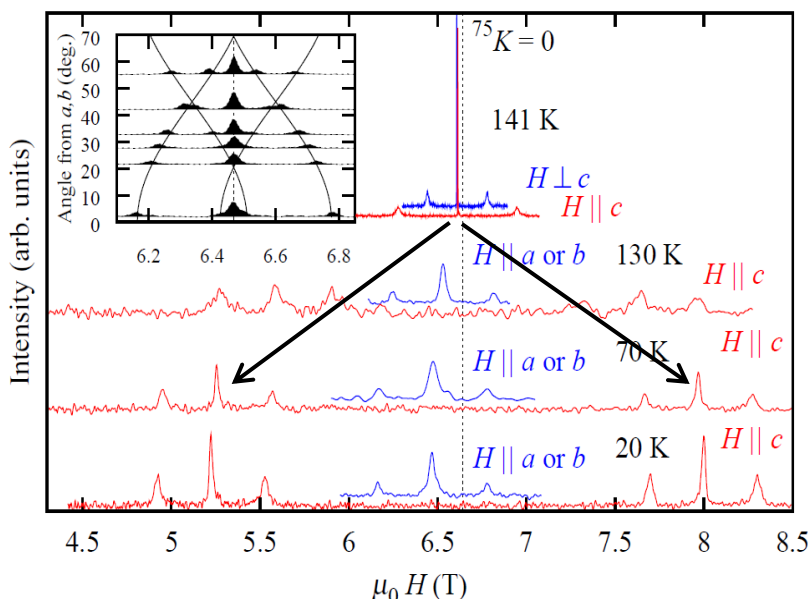
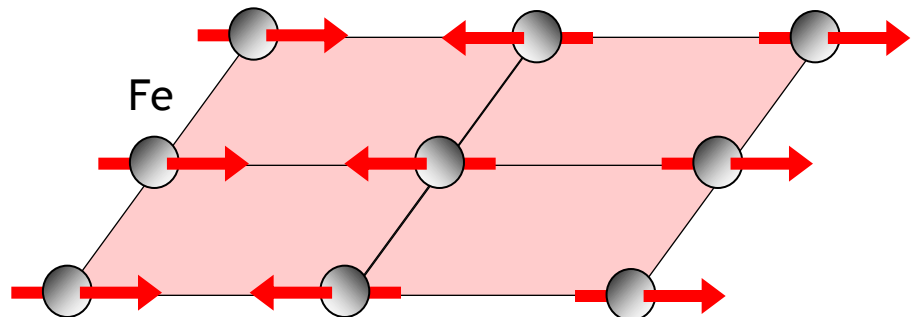
$T < T_C$



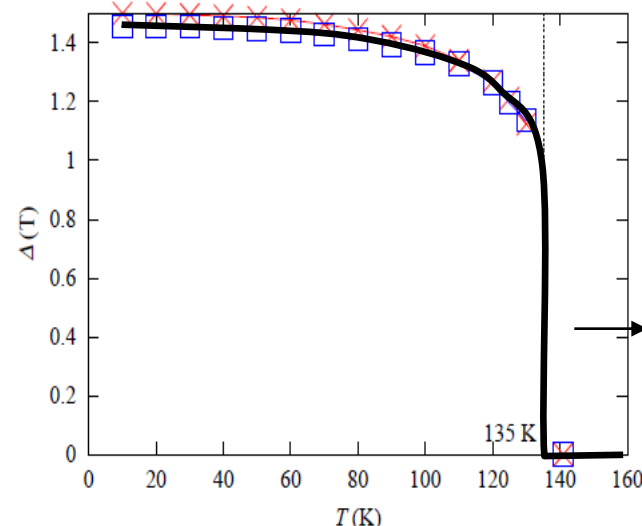
# Magnetic ordering: local field vs T, structure



pnictides  $\text{BaFe}_2\text{As}_2$



- $H$  is parallel to  $c$
- Dipolar coupling
- Discussion of the magnetic structure

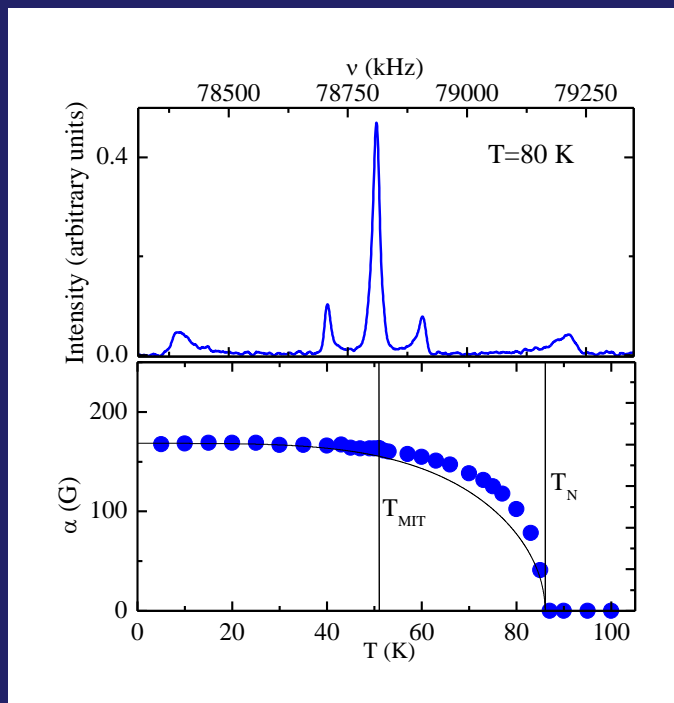


Kitagawa, Takigawa, JPSJ 08

# Magnetic ordering: various types

- Field distribution gives information on the type of ordering

Antiferromagnetic ordering  
eg: Na<sub>0.5</sub>CoO<sub>2</sub>  
Splitting of the lines



Spin density wave  
eg: Cr: distributed field

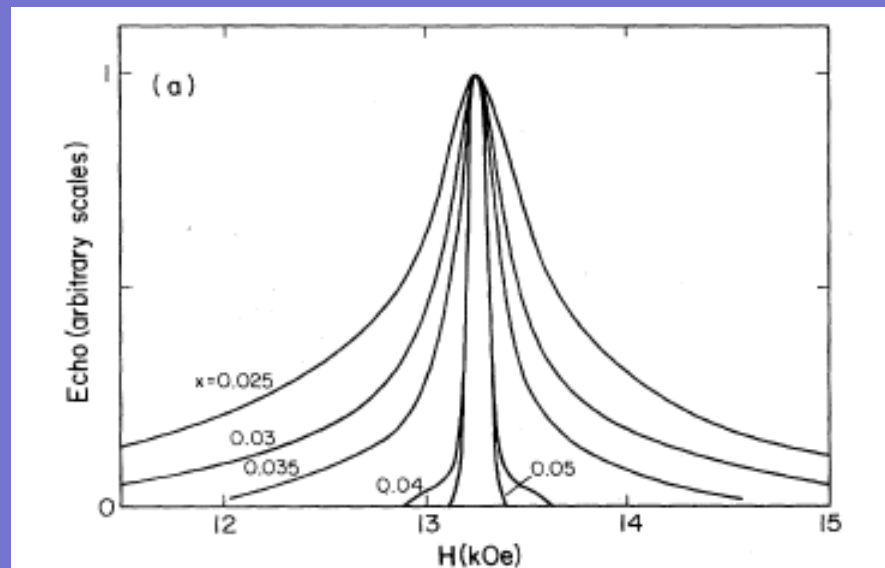
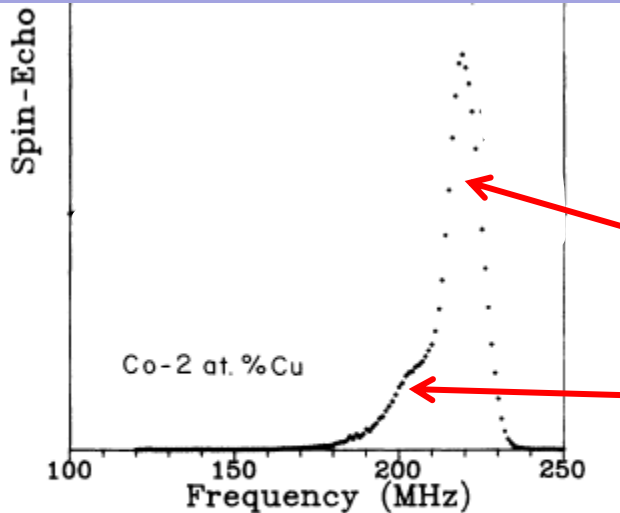


FIG. 74. NMR spectra for Cr-V alloys: (a) Spin echo of <sup>51</sup>V in magnetic field  $H$  at frequency 15 MHz and temperature in the AF<sub>1</sub> phase of  $\text{Cr}_{1-x}\text{V}_x$  alloys (from Kontani *et al.*, 1983); (b)

# Ferromagnets



Cu/Co ferromagnetic multilayers

Panissod *et al.*, PRB 1992

Co surrounded by Co

Co surrounded by Co and Cu

FIG. 1.  $^{59}\text{Co}$  NMR spectra of cobalt-copper alloys with 2, 6, and 10 at. % of copper. The main line is attributed to Co with 12 Co nearest neighbors and each successive satellite to the successive substitution of Cu for Co in the vicinity of Co.

Cr inside the domain

Cr in the domain wall

NArath, Phys Rev 1965

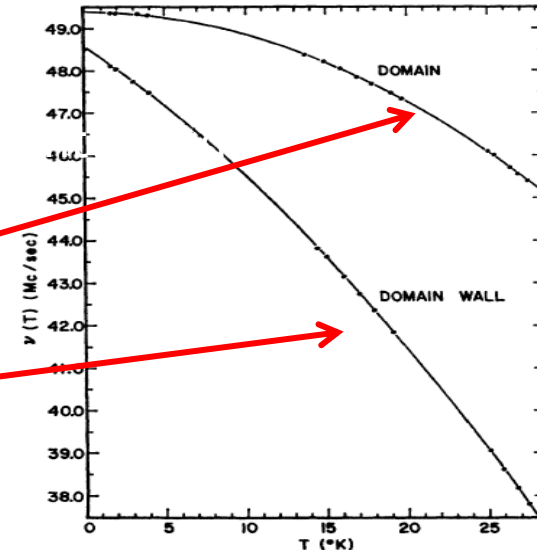


FIG. 1. Plot of the domain and domain-wall  $^{53}\text{Cr}$  NMR in ferromagnetic  $\text{CrI}_3$  as a function of temperature. For the domain resonance only the central ( $\frac{1}{2} \leftrightarrow -\frac{1}{2}$ ) transition frequency is shown. The solid lines are smooth fits to the data.

# NMR in ferromagnetic multilayers

Co-Cu multilayers:  
Co resonance depends  
on local environment

- 12 Co
- 11 Co, 1 Cu, intensity  $\sim c_{\text{Cu}}$
- 10 Co, 2 Cu, intensity  $\sim c_{\text{Cu}}^2$

Work from Panissod  
Co/Cu multilayers (1992)

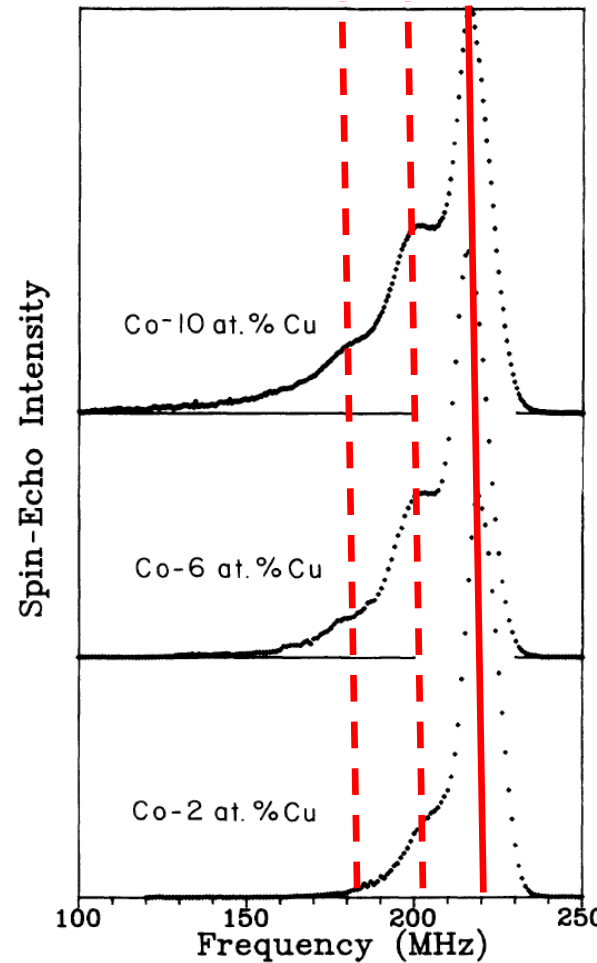


FIG. 1.  $^{59}\text{Co}$  NMR spectra of cobalt-copper alloys with 2, 6, and 10 at. % of copper. The main line is attributed to Co with 12 Co nearest neighbors and each successive satellite to the successive substitution of Cu for Co in the vicinity of Co.

Marginal as compared to the world of thin films

# NMR in ferromagnetic multilayers

## Multilayer cross section

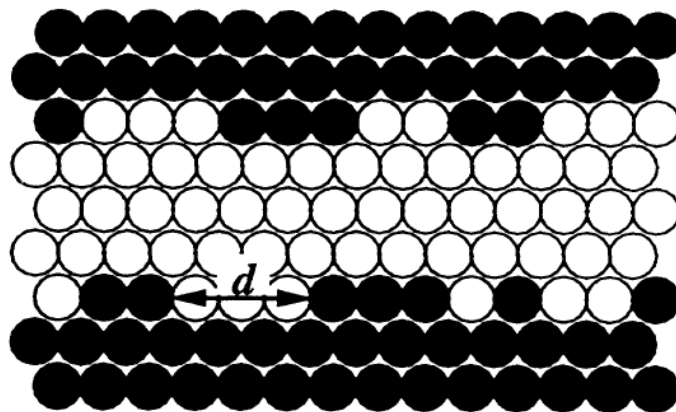


TABLE III. Number of cobalt atoms in the interfaces of the multilayers in units of full Co monolayers per interface (FML).

Sample	Co in the interface (FML)
(15-Å Co)/(15-Å Cu)	1.7
(15-Å Co)/(20-Å Cu)	1.7
(60-Å Co)/(20-Å Cu)	3.0
(60-Å Co)/(60-Å Cu)	3.8
(60-Å Co)/(90-Å Cu)	3.5

Work from Panissod  
Co/Cu multilayers (1992)

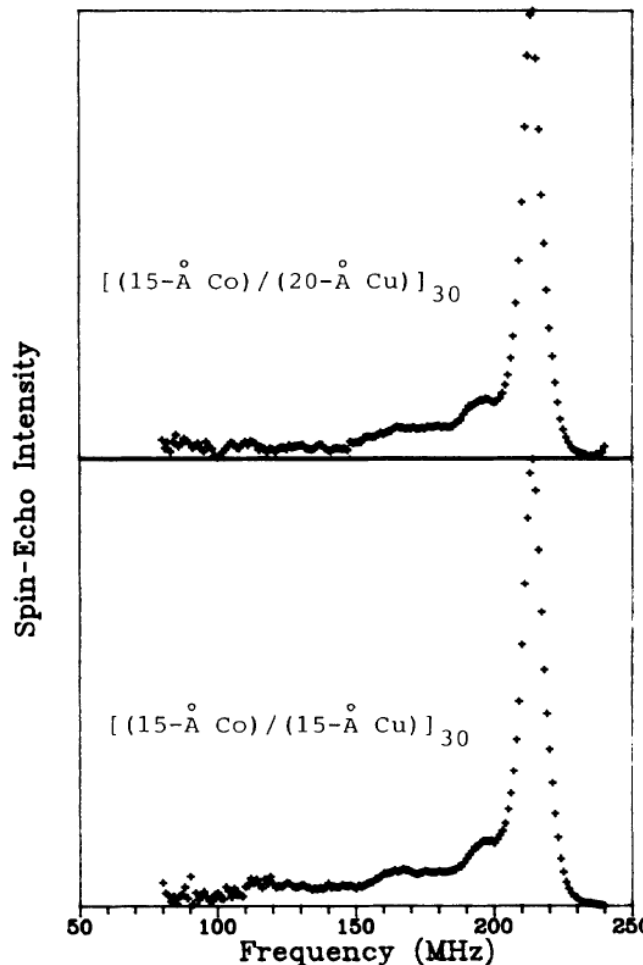
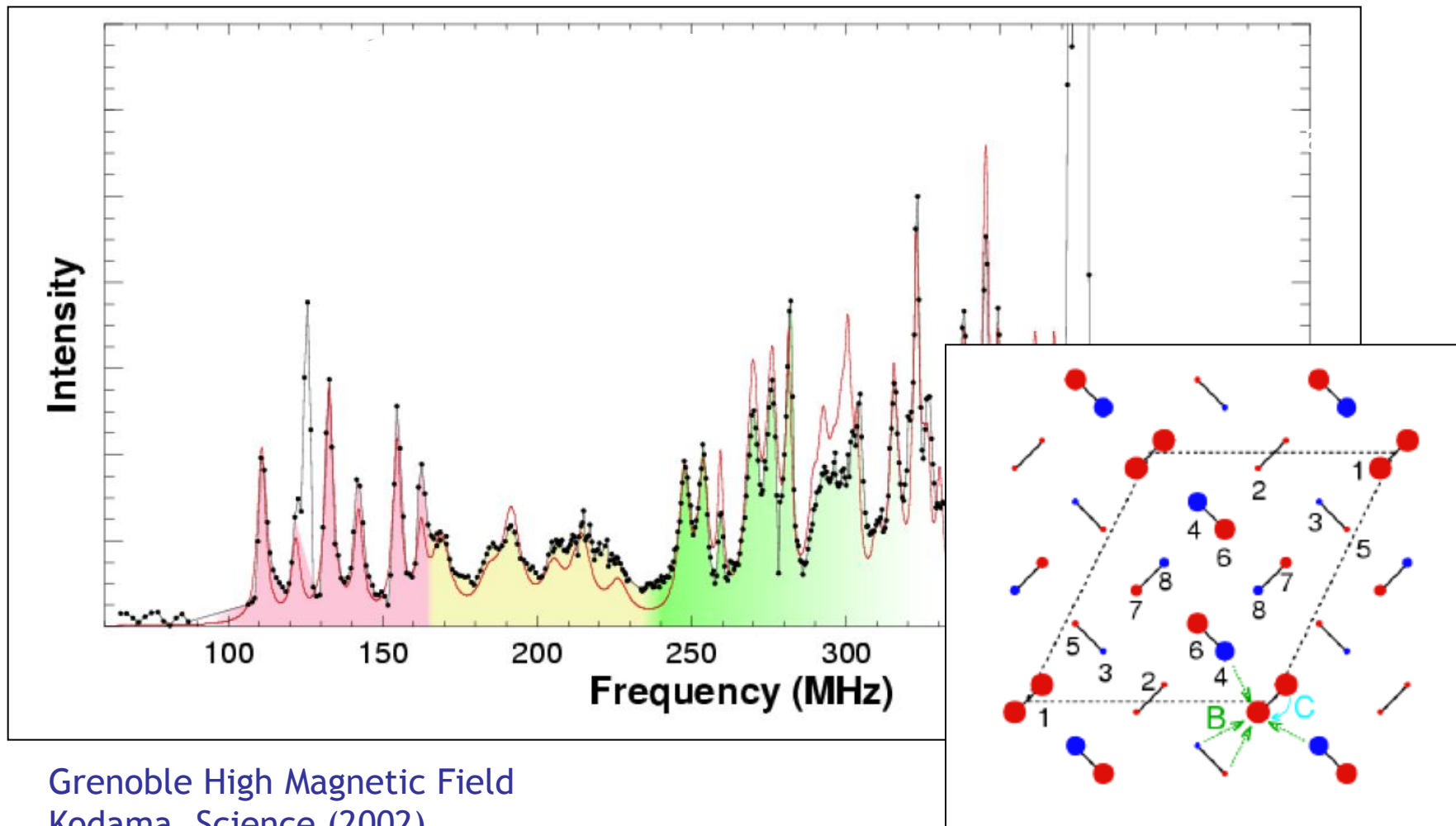


FIG. 3. NMR spectra of the multilayers with 15-Å cobalt thickness. The main line is attributed to fcc Co and the satellites to Co at the interfaces of the multilayers.

Marginal as compared to the world of thin films

# Quantum dimers: model Hamiltonians

## Magnetic Superstructure in the Two-Dimensional Quantum Antiferromagnet $\text{SrCu}_2(\text{BO}_3)_2$



# Summary: observables

## Static

- Orbital susceptibility
- Spatially resolved static susceptibility
- Inhomogeneities, distribution of local fields
- Charge effects
- Ordered phases (charge or magnetic order)

## Techniques

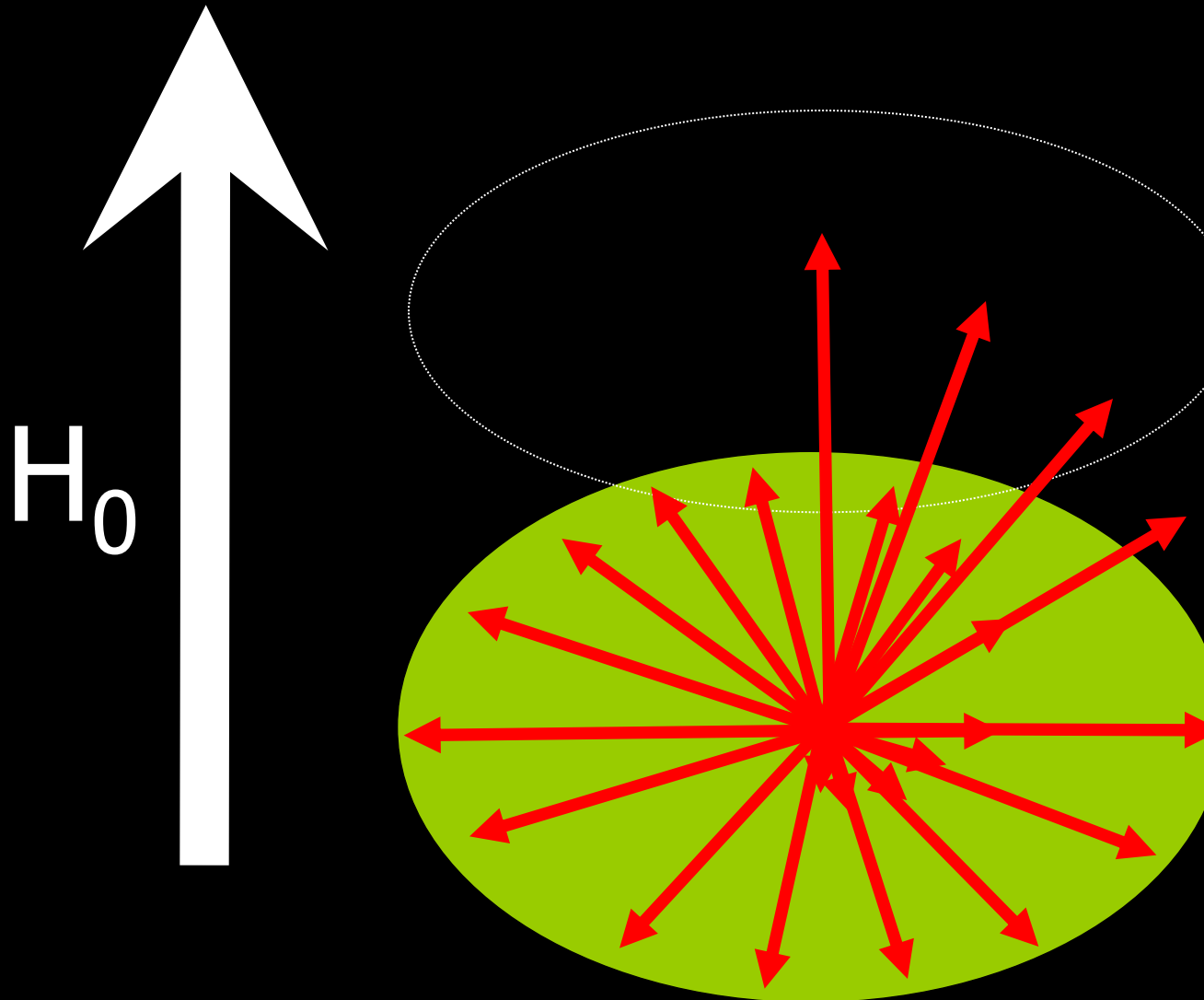
- In applied field: NMR: easy for  $I=1/2$  on powders  
For  $I>1/2$ , quadrupolar effects, much better with single crystals
- Zero applied field: NQR (no probe of  $\chi$ ), ZFNMR  
~ single crystals

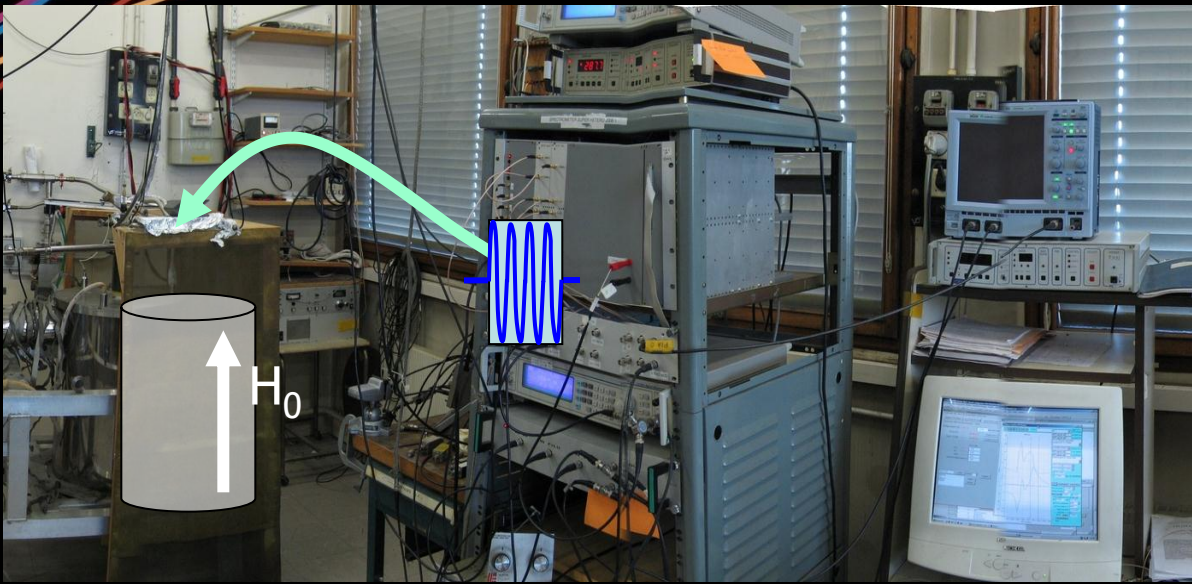
## Dynamics $\langle h_{loc}^+(t) h_{loc}^-(0) \rangle$

- Magnetic correlations  $\xi(T)$
- Excitations (gapped or not gapped)  $\Delta$
- Critical regime

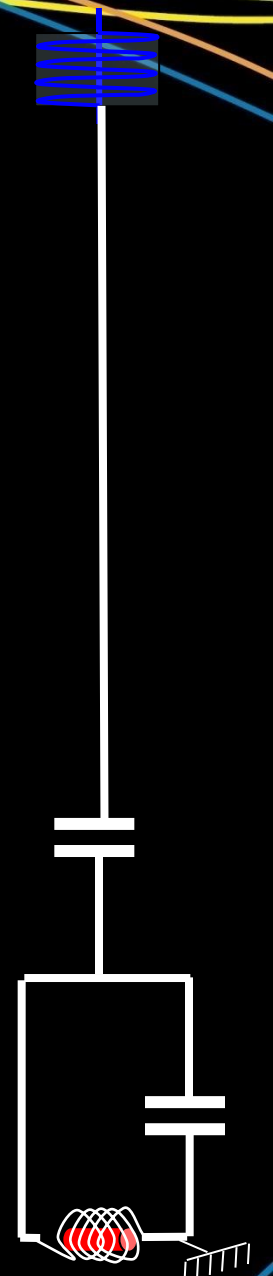
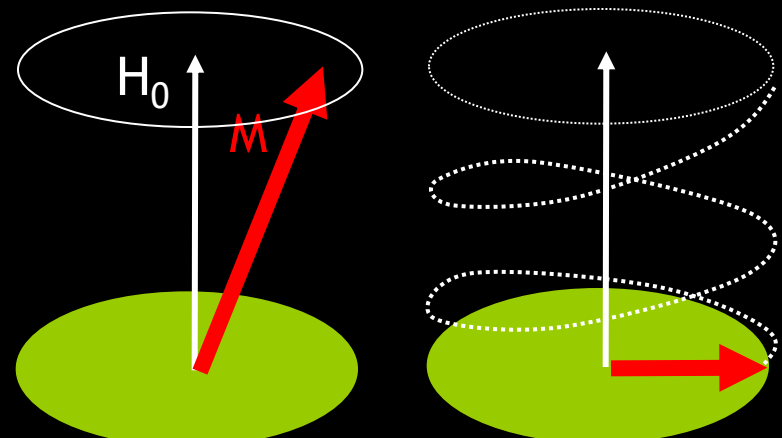
Compare timescales of the probes vs coupling constant

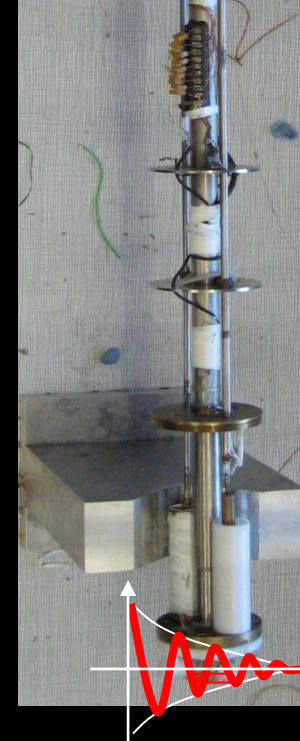
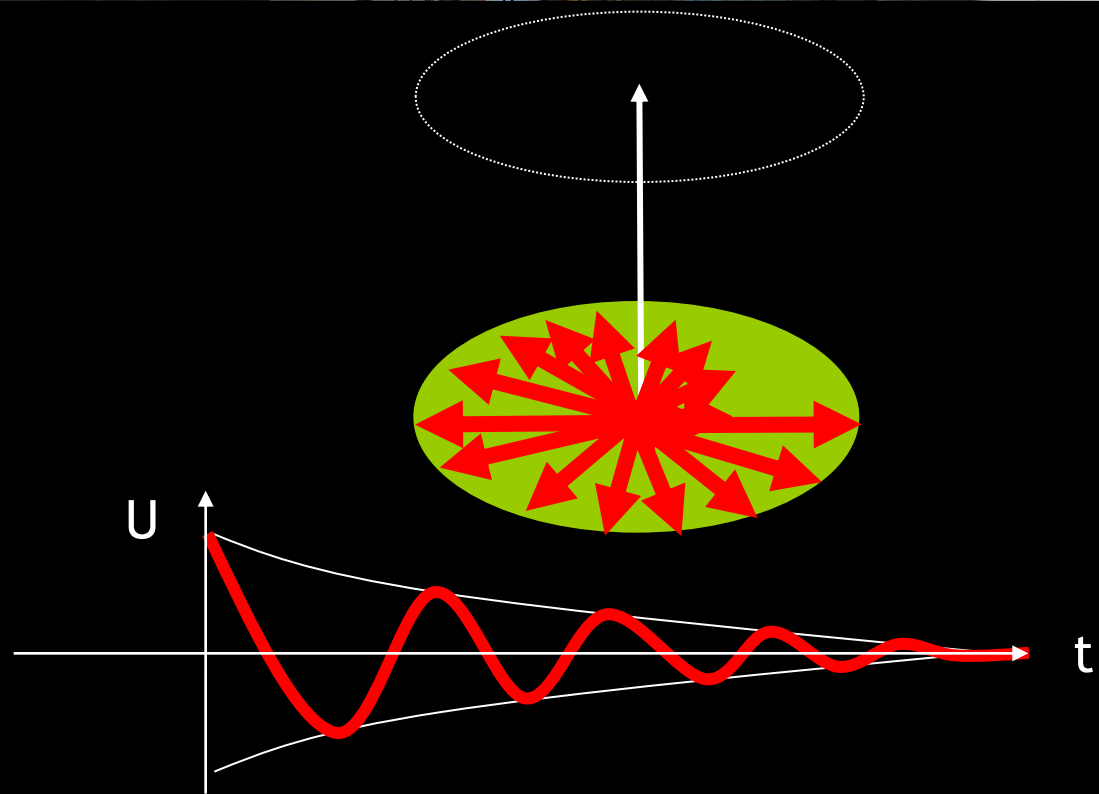
# What about an experiment?

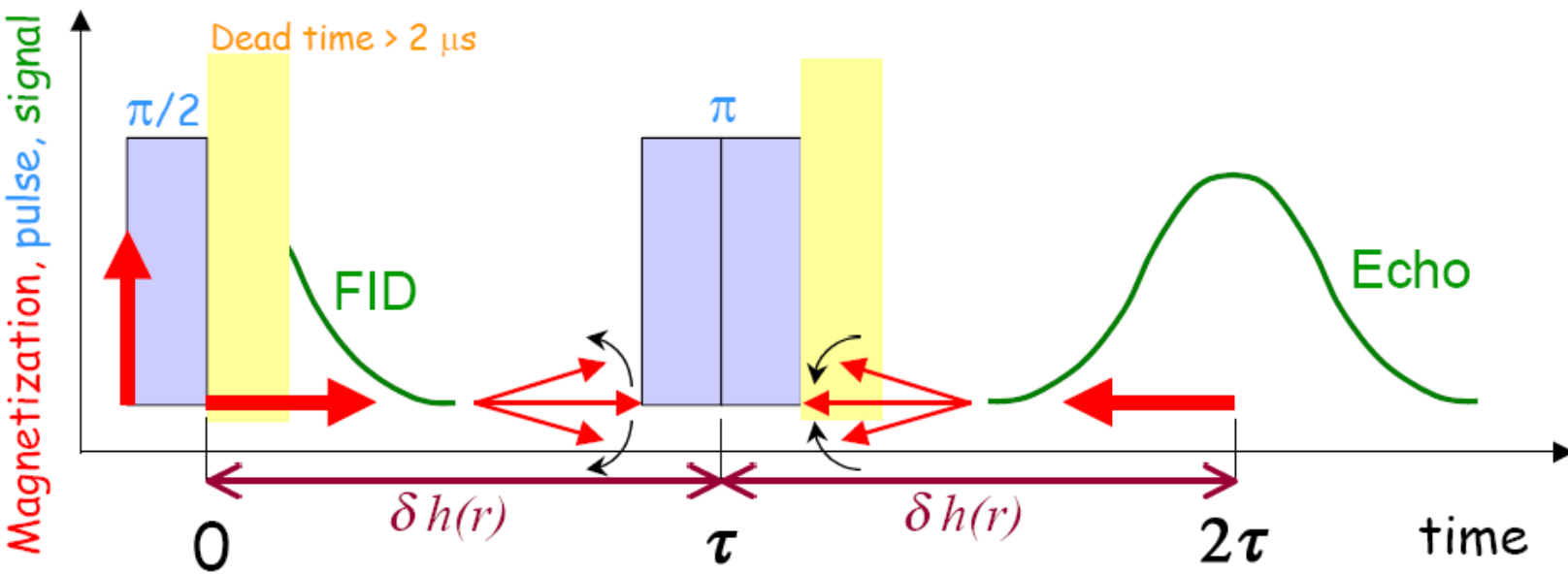
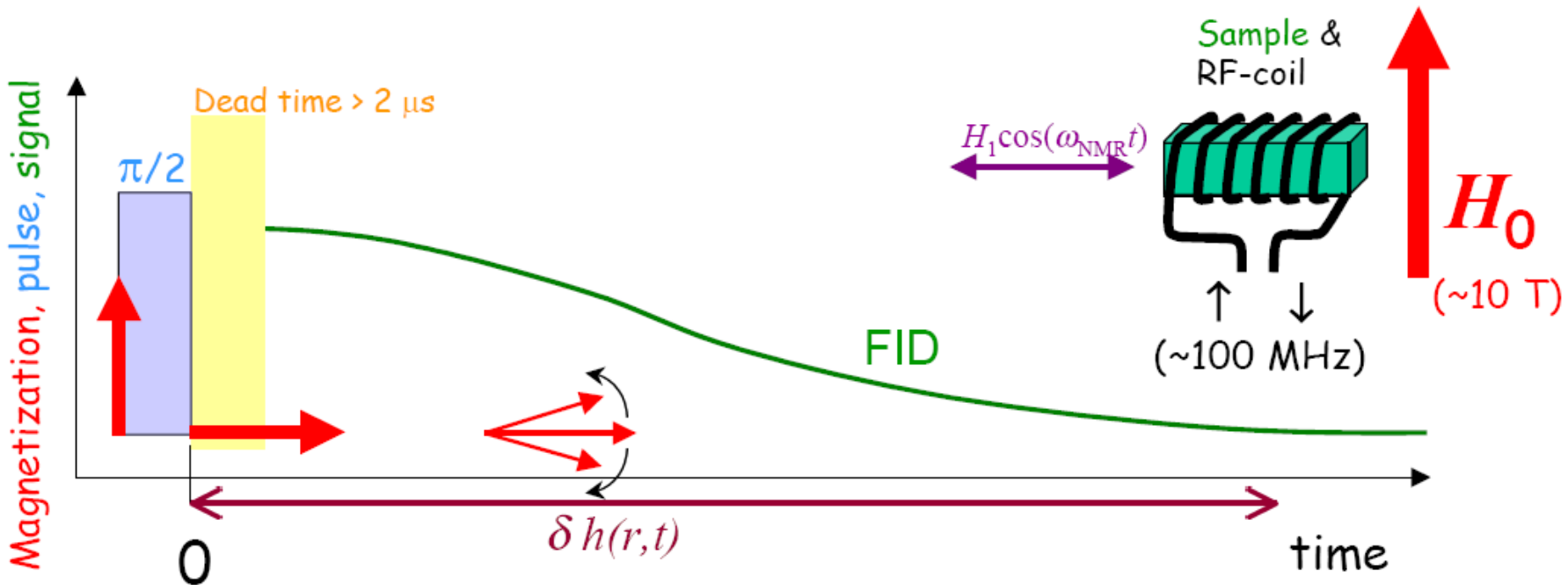




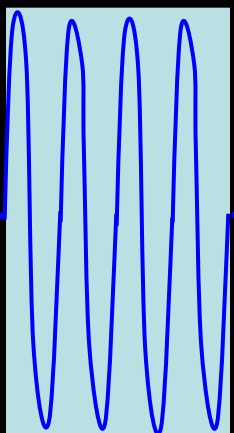
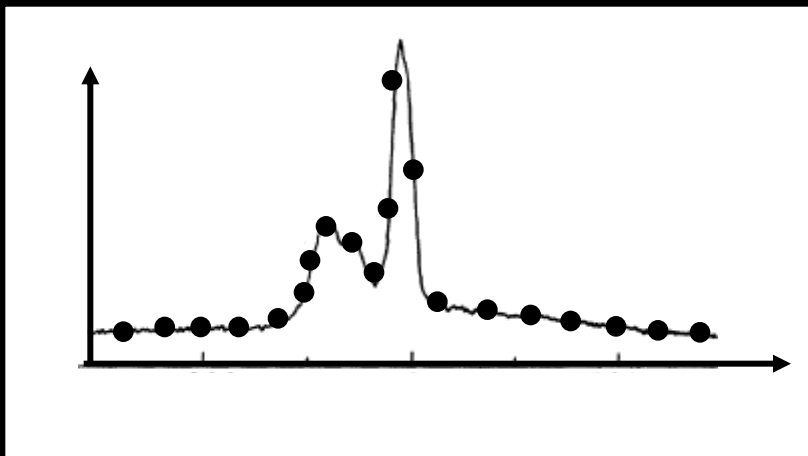
Radiofrequency pulse ~ few  $\mu\text{sec}$



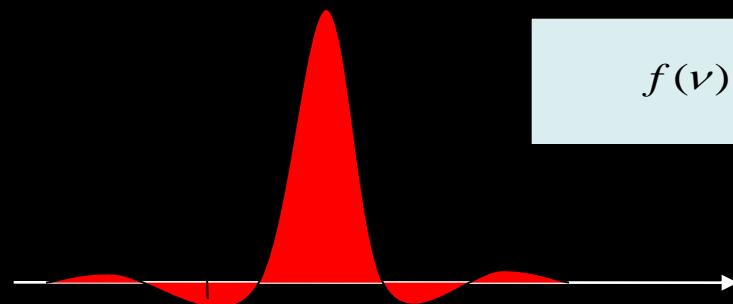




# Why pulsed NMR?



$\Delta t$



$$f(\nu) = f_0 \frac{\sin(\pi\Delta t(\nu - \nu_0))}{\pi\Delta t(\nu - \nu_0)}$$

A pulse has a spectral width in Fourier space.  
Fourier transform yields the response of the sample in the frequency domain of the pulse.

# Experimental set-ups

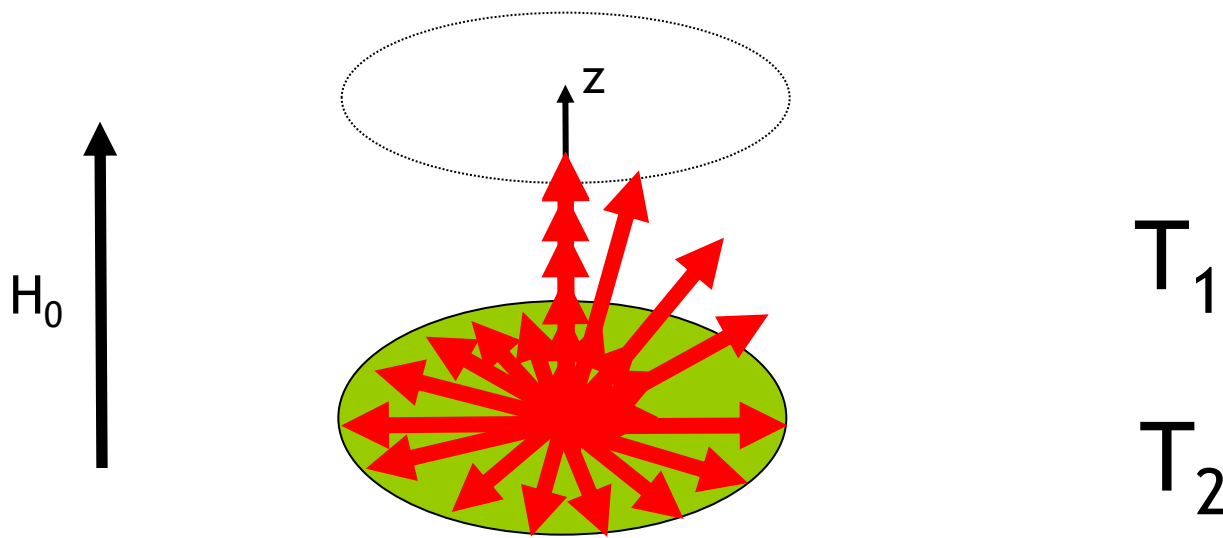
Field range: 1T - 45 T

T-range: 10 mK - 1000 K

Sensitivity: 1 mMole... depends on sensitivity

Misc: pressure (few GPa), in-situ rotation

# Dynamics as probed by NMR: relaxation times



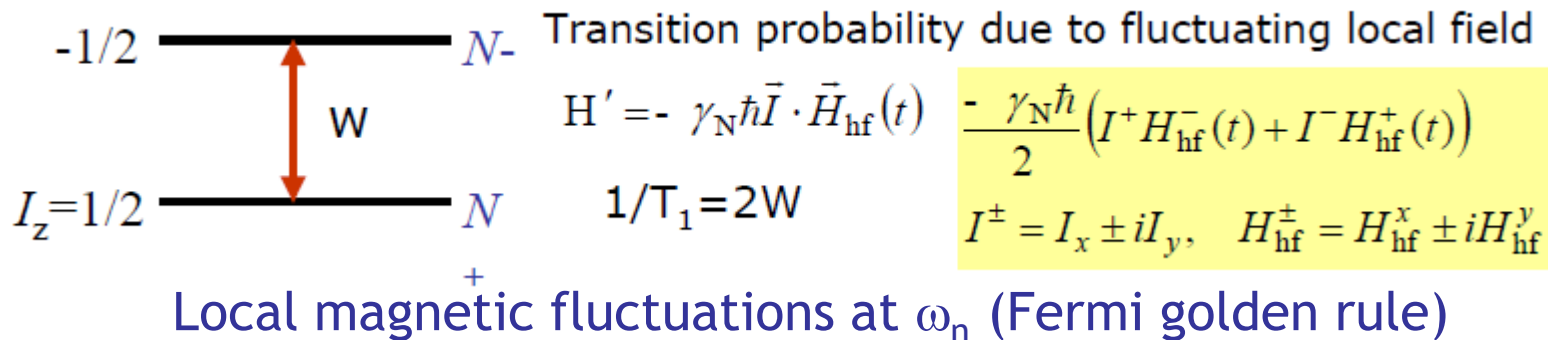
transverse relaxation :  $T_2$   
Energy is conserved

$$\frac{dM_{X,Y}}{dt} = \frac{-M_{X,Y}}{T_2} + \gamma(\vec{M} \times \vec{H})_{X,Y}$$

Longitudinal relaxation :  $T_1$   
Energy exchange  
with the lattice

$$\frac{dM_Z}{dt} = \frac{M_{equilibrium} - M_Z}{T_1} + \gamma(\vec{M} \times \vec{H})_Z$$

# Relaxation time $T_1$



$$\frac{1}{T_1} \sim \int_{-\infty}^{\infty} \langle B_L^+(t) B_L^-(0) \rangle \exp(-i\omega_n t) dt$$

$$B(t) = \sum_{\text{coupled nuclei } r_i} \vec{A}_{\text{hf}}(r_i) \vec{I} \cdot \vec{S}(r_i, t)$$

Fourier transform       $\frac{1}{T_1} \sim \int_{-\infty}^{\infty} \sum_q |A_{\text{hf}}(q)|^2 \langle s^+(q, t) s^-(q, 0) \rangle \exp(-i\omega_n t) dt$

Fluctuation - Dissipation       $\frac{1}{2\hbar} (1 - \exp \frac{-\hbar\omega_n}{k_B T}) \int_{-\infty}^{\infty} \langle S^+(q, t) S^-(-q, 0) \rangle \exp(-i\omega_n t) dt = \chi''(q, \omega_n)$

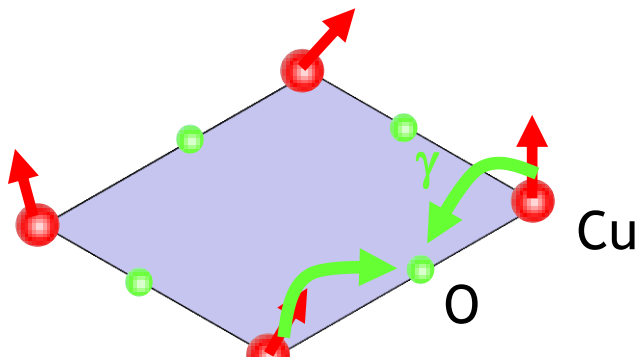
$\hbar\omega_n \ll k_B T \Rightarrow \frac{1}{T_1} = \frac{1}{\hbar^2} \frac{k_B T}{(g\mu_B)^2} \sum_q |A(q)|^2 \frac{\chi''(q, \omega_n)}{\omega_n}$

$\omega_n$  is small  $\approx 0$  as compared to neutrons, integrate over  $q$

# Relaxation time $T_1$ : electronic spins

$$\frac{1}{T_1} = \frac{1}{\hbar^2} \frac{k_B T}{(g\mu_B)^2} \sum_q |A(q)|^2 \frac{\chi''(q, \omega_n)}{\omega_n} \quad A(\vec{q}) = \sum_{r_i} A(\vec{r}_i) e(-i\vec{q} \cdot \vec{r}_i)$$

$A(q)$  form factor and favours some  $q$ .

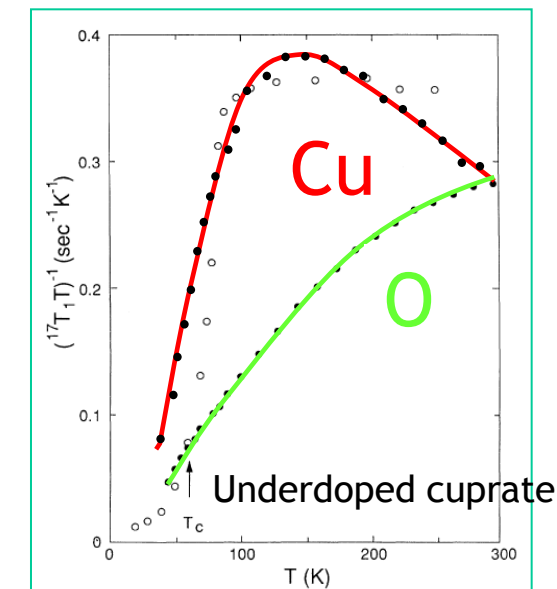
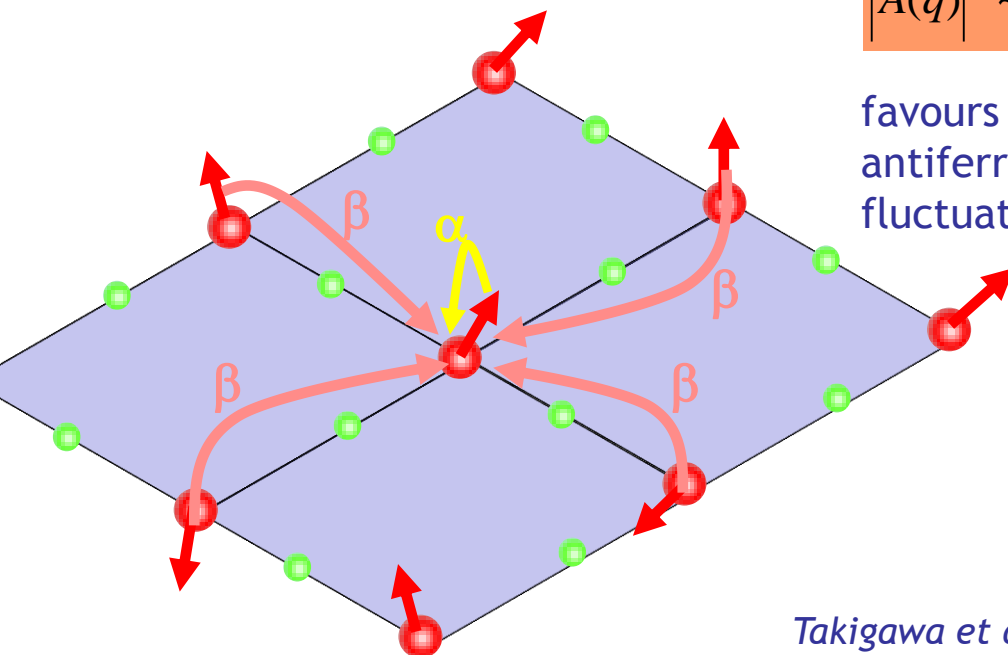


$$|A(\vec{q})|^2 \sim 2\gamma \left[ 1 + \frac{1}{2} (\cos(q_x a) + \cos(q_y b)) \right]$$

favours  $q=0$ , ferromagnetic fluctuations between Cu

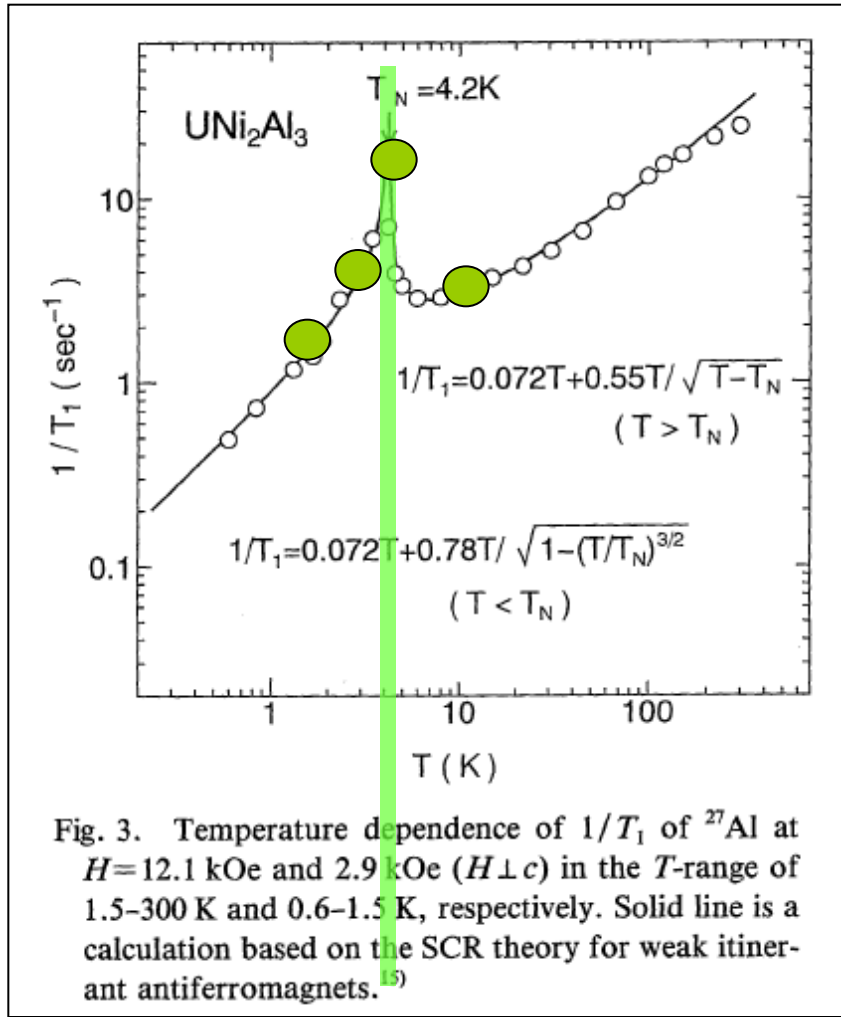
$$|A(\vec{q})|^2 \sim [\alpha + 2\beta (\cos(q_x a) + \cos(q_y b))]^2$$

favours  $q=\pi, \pi$ , antiferromagnetic fluctuations

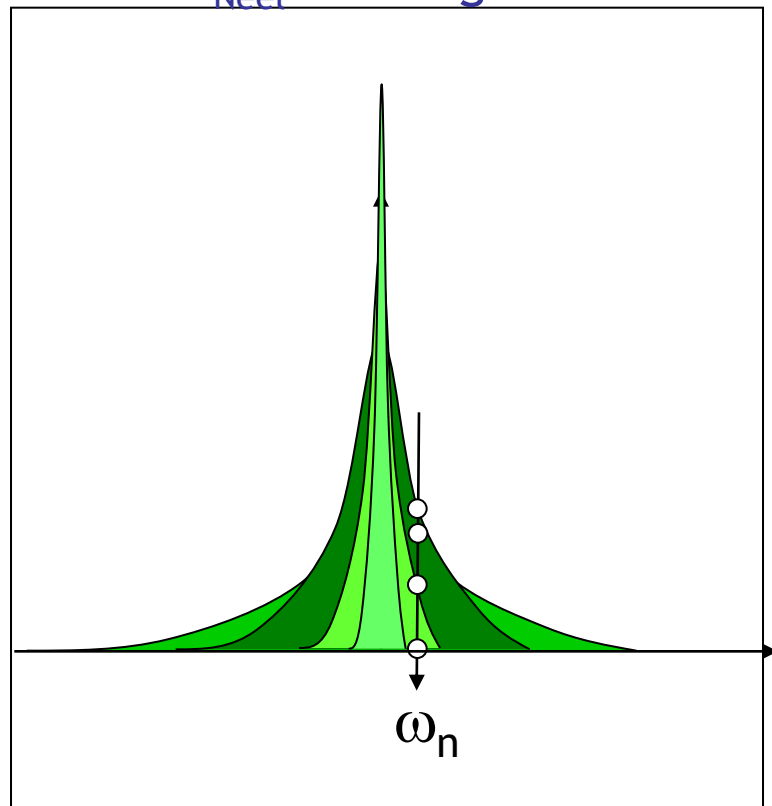


# Magnetic transition: divergence of $T_1$

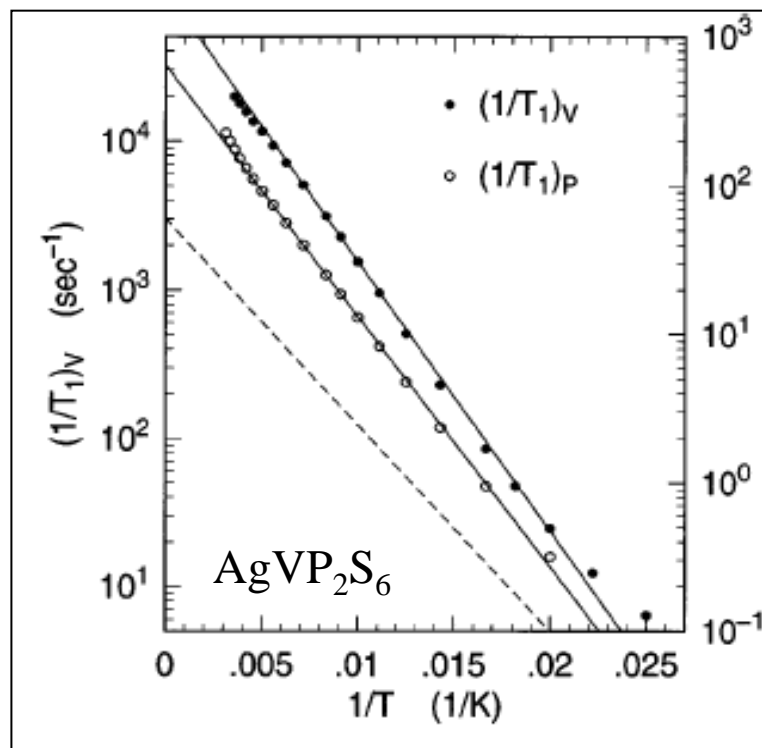
Slowing down of fluctuations  
In a weak metallic antiferromagnet



- Above  $T_{\text{Neel}}$  :  $T_1 T \text{K} = \text{cst}$
- At  $T_{\text{Neel}}$  : divergence of  $1/T_1$



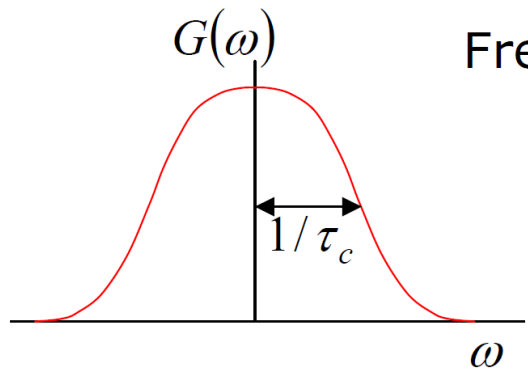
# $T_1$ : Gapped magnetic insulator - Haldane chain ( $S = 1$ )



Shimizu et al., PRB (1995)

$$\frac{1}{T_1} \sim e^{-\frac{\Delta}{T}} \xrightarrow{\text{Haldane gap}}$$

# T<sub>1</sub>: High-T regime for an insulator $\oplus$ exchange (J)



Frequency spectrum of local field fluctuations

$$G(\omega) = \frac{1}{2} \int_{-\infty}^{\infty} \langle \{H_{\text{hf}}^-, H_{\text{hf}}^+(t)\} \rangle \exp\left(\frac{i\omega t}{\hbar}\right) dt$$

$$\int_{-\infty}^{\infty} G(\omega) d\omega = 2\pi \langle H_{\text{hf}}^2 \rangle \approx \frac{2G(0)}{\tau_c}$$

$\tau_c$  : correlation time

If  $\frac{1}{\tau_c} \gg \omega_n$  and  $\gamma_N H_{\text{hf}}$ ,

$$\frac{1}{T_1} = \gamma_N^2 G(\omega_N) \approx \gamma_N^2 G(0) \approx \pi \gamma_N^2 \langle H_{\text{hf}}^2 \rangle \tau_c$$

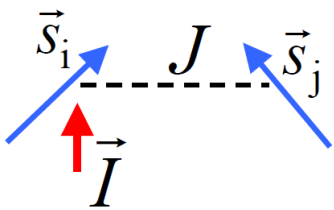
$$= |\gamma_N H_{\text{hf}}| \cdot \frac{|\gamma_N H_{\text{hf}}|}{1/\tau_c}$$

$|\gamma_N H_{\text{hf}}|$ : instantaneous Larmor frequency

motional narrowing

# $T_1$ : High-T regime for an insulator $\oplus$ exchange ( $J$ )

$$\frac{1}{T_1} = \gamma_N^2 G(\omega_N) \approx \gamma_N^2 G(0) \approx \pi \gamma_N^2 \langle H_{\text{hf}}^2 \rangle \tau_c$$



$$\langle H_{\text{hf}} \rangle \approx \frac{A}{\gamma_N \hbar} S$$

$$\frac{1}{\tau_c} \approx \sqrt{z} \frac{JS}{\hbar} \quad \text{exchange frequency}$$

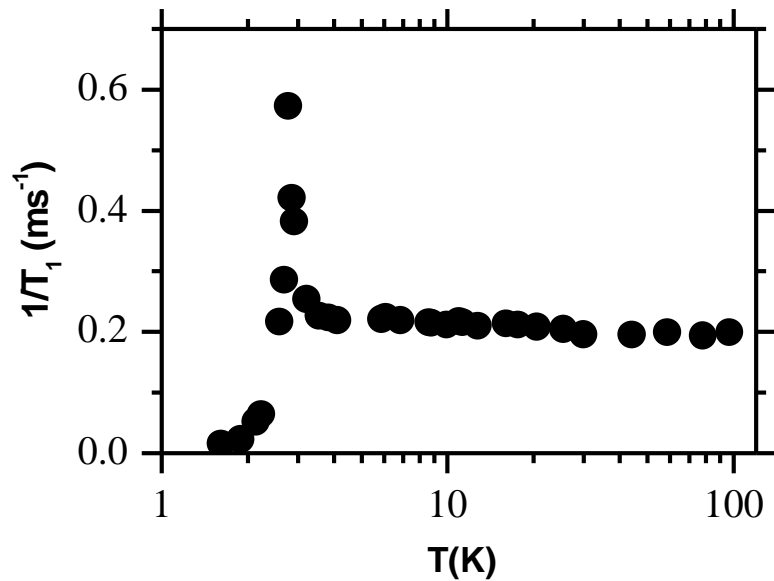
$$\frac{1}{T_1} \approx \frac{A^2 S}{\hbar \sqrt{z} J}$$

( $z$  : number of nearest neighbor

More accurate expression  
(Moriya 1956)

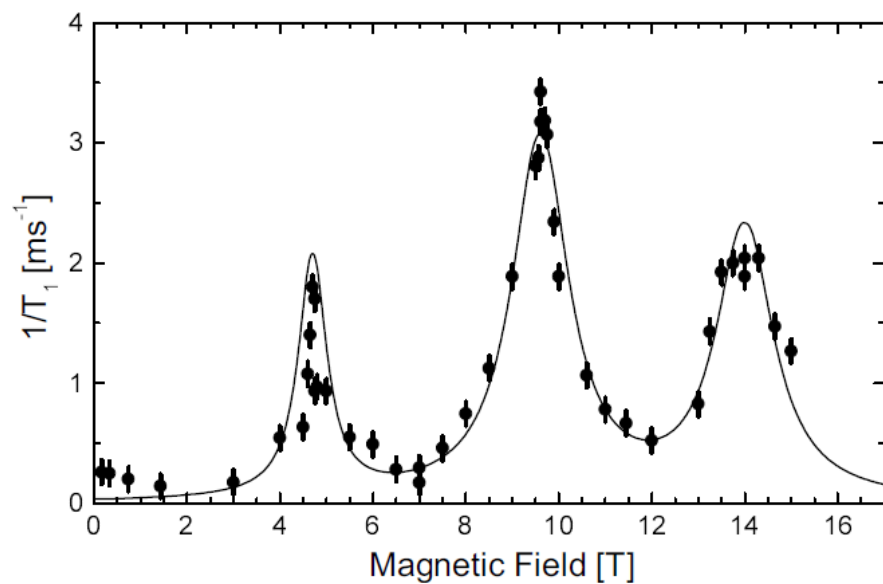
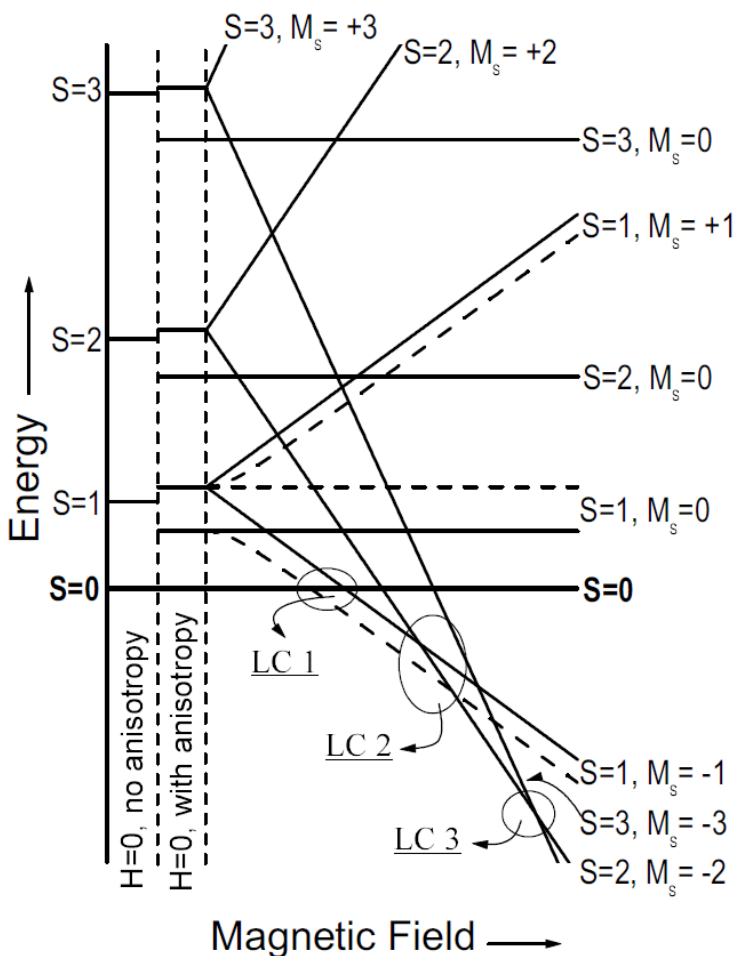
$$\frac{1}{T_1} = \sqrt{\frac{\pi}{3}} \frac{A^2 \sqrt{S(S+1)}}{\hbar J \sqrt{z}}$$

# $T_1$ : High-T regime for an insulator $\oplus$ exchange ( $J$ )



*Frustrated 2D HAF  $S=1/2$*

# Single molecule magnets



cross-relaxation effect between the nuclear Zeeman reservoir and the reservoir of the Zeeman levels of the molecule. This effect provides a powerful tool to investigate quantum dynamical phenomena

# Mössbauer spectroscopy

(Or nuclear  $\gamma$ -ray spectroscopy)

1958: Discovery and interpretation  
by Rudolf Mössbauer

1961: Nobel Prize



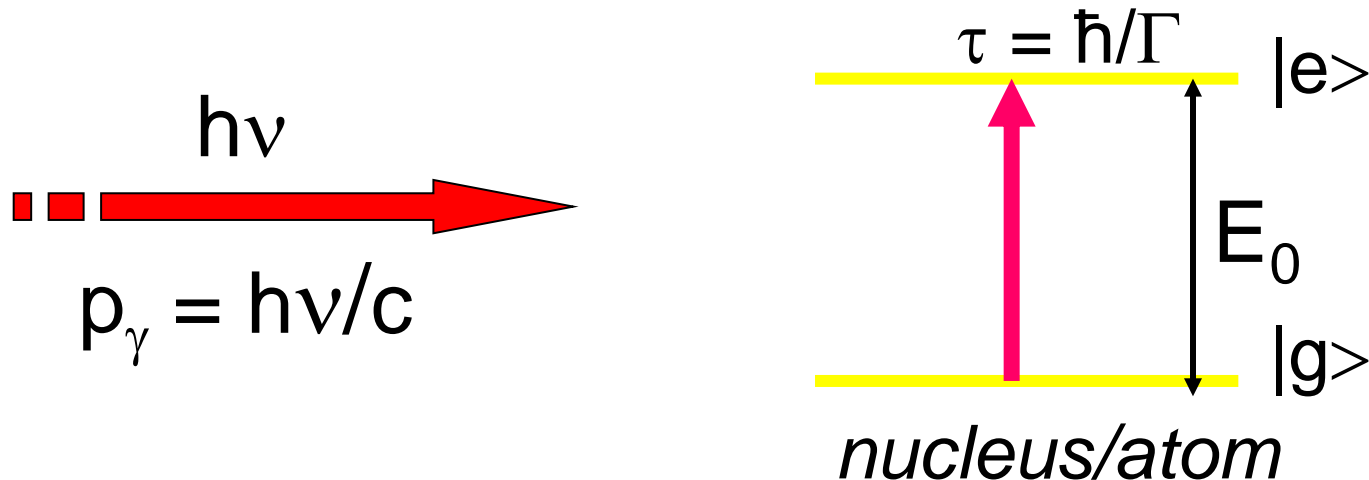
Born 1929

- Transition between nuclear levels
- Emitter (source)  $\oplus$  Absorber
  - transmission geometry for bulk samples
  - Surface studies: Conversion Electron Spectroscopy

Thanks to P. Bonville, CEA Saclay

# Is nuclear $\gamma$ -ray spectroscopy possible ?

Conservation of energy and momentum



$$h\nu = E_0 + P^2/2M_n$$

$$h\nu/c = P$$

$$\text{Recoil energy } E_R = P^2/2M_n \approx \frac{1}{2} \frac{E_0^2}{M_n c^2}$$

$$M_n c^2 \sim 100 \text{ GeV} ; E_0 \sim 100 \text{ keV} ; E_R \sim 1 \text{ meV}$$

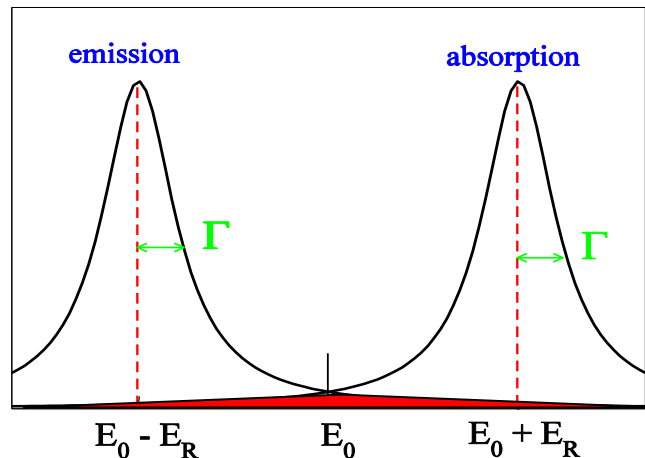
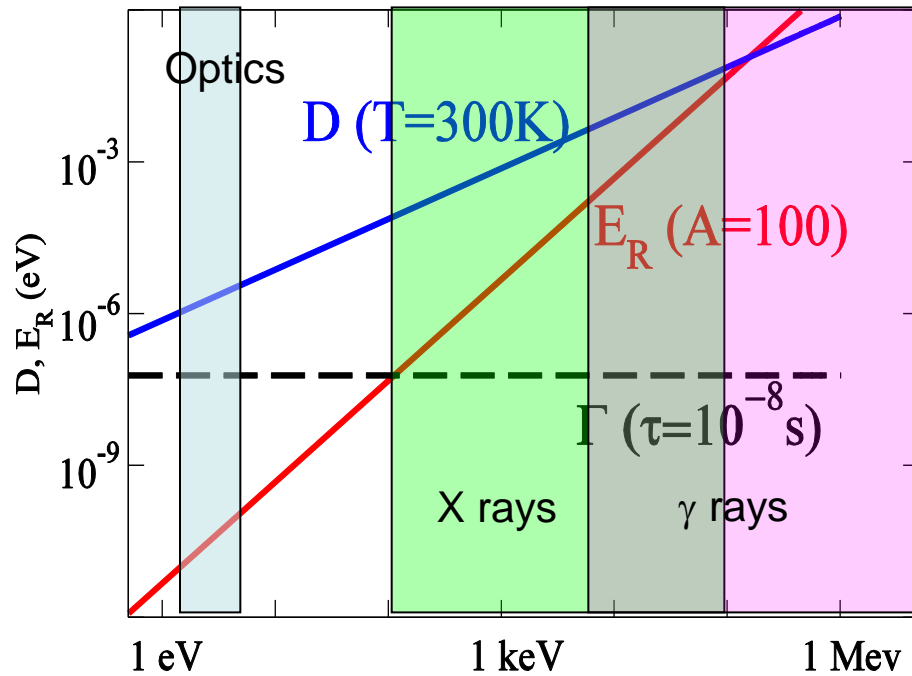
Care about recoil energy

# Is nuclear $\gamma$ -ray spectroscopy possible ?

Energy conservation:

- emission:  $h\nu = E_0 - E_R$
- absorption:  $h\nu = E_0 + E_R$

if  $\Gamma \ll E_R$ , no overlap



At temperature T:  
moving emitter/abs  
⇒ Doppler broadening  
 $D \approx 2 \sqrt{k_B T} E_R$

for  $\gamma$  rays:  $\Gamma \ll E_R$

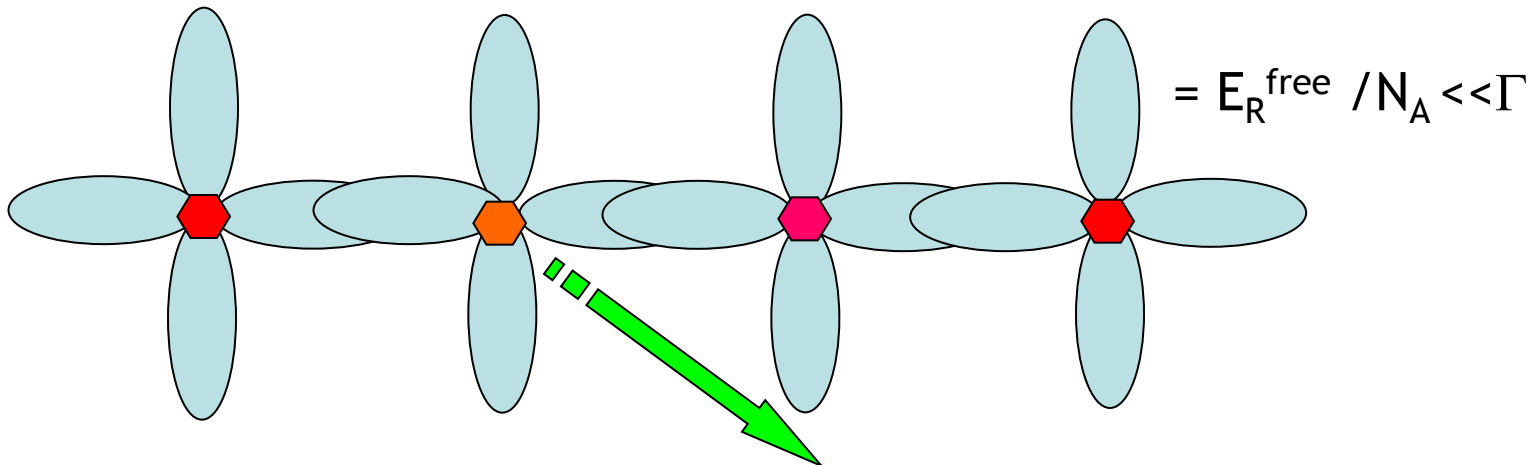
Impossible in free atoms / nuclei ≠ Atomic spectroscopy

# Is nuclear $\gamma$ -ray spectroscopy possible ?

For  $\gamma$  rays,  $\Gamma \ll E_R$  and  $D \sim E_R \Rightarrow$  weak overlap

On cooling, not on heating ( $D \uparrow$  as  $T \uparrow$ ), R.M. observes an increase of the resonant absorption in  $^{191}\text{Ir}$  ...

Interpretation: nucleus bound in a solid  $\Rightarrow E_R \approx \frac{1}{2} \frac{E_0^2}{M_{solid} c^2}$



photon emitted without recoil of the nucleus  
(for rigid atomic bonds)

# In practice

Lamb-Mössbauer factor:  $f(T) = |J_0(kx_0)|^2 \approx 1 - \frac{1}{2} k^2 x_0^2$

$$f(T) \approx 1 - k^2 \langle x^2 \rangle_T \approx \exp\left(-\frac{E_0^2 \langle x^2 \rangle_T}{\hbar^2 c^2}\right)$$

⇒ finite probability  $f(T)$  of nuclear resonant absorption  
of a photon with no phonons absorbed or emitted allows  
Mössbauer spectroscopy of hyperfine (electro-nuclear)  
interactions ( $\sim 10^{-6}$  eV) if  $\Gamma \ll \omega_{hf}$

*radioactive source*

continuous Doppler energy sweep

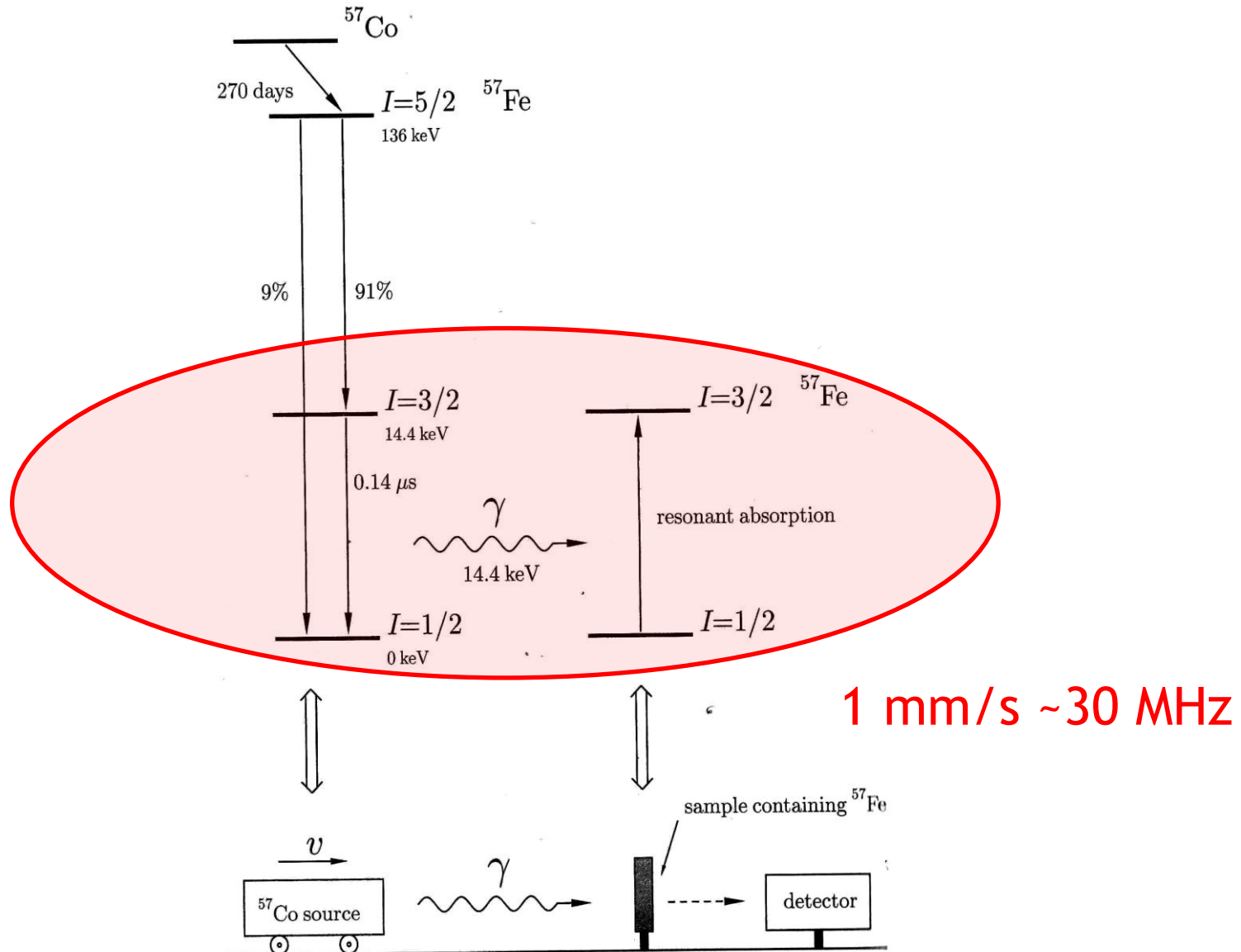
$$\omega = \omega_0 (1 + v/c)$$

$$\omega_0 v_{max}/c > \omega_{hf}$$

⇒ *abs./em. energy spectrum*

Recoilless is for source and absorber!

# In practice



Vary the speed of the source ~ sweep the frequency (Doppler)

# In practice

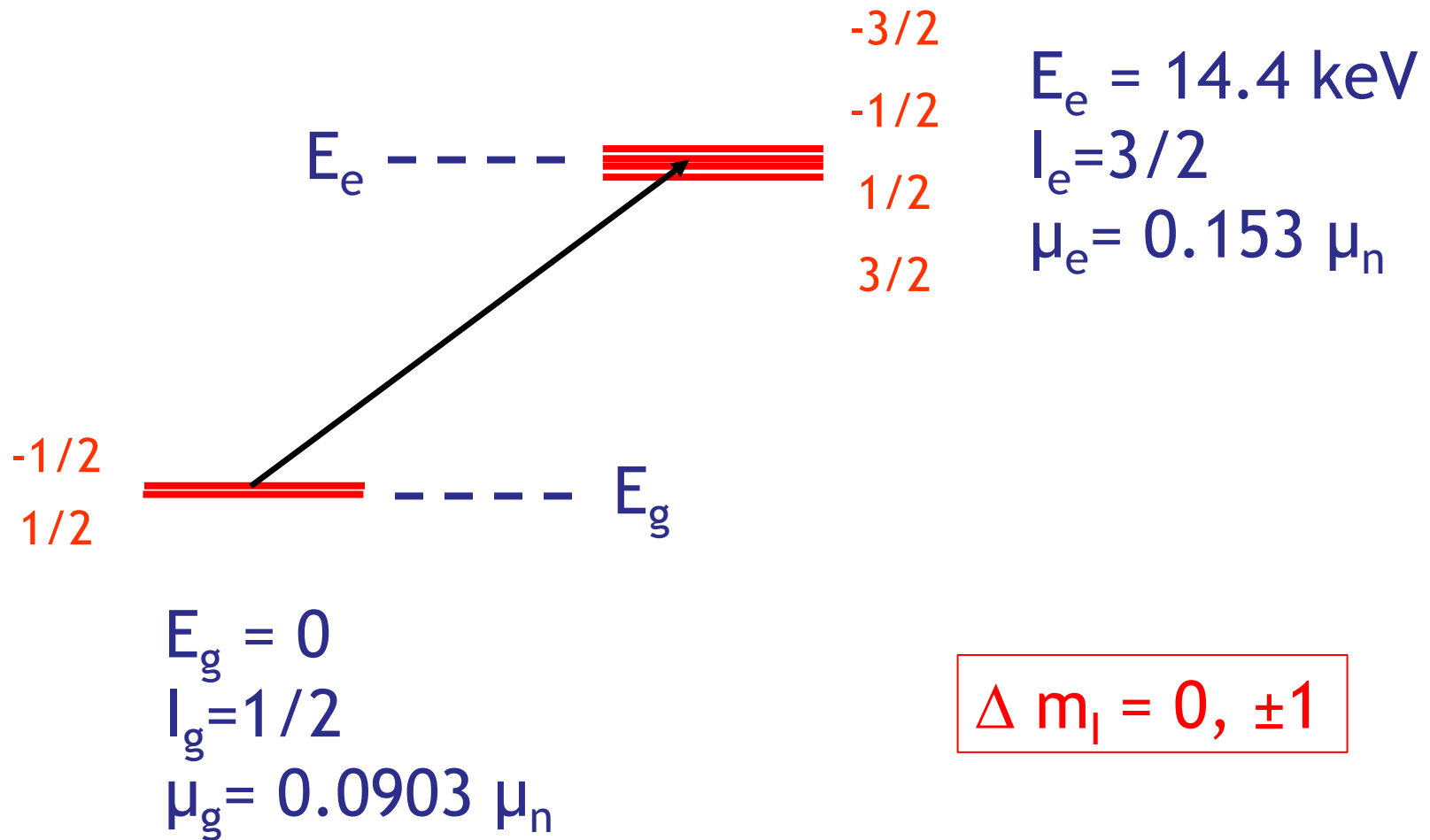
## Mössbauer Active Elements

IA		VIIIA																	
H	Be											He							
Li	Mg	IIIB		IVB	VB	VIB	VIIB	VIIIB			IB	IIB	III A	IV A	V A	VIA	VIIA		
K	Ca	Sc	Ti	V	Cr	Mn	Fe	Co	Ni	Cu	Zn	Ga	Ge	As	Se	Br	Kr		
Rb	Sr	Y	Zr	Nb	Mo	Tc	Ru	Rh	Pd	Ag	Cd	In	Sn	Sb	Te	I	Xe		
Cs	Ba	La	Hf	Ta	W	Re	Os	Ir	Pt	Au	Hg	Tl	Pb	Bi	Po	At	Rn		
Fr	Ra	Ac																	
			Ce	Pr	Nd	Pm	Sm	Eu	Gd	Tb	Dy	Ho	Er	Tm	Yb	Lu			
			Th	Pa	U	Np	Pu	Am	Cm	Bk	Cf	Es	Fm	Md	No	Lw			

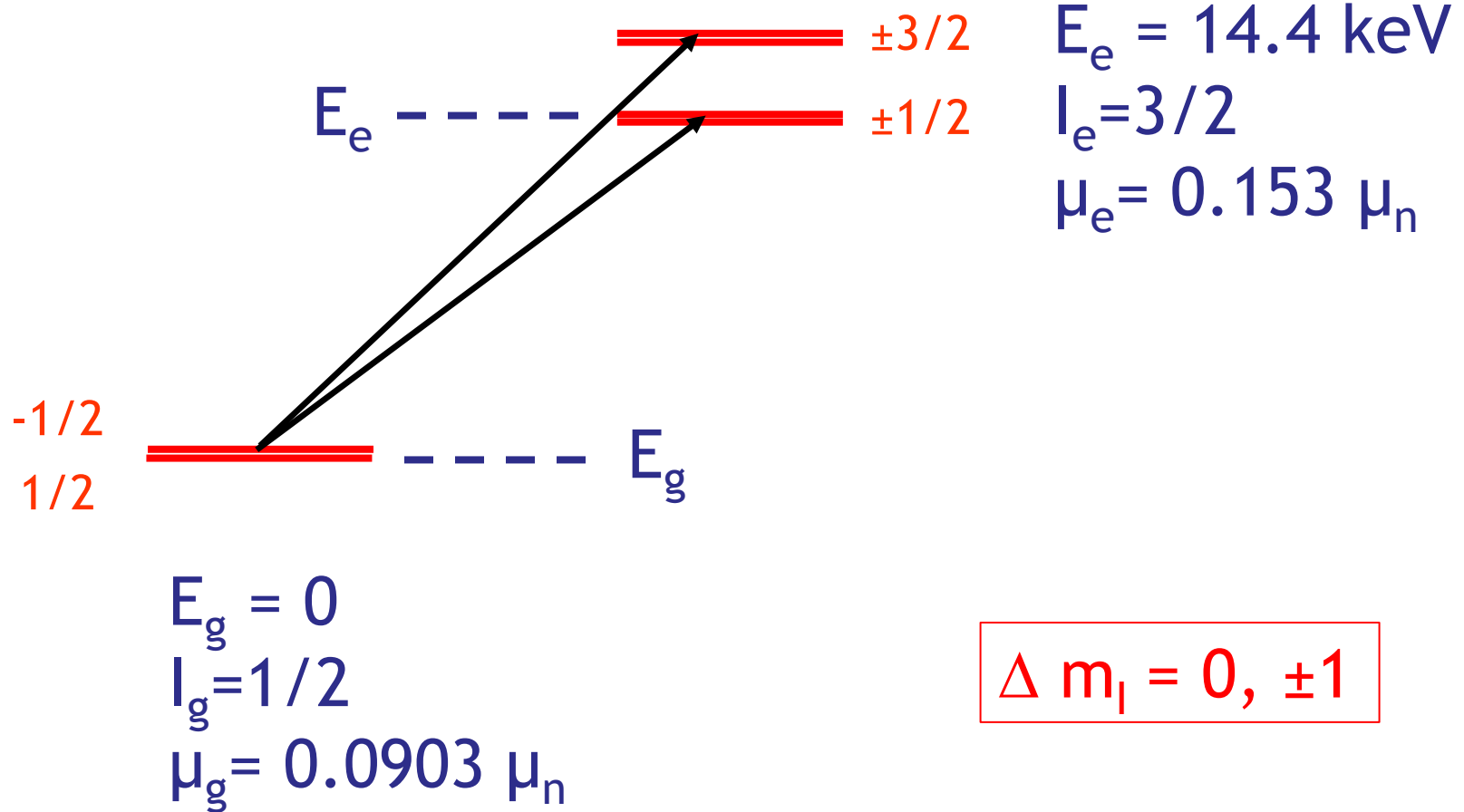
46 elements, 89 isotopes, 104 Mössbauer transitions

~10 used in condensed matter!

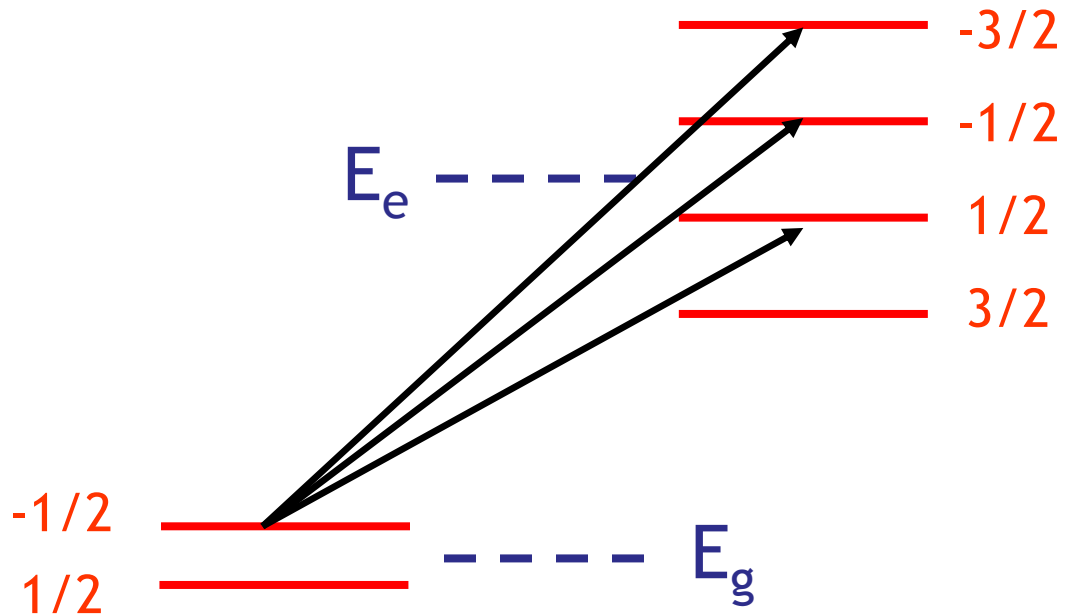
# In practice: $^{57}\text{Fe}$ , no EFG, no field



# In practice: $^{57}\text{Fe}$ , EFG, no field



# In practice: $^{57}\text{Fe} \oplus$ field (no EFG)

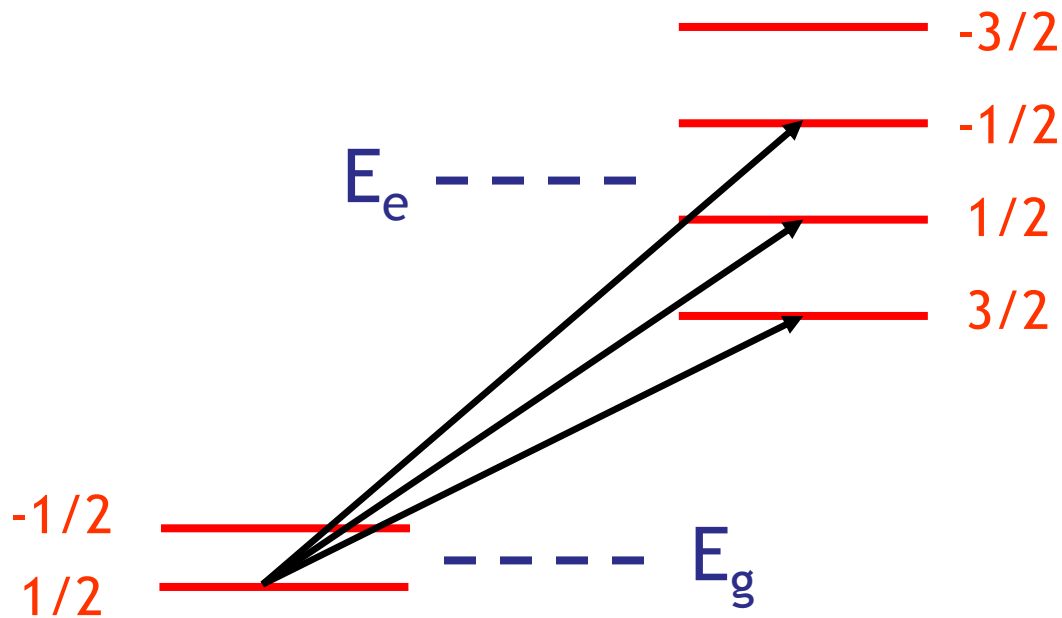


$$\begin{aligned}E_e &= 14.4 \text{ keV} \\I_e &= 3/2 \\ \mu_e &= 0.153 \mu_n\end{aligned}$$

$$\begin{aligned}E_g &= 0 \\I_g &= 1/2 \\ \mu_g &= 0.0903 \mu_n\end{aligned}$$

$$\Delta m_I = 0, \pm 1$$

# In practice: $^{57}\text{Fe} \oplus$ field (no EFG)



$$E_g = 0$$

$$I_g = 1/2$$

$$\mu_g = 0.0903 \mu_n$$

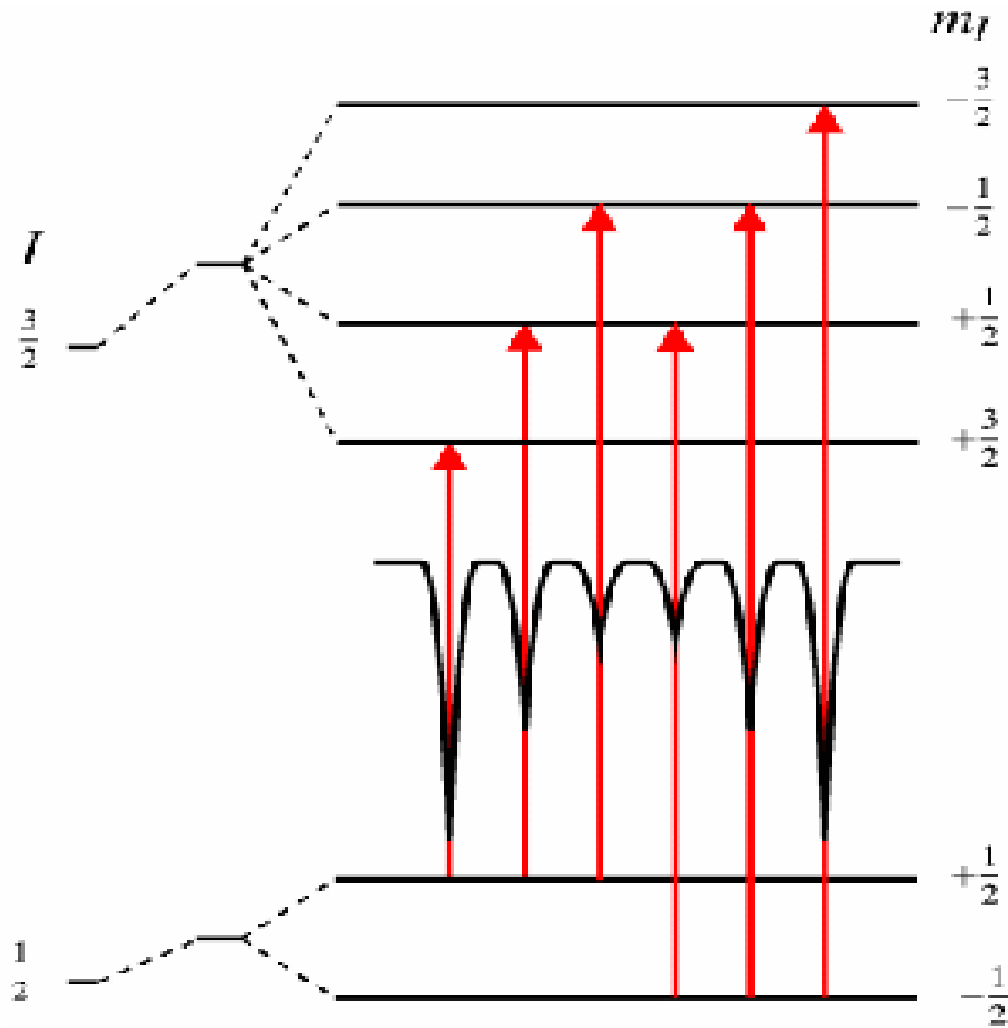
$$E_e = 14.4 \text{ keV}$$

$$I_e = 3/2$$

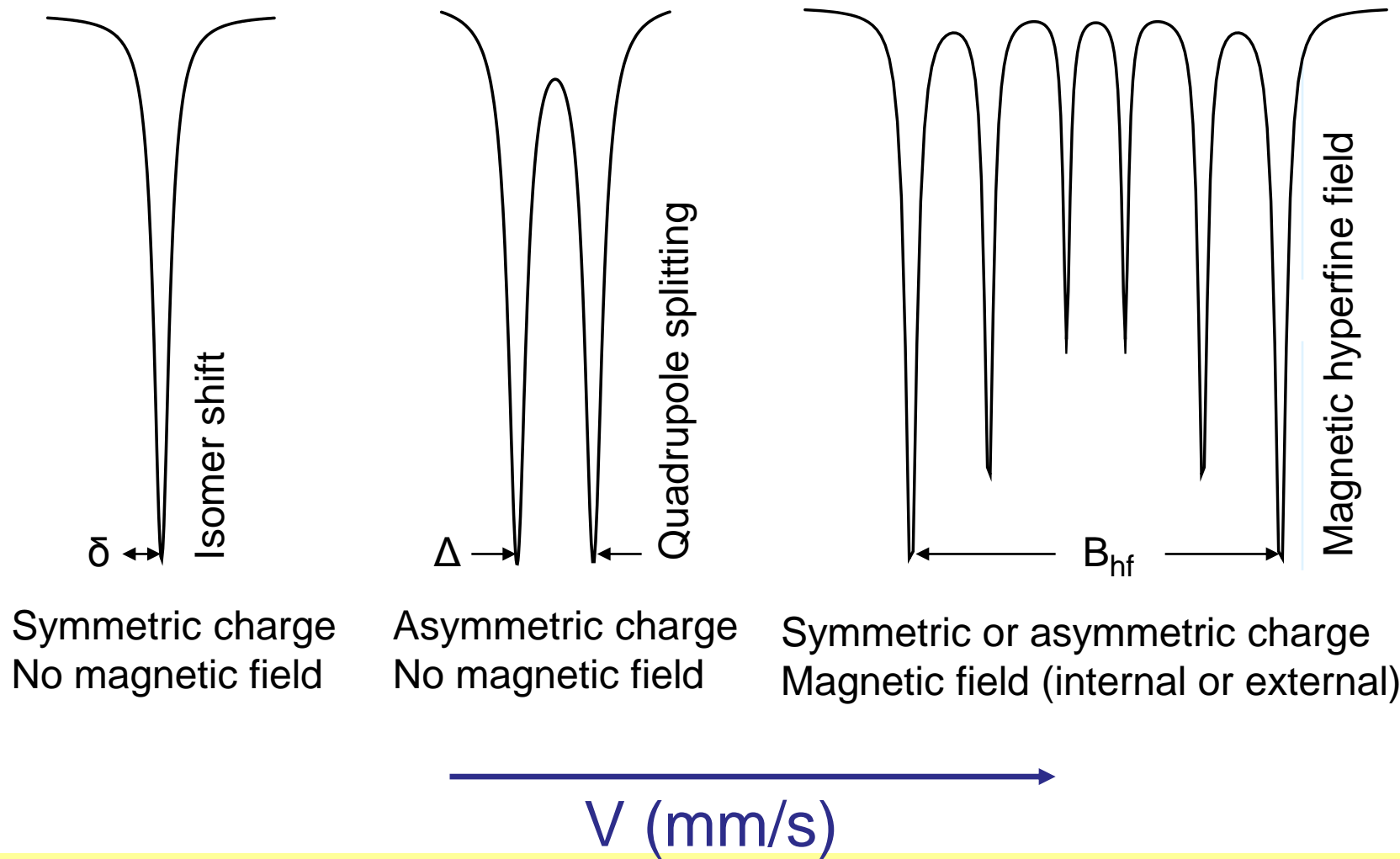
$$\mu_e = 0.153 \mu_n$$

$$\Delta m_I = 0, \pm 1$$

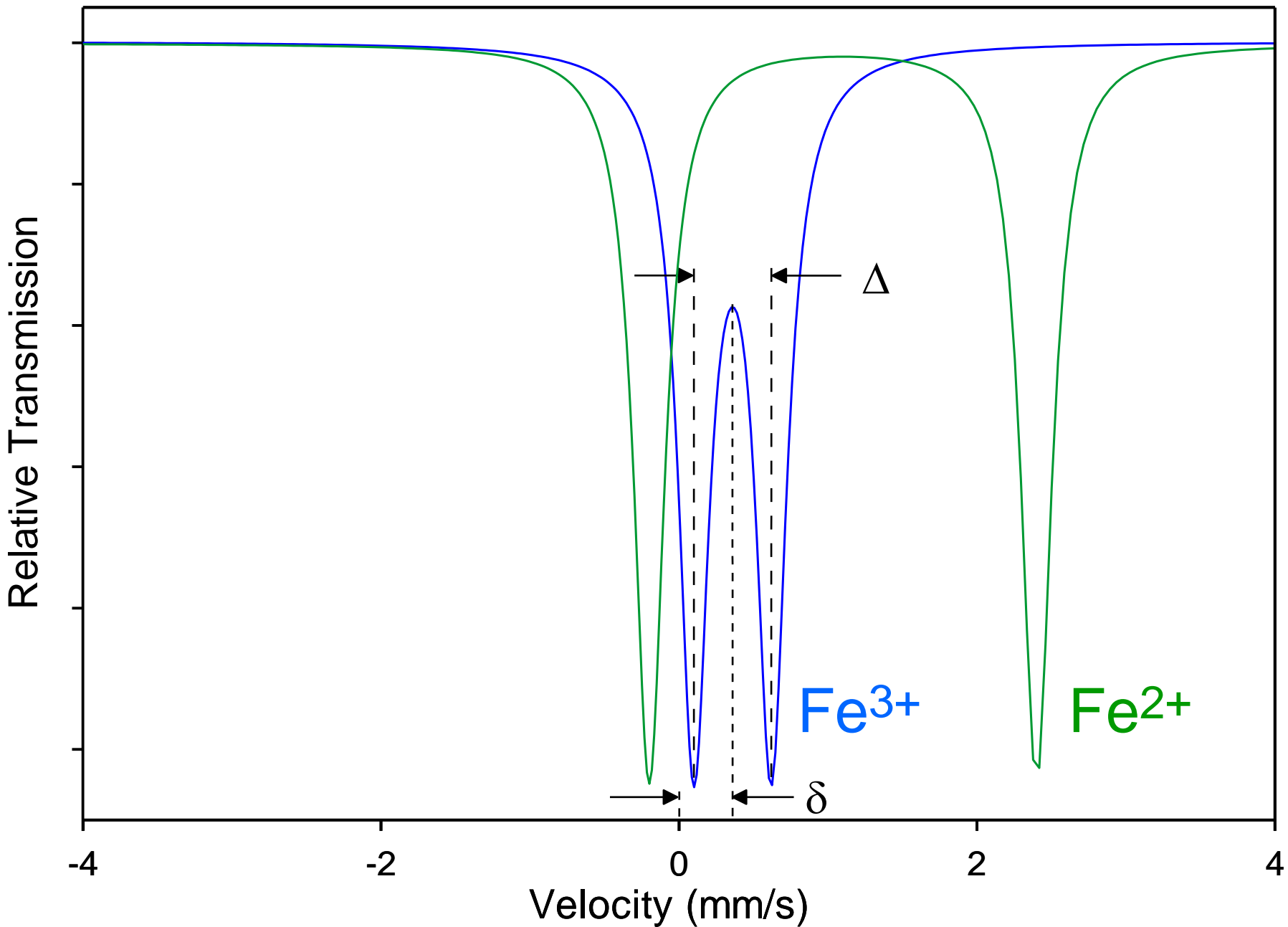
# In practice: $^{57}\text{Fe} \oplus$ field (no EFG)



# Static: Orbitals, surrounding charges, fields



# Isomer shift $\oplus$ local environment

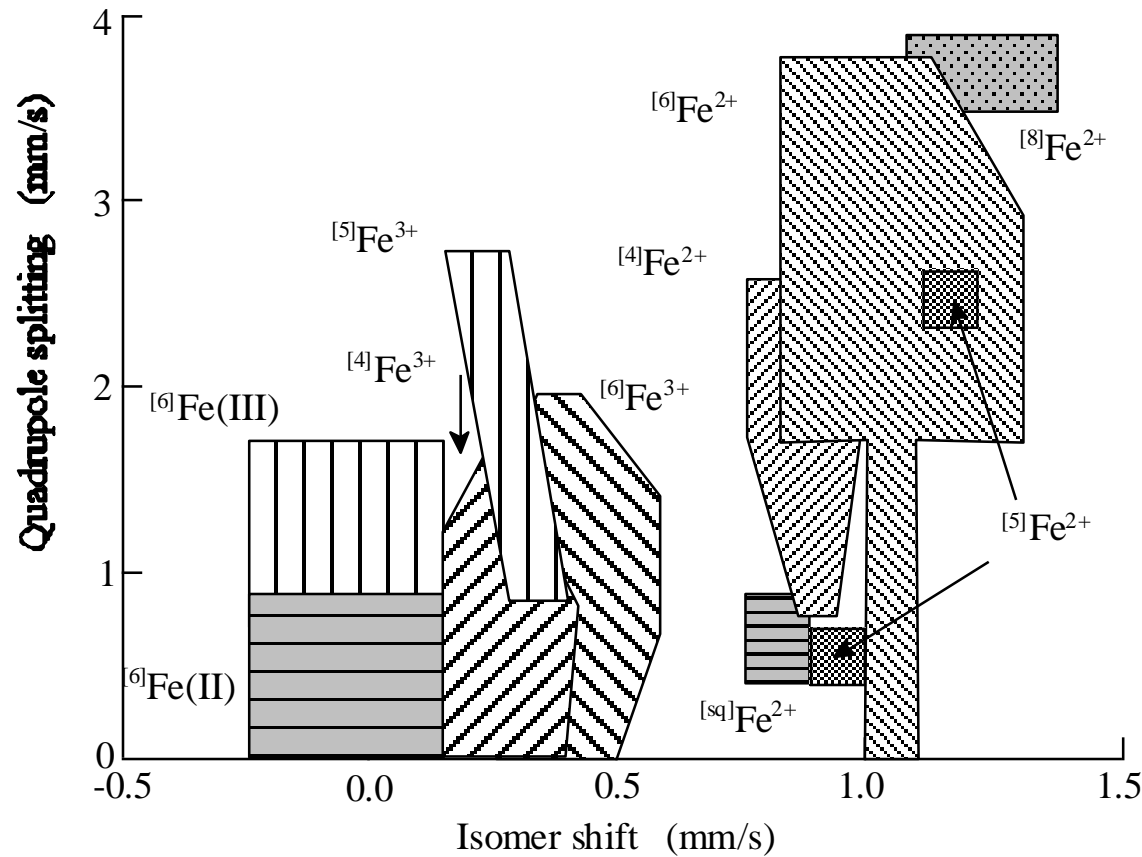


# Isomer shift $\oplus$ local environment

## Use of Mössbauer spectroscopy as a “fingerprinting” technique

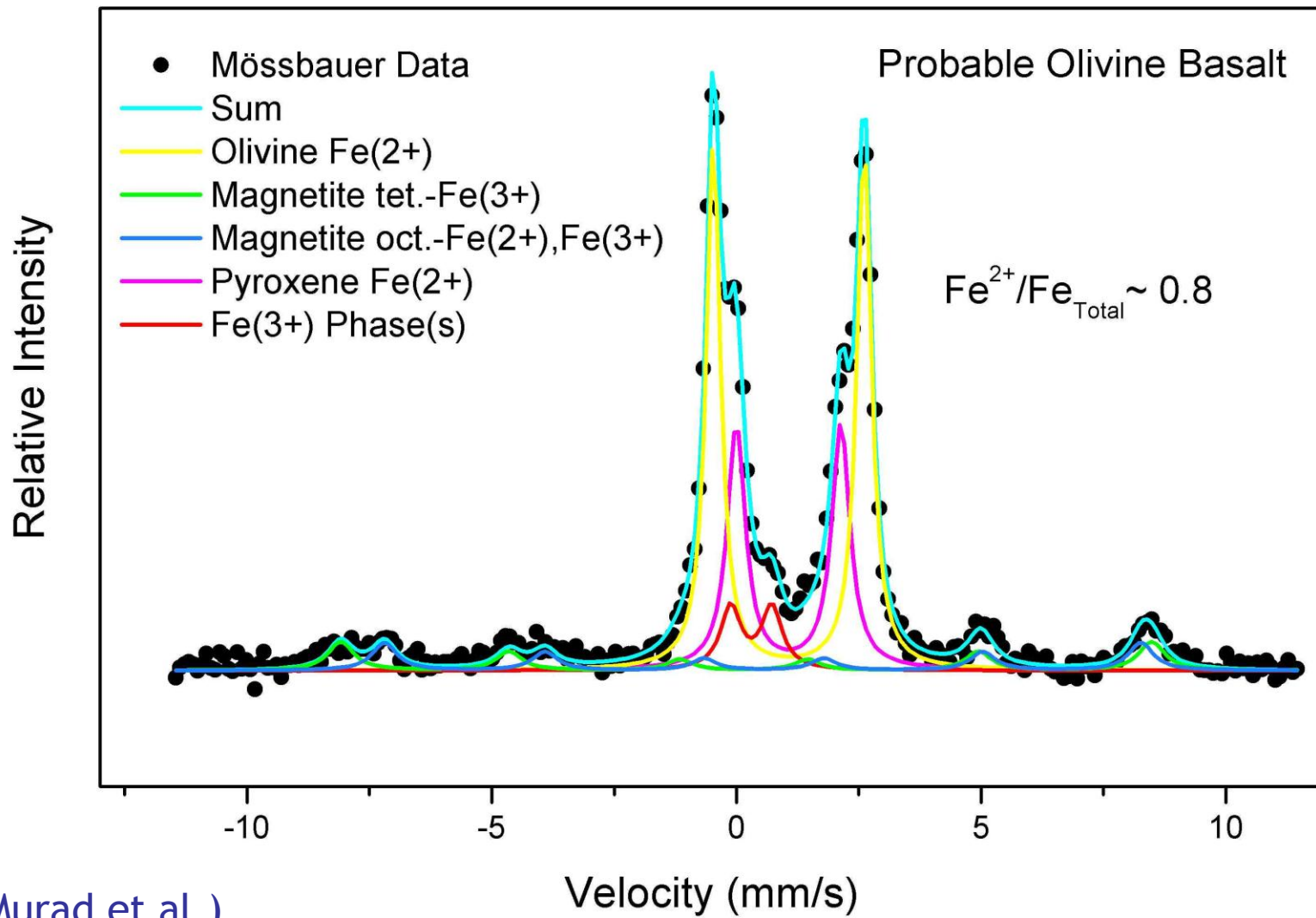
Isomer shifts and quadrupole splittings of Fe-bearing phases vary systematically as a function of Fe oxidation, Fe spin states, and Fe coordination.

Knowledge of the Mössbauer parameters can therefore be used to “fingerprint” an unknown phase.

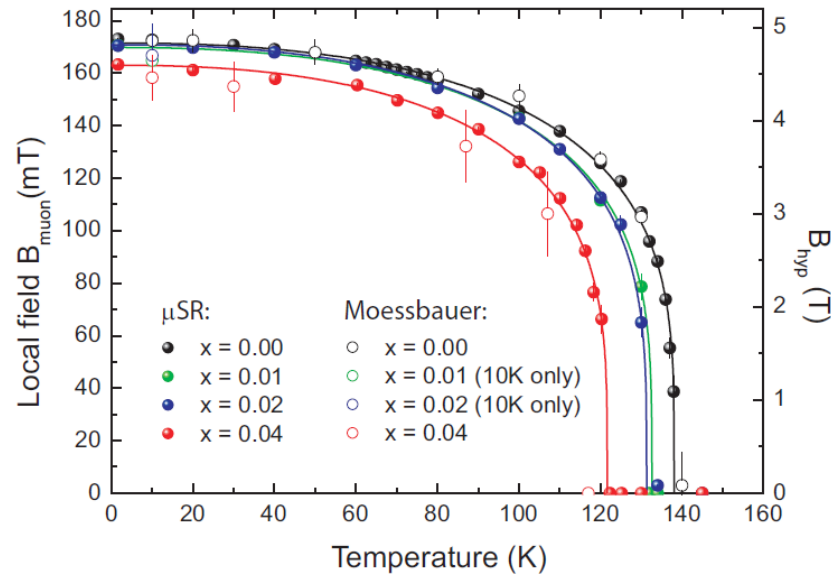
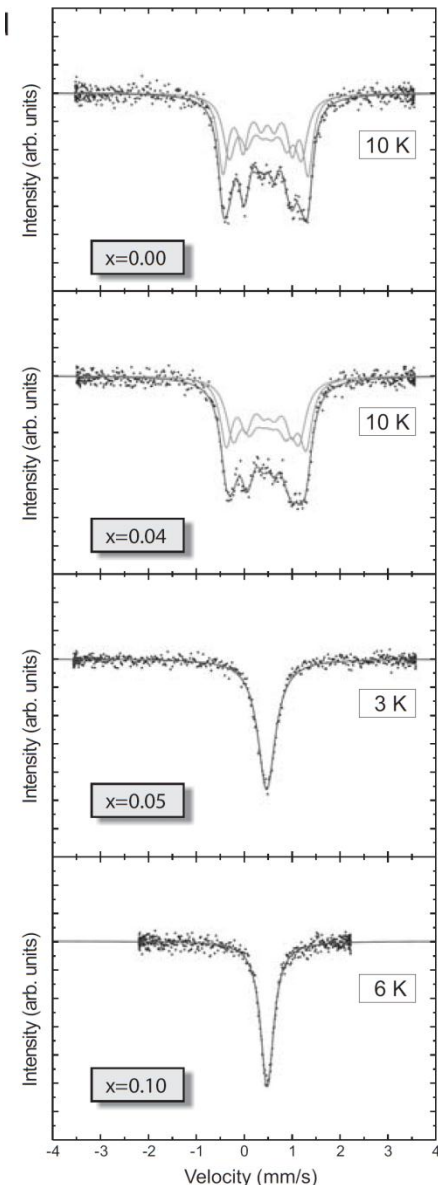


# Isomer shift $\oplus$ local environment

Mössbauer Spectrum of Adirondack Rock  
(Sol 18, Gusev Crater, Mars)



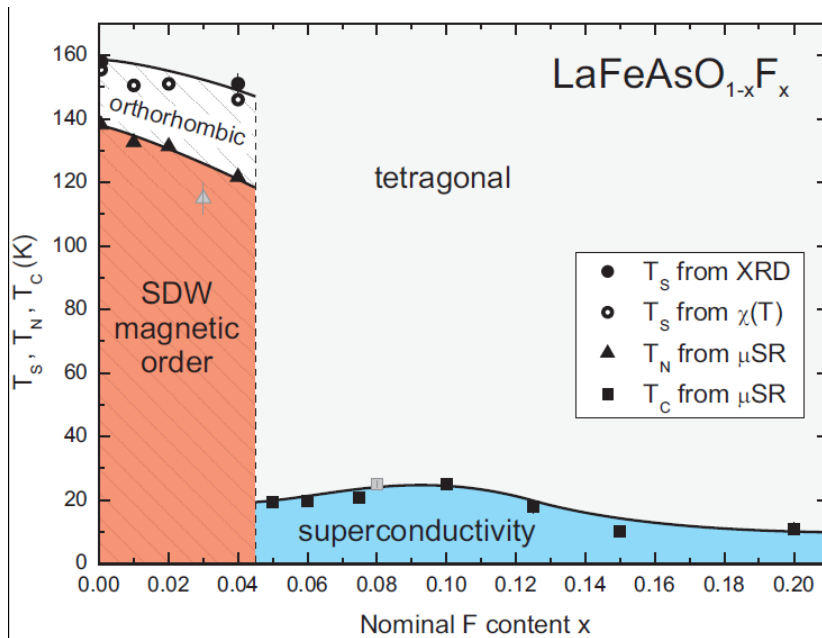
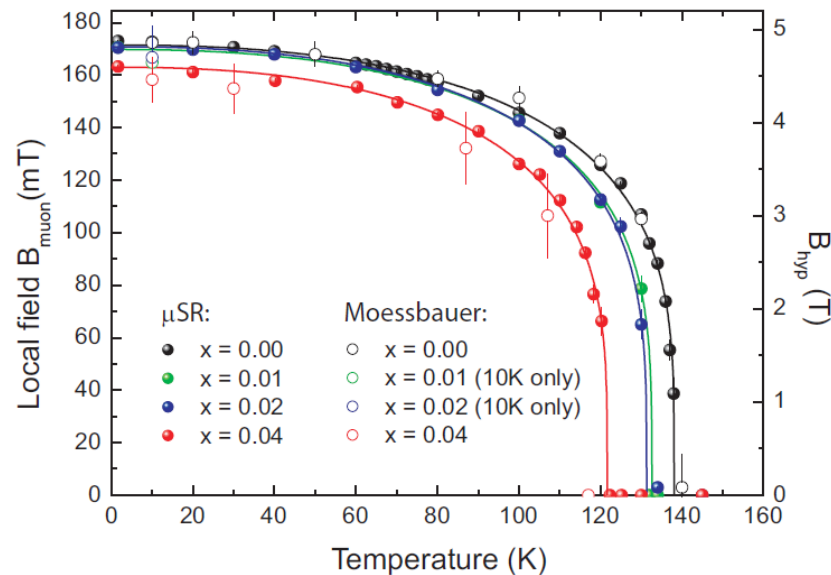
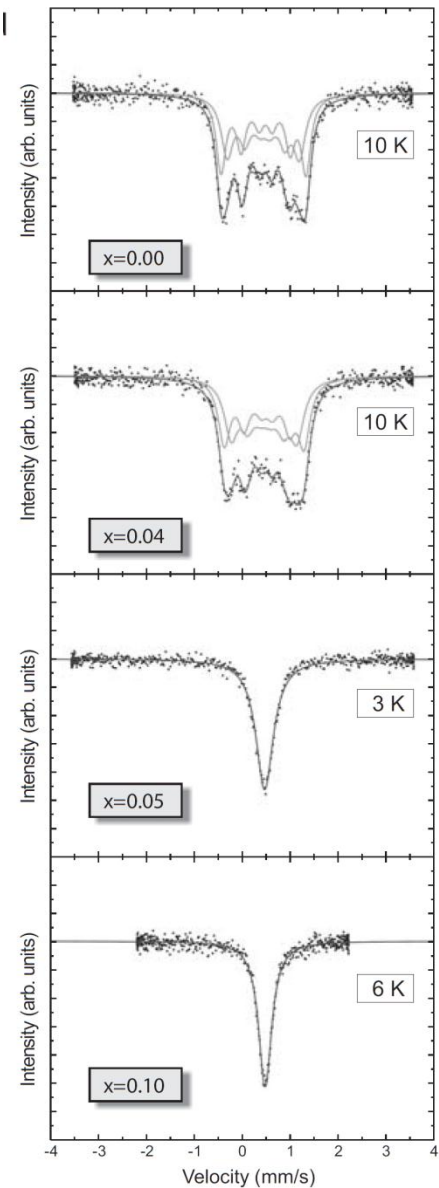
# Magnetic properties of Fe-pnictides



- Isomer shift typical of Fe(II) low or intermediate spin state
- Small internal field
- Fe<sup>2+</sup> hyperfine coupling well known
- Extraction of a small moment  $0.25(5) \mu_B$ : first indication in favour of a **commensurate Spin Density Wave**
- Note: disorder fitted with a double sextet

(Klauss, Luetkens et al.)

# Magnetic properties of Fe-pnictides

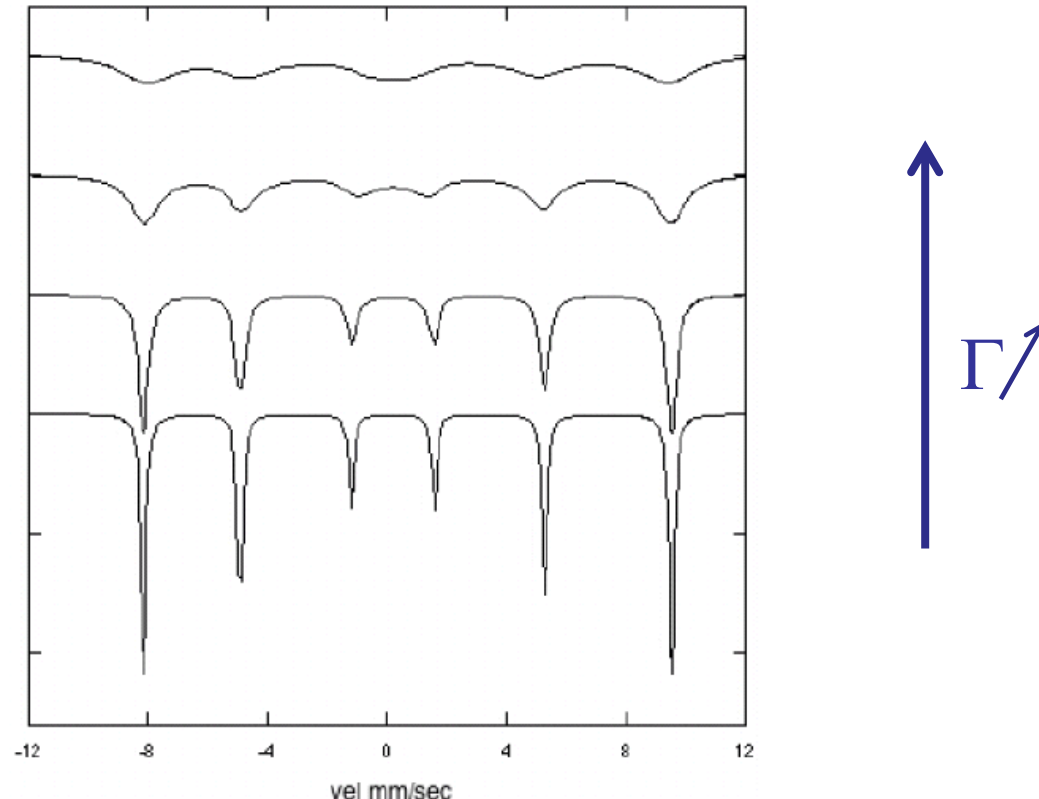


(Klauss, Luetkens et al.)

# Dynamics: Linewidth

- $\Delta E \Delta t \sim \hbar$
- Lifetime  $\tau$ , linewidth  $\Gamma$ :  $\Delta E = \Gamma \sim \hbar/\tau$
- $\tau \sim 10^{-5} - 10^{-11} \text{ s}$

Slow relaxation

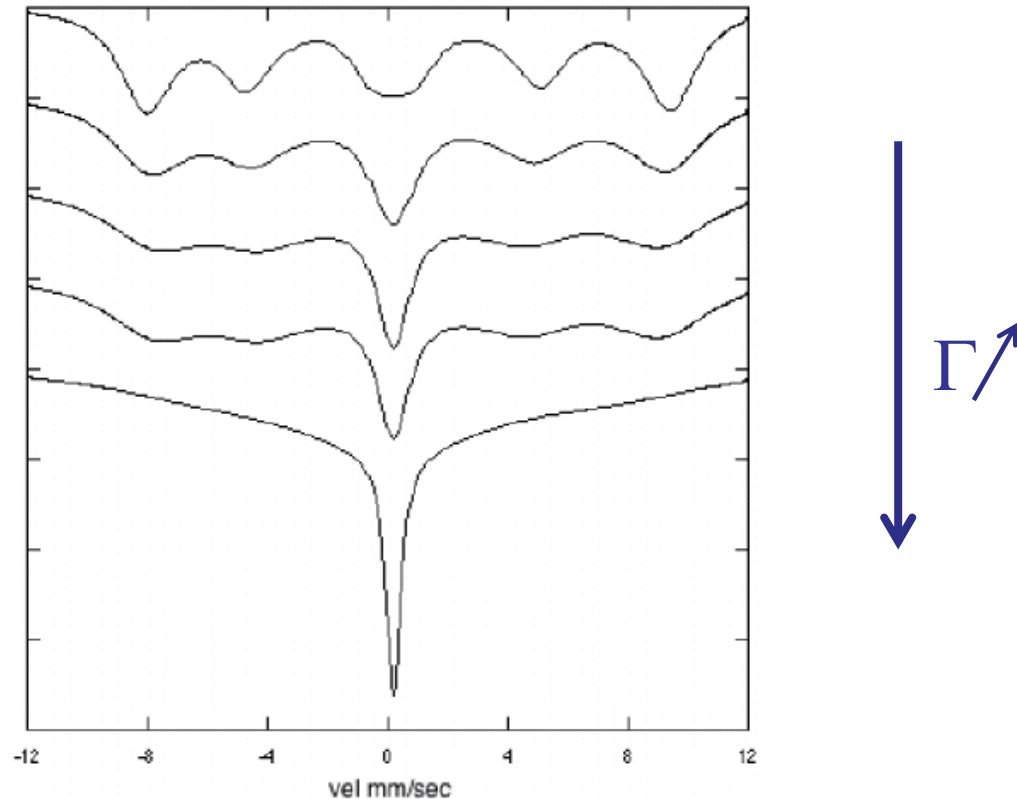


Note: effects are not the same on all lines: outer are more « protected »

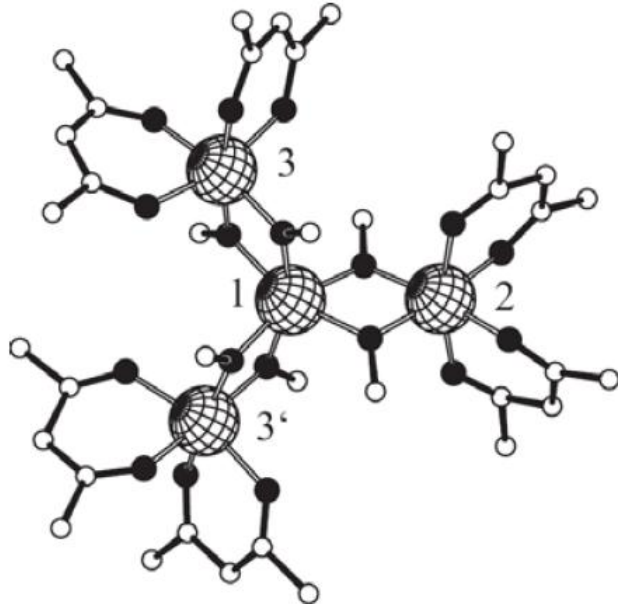
# Dynamics: Linewidth

- $\Delta E \Delta t \sim \hbar$
- Lifetime  $\tau$ , linewidth  $\Gamma$ :  $\Delta E = \Gamma \sim \hbar/\tau$
- $\tau \sim 10^{-5} - 10^{-11} \text{ s}$

Intermediate  
relaxation



# Example: Fe<sub>4</sub> molecular magnet



$S=5$   
AF interactions  
3 ineq sites, EFG  $\neq 0$

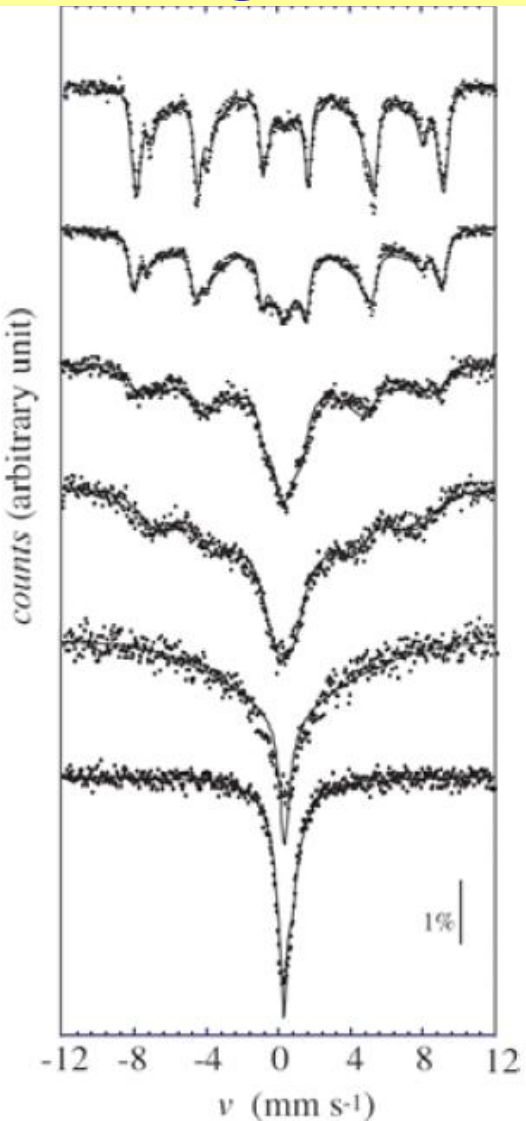


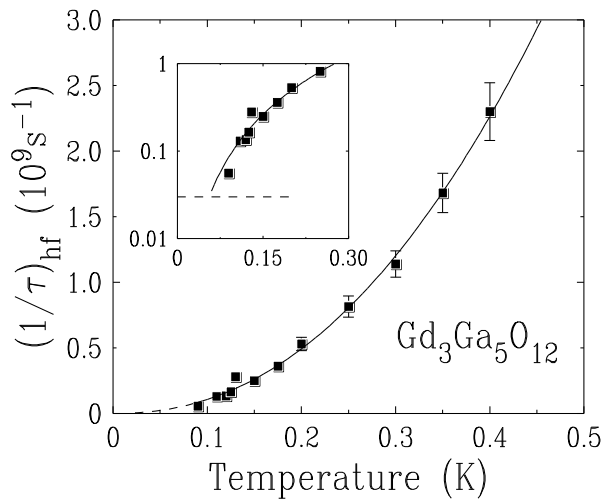
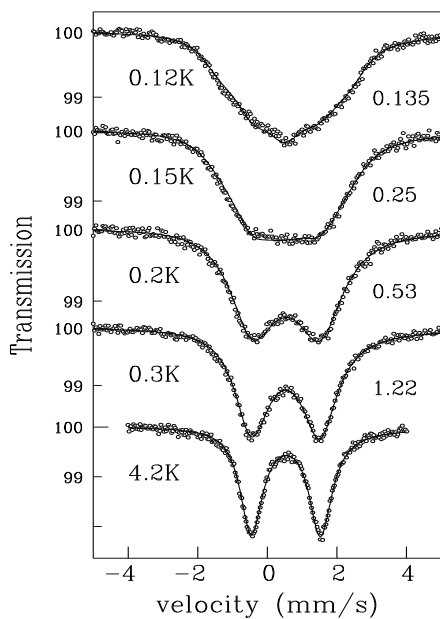
**Fig. 2.** Mössbauer spectra of the Fe<sub>4</sub> molecule at the temperatures of (starting from the top) 1.38, 4.25, 12.5, 25.7, 45, 77 K.

# Example: persistent fluctuations in frustrated magnets

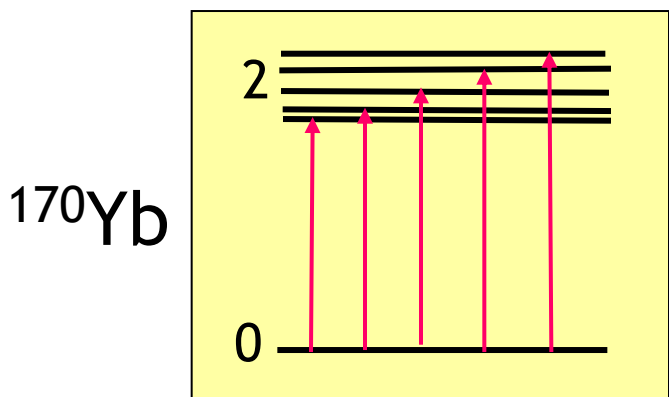
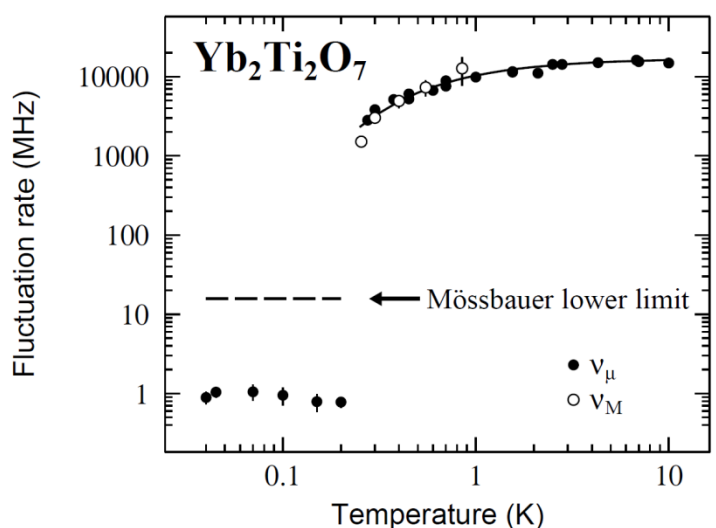
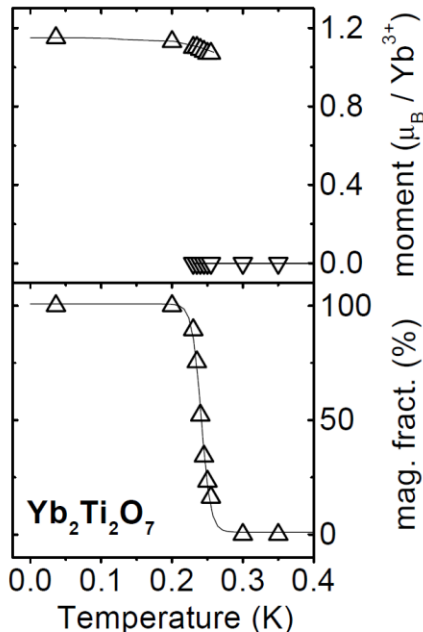
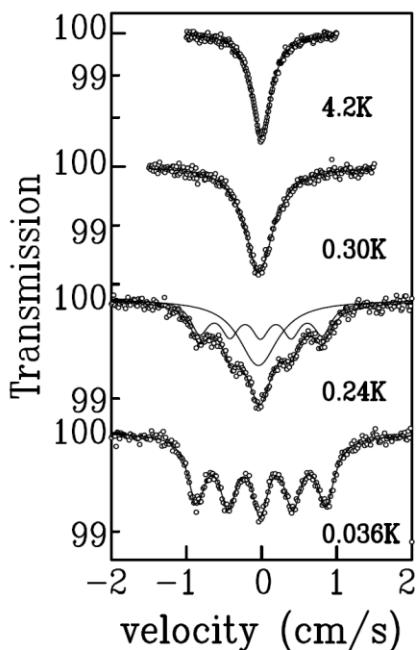
$^{155}\text{Gd}$  in  $\text{Gd}_3\text{Ga}_5\text{O}_{12}$

No magnetic order  
of  $\text{Gd}^{3+}$  moments due to  
geometrical frustration

*P.Bonville et al*  
*PRL 92 (2004) 167202*



# Example: phase transition in $\text{Yb}_2\text{Ti}_2\text{O}_7$



5 lines  
with equal  
intensities

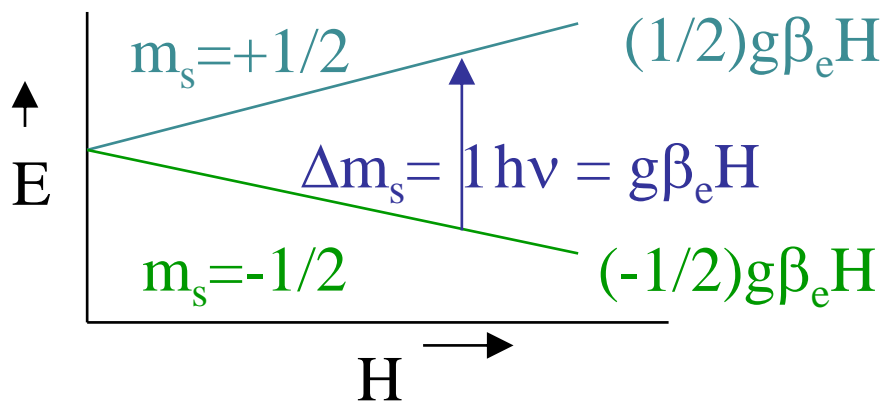
# NMR/Mössbauer: a comparative summary

	Mössbauer	NMR
Which sample?	Needs a source	Many...needs time
Fluctuation rate	Few 10 GHz... MHz	100 MHz - fraction of Hz
Location/coupling	At. Site, hyperfine 0.1 T - 10 T/ $\mu_B$	At. Site, hyperfine 0.1 T - 10 T/ $\mu_B$
Observables	Magnetic transitions	Magnetic susceptibilities
Temperature range	10 mK - ... K	10 mK - 1000 K
Field range	0 - (few T)	1 - 45 T
Intrinsic drawback	Need a source	r.f. field needed, field needed Tuning of the probe

$$\text{Fast fluctuations } 1/T_1 \sim A^2 \tau_c$$

# ESR: principle

- Angular momentum  $\hat{\vec{I}} = \hbar \hat{\vec{S}} \Rightarrow \hat{\vec{\mu}_e} = -\gamma_e \hbar \hat{\vec{S}}$
- Magnetic moment  $\mu_e = -\sqrt{S(S+1)} \frac{e\hbar}{m_e} = -\sqrt{S(S+1)} g \mu_B$
- Bohr magneton  $\mu_B = \frac{e\hbar}{2m_e} = 9.274 \cdot 10^{24} \text{ Am}^2$
- Landé factor  $g=2(1+\alpha/2\pi+...)$
- $\Delta m_s = \pm 1$   $\Delta E = g\beta_e H$



# ESR and NMR comparison!

	<i>electron</i>	<i>proton</i>	<i>ratio</i>
Rest mass	$m_e = 9.1094 \times 10^{-28} \text{ g}$	$m_p = 1.6726 \times 10^{-24} \text{ g}$	$5.446 \times 10^{-4}$
Magnetic dipole moment	$\mu_S = -g_e \mu_e \mathbf{S}$ $g_e = 2.002322$ $\mu_e = e\hbar / 4\pi m_e c =$ $9.274 \times 10^{-21} \text{ erg/G}$	$\mu_S = -g_N \mu_N \mathbf{S}$ $g_N = 5.5856$ $\mu_N = e\hbar / 4\pi m_N c =$ $5.0504 \times 10^{-24} \text{ erg/G}$	1836.12

**Frequency:** Factor 1000 larger in EPR ! (*GHz instead of MHz*)

**Dipolar coupling:** Factor 1 000 000 larger in EPR ! (*MHz instead of Hz*)

**Relaxation Times:** Factor 1000 000 smaller in EPR ! (*ns instead of ms*)

= much higher technical requirements, but unique sensitivity to molecular motion

**Sensitivity :** Factor 1 000 000 better than in NMR !! (*1nM instead of 1mM* )

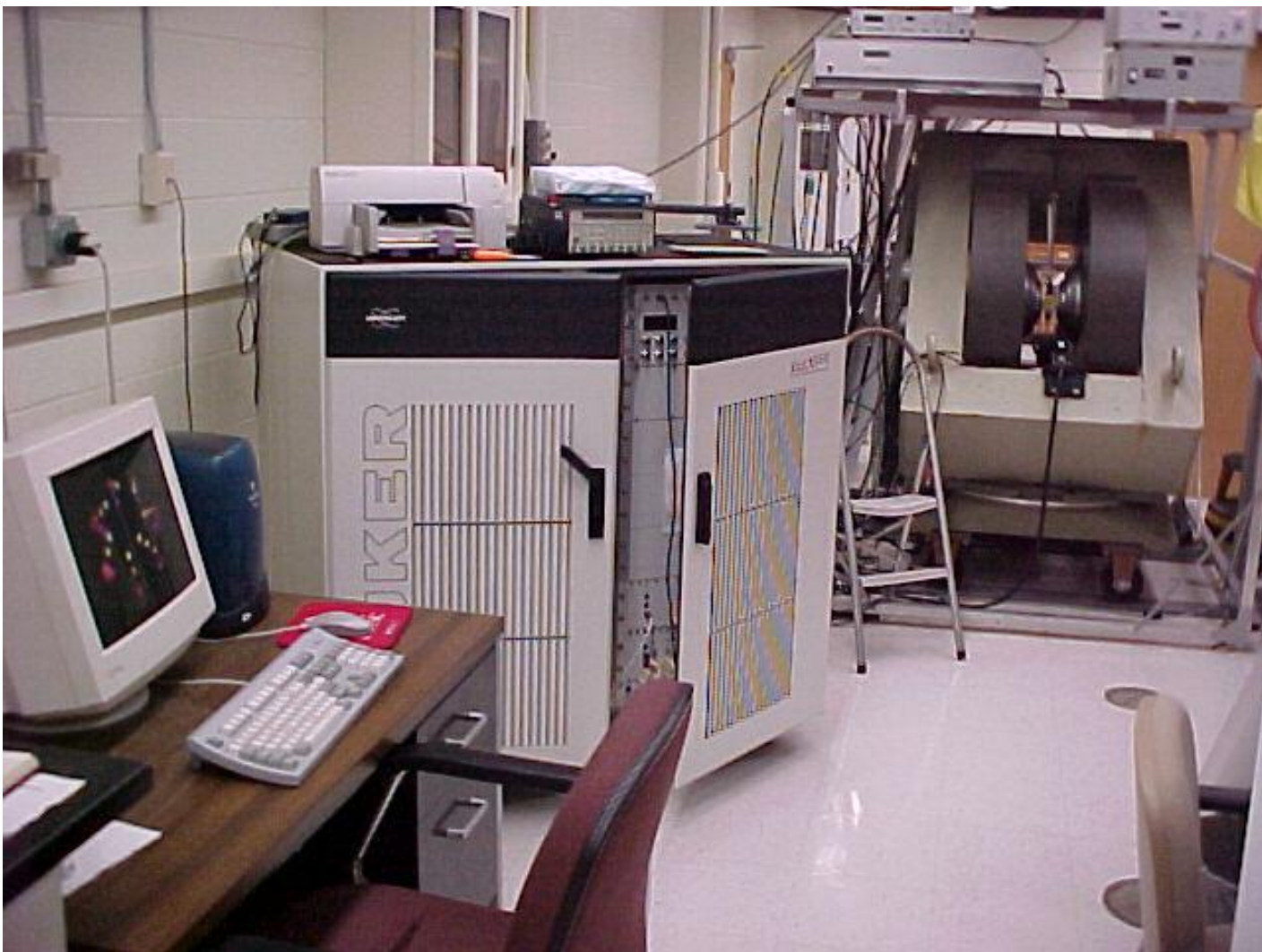
*An ideal case, though*

# ESR: in practice

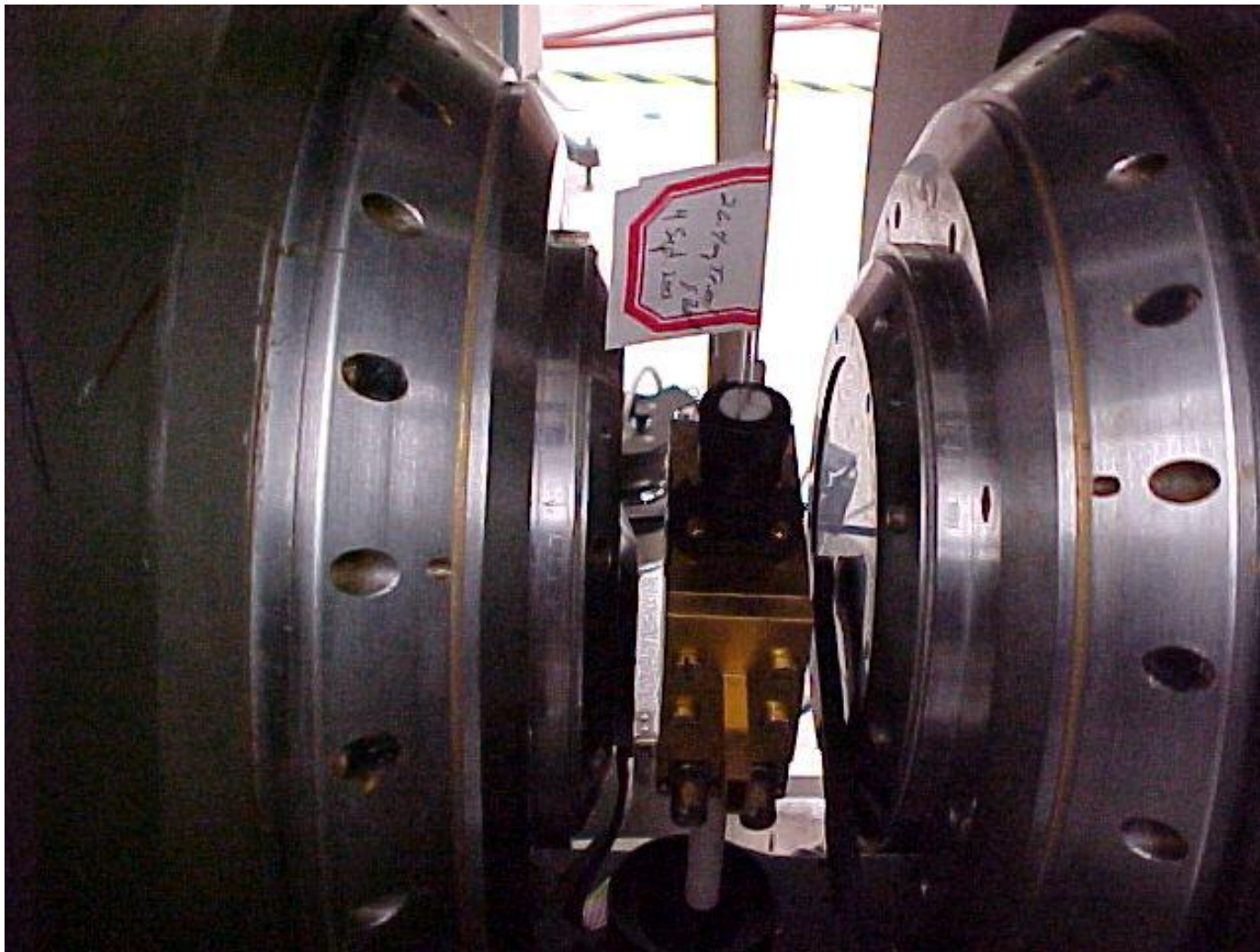
~ 33 GHz / Tesla

- Traditional frequencies,  $\nu$ , used are microwave bands originally developed for radar:
  - X band; ~9-9.5 GHz, in most widespread use ( $\lambda \sim 3$  cm).
  - K band; ~ 24 GHz ( $\lambda \sim 1$  cm)
  - Q band; ~ 35 GHz ( $\lambda \sim 0.8$  cm)
  - W band; ~ 95 GHz
- Traditional electromagnets with fields up to 3 Tesla.
  - At  $g=2$ , about which most spectra are centered, X-band setups have resonances at 3,000-3,500 Gauss.
- Cutting edge EPR is going to ever higher and ever lower  $\nu$ .

# ESR apparatus



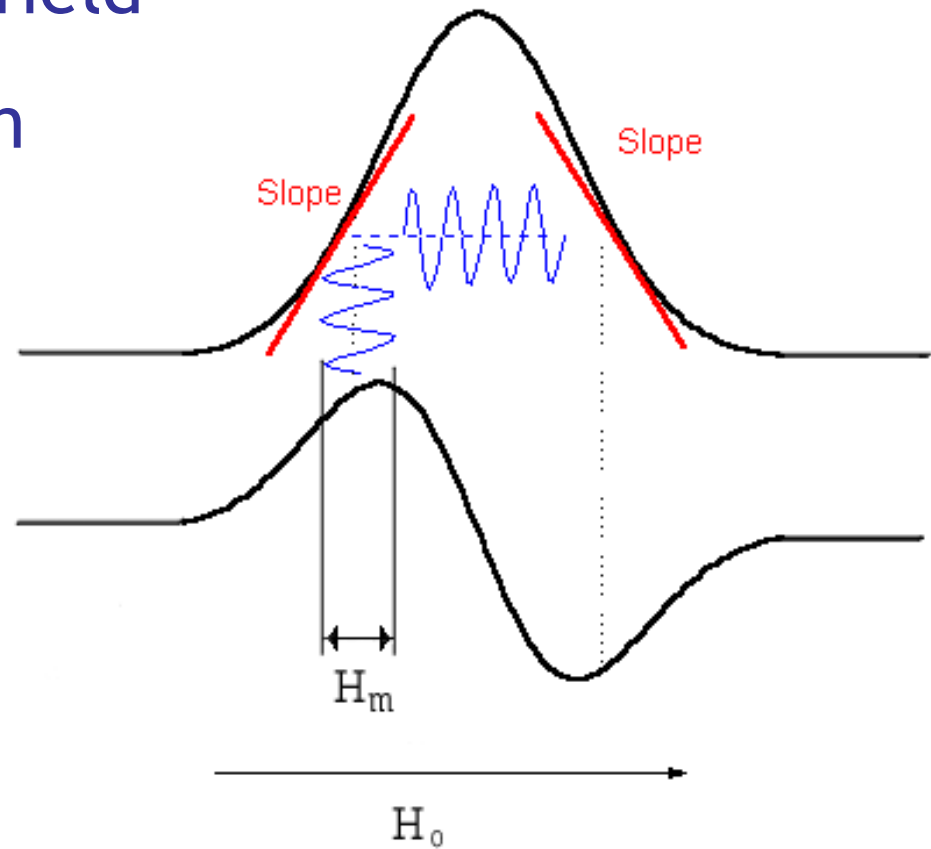
# ESR apparatus



Use of a cavity (except at high frequencies) → sweep the field

# ESR detection

- Modulation of magnetic field
- Phase sensitive detection
- Spectrum = derivative



- Intensity by double integration ~ static susceptibility

# Spin(s) Hamiltonian for EPR

$$H = H_{eZ} + H_{ZFS} + H_{ee} + H_{en} + H_{nZ}$$

$H_{eZ}$  = Electron Zeeman interaction: *g tensor*

$H_{ZFS}$  = Zero-field splitting interaction: **anisotropy, dipolar**

$H_{ee}$  = Interactions between electron moments: **exchange**

$H_{en}$  = Electron - nucleus interaction

$H_{NZ}$  = Nuclear zeeman interaction

Hilbert space of coupled electrons and nuclear spins has a dimension  $n_H = \prod_m (2S_m + 1) \prod_n (2I_n + 1)$

# e-Zeeman interaction

$$H_{eZ} = \mu_B \vec{B} \cdot \underline{\underline{g}} \cdot \vec{S}$$

- « Effective » g
- Crystal Field + Spin Orbit
- Different hierarchy for 3d and 4f
- 3d:  $\langle \mathbf{L} \rangle = 0$  Crystal field dominates, Spin orbit = small corr.

$$H_{eZ} + H_{LS} = g_e \mu_B \vec{B} \cdot (\vec{L} + \vec{S}) + \lambda \vec{L} \cdot \vec{S} = g_e \mu_B \vec{B} \cdot \underline{\underline{g}} \cdot \vec{S} + \vec{S} \cdot \underline{\underline{D}} \cdot \vec{S}$$

4f: use  $g_J$  (free atom) instead of  $g$  (takes into account the spin orbit term)

# e-Zeeman interaction

$$H_{eZ} + H_{LS} = g_e \mu_B \vec{B} \cdot (\vec{L} + \vec{S}) + \lambda \vec{L} \cdot \vec{S} = g_e \mu_B \vec{B} \cdot \underline{\underline{g}} \cdot \vec{S} + \vec{S} \cdot \underline{\underline{D}} \cdot \vec{S}$$

$$\underline{\underline{g}} = g_e (1 + 2\lambda \underline{\underline{\Lambda}}) \quad g_e = 2.0023$$

$$\underline{\underline{D}} = \lambda^2 \underline{\underline{\Lambda}}$$

$$\Lambda_{ij} = \sum_{n \neq 0} \frac{\langle \psi_0 | L_i | \psi_n \rangle \langle \psi_n | L_j | \psi_0 \rangle}{E_0 - E_n}$$

$$H_{eZ} = \mu_B \vec{B} \cdot \underline{\underline{g}} \cdot \vec{S}$$

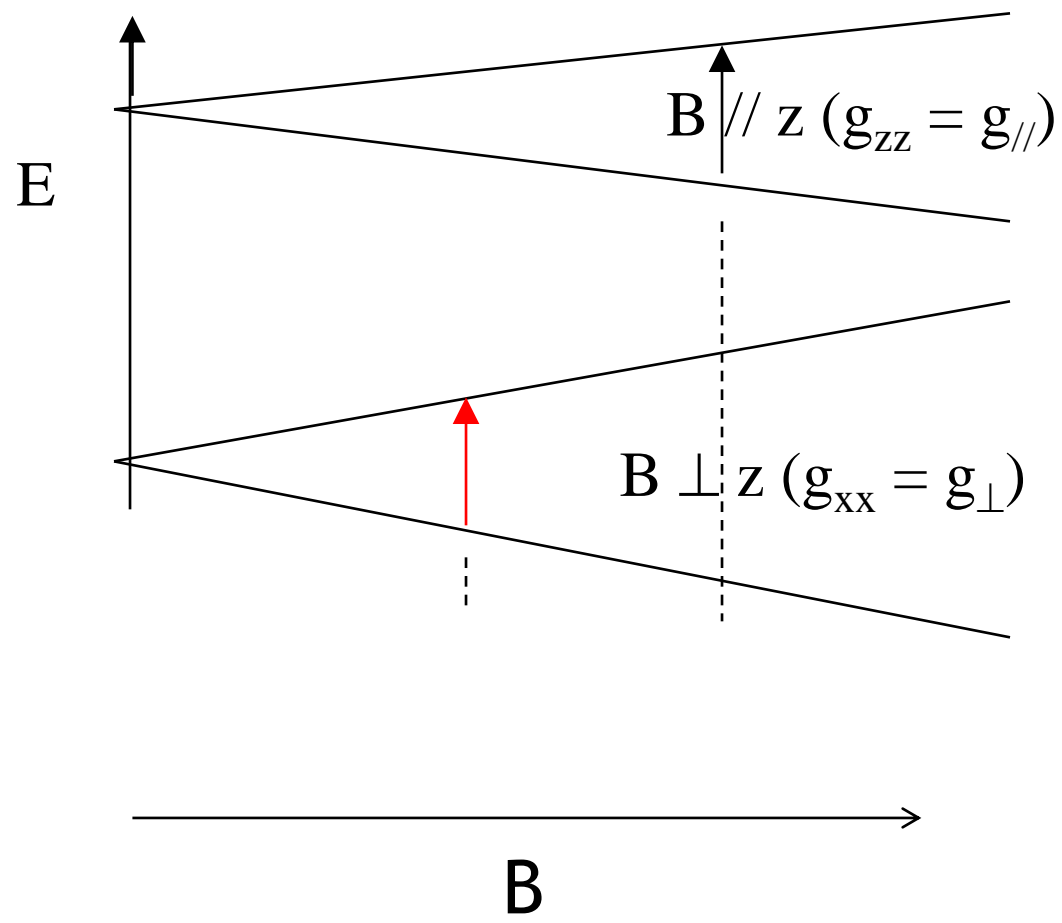
$$\underline{\underline{g}} = \begin{pmatrix} g_{xx} & 0 & 0 \\ 0 & g_{yy} & 0 \\ 0 & 0 & g_{zz} \end{pmatrix}$$

$$\begin{aligned} h\nu &= g_{xx} \mu_B B, & \underline{B} // x, \\ h\nu &= g_{yy} \mu_B B, & \underline{B} // y \\ h\nu &= g_{zz} \mu_B B, & \underline{B} // z. \end{aligned}$$

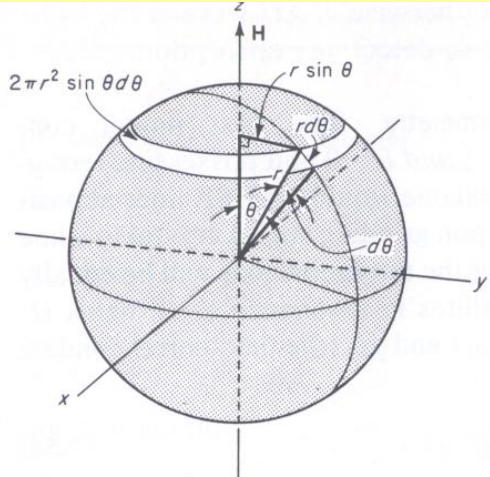
- Cubic symmetry:  $g_{xx} = g_{yy} = g_{zz}$
- Axial symmetry (trigonal, tetragonal, hexagonal):  $g_{xx} = g_{yy} = g_{\perp}$  and  $g_{zz} = g_{||}$
- Orthorhombic symmetry:  $g_{xx} \neq g_{yy} \neq g_{zz}$

# g-tensor: axial case

$$H_{eZ} = \mu_B \vec{B} \cdot \underline{\underline{g}} \cdot \vec{S}$$



# g-tensor: axial case, powder lineshape



$S=1/2, l=0, g_x=g_y>g_z$  **Axially symmetric g-factor**

$$B_r = \frac{h\nu}{g_{eff}\mu_B} = \frac{h\nu}{\mu_B} [g_{II}^2 \cos^2 \theta + g_{\perp}^2 \sin^2 \theta]^{-1/2}$$

$\theta$  is the angle between a z-principal axis and the magnetic field direction

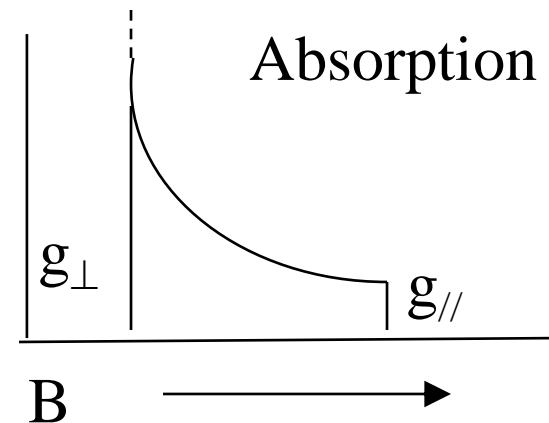
The given solid angle  $\Omega$  is defined to be the ratio of the surface area  $S$  to the total surface area on the sphere:  $\Omega = S/4\pi r^2$ :  $d\Omega/\Omega = 2\pi r^2 \sin \theta d\theta / 4\pi r^2 = \sin \theta d\theta / 2$

$$f(B)dB \propto \sin \theta d\theta$$

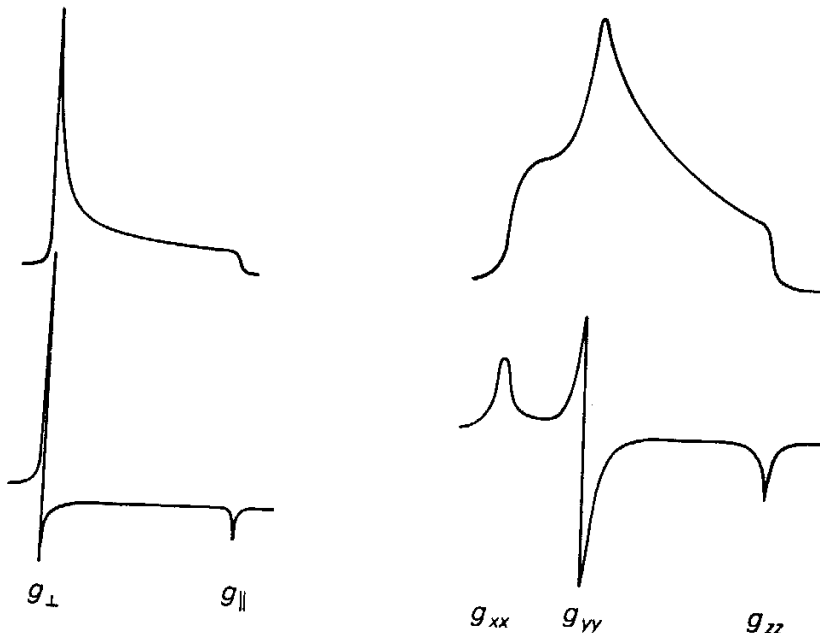
$$f(B) \propto \frac{1}{|dB/d \cos \theta|}$$

$$f(B) \propto \frac{\mu_B}{h\nu} \frac{(g_{II}^2 \cos^2 \theta + g_{\perp}^2 \sin^2 \theta)^{3/2}}{(g_{II}^2 - g_{\perp}^2) \cos \theta}$$

$$f(B) \propto \frac{\mu_B}{h\nu} \frac{1}{B_r^3 (g_{II}^2 - g_{\perp}^2) \cos \theta}$$



# Lineshape: g tensor



$g_{xx} = 2.0507$ ;  $g_{yy} = 2.080$ ;  
 $g_{zz} = 2.230$ .

Absorption

Observed

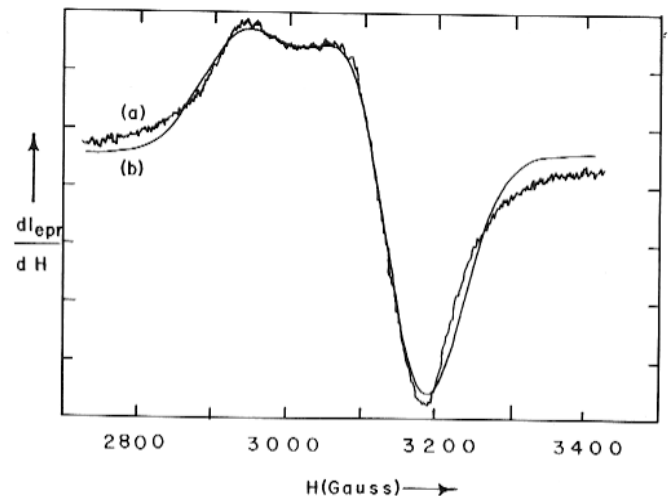


FIG. 5. Experimental (a) and best-fit (b) EPR first-derivative spectra of a powder sample of  $\text{Y}_2\text{BaCuO}_5$  at room temperature. The microwave frequency was 9.160 GHz.

g tensor  $\longleftrightarrow$  spin orbit

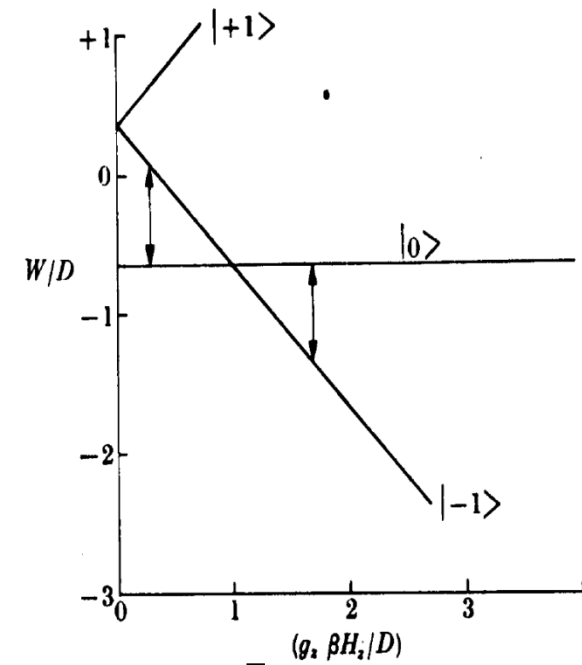
# Zero Field Splitting: single ion anisotropy

$$H_{ZFS} = \mu_B \vec{S} \cdot \underline{\underline{D}} \cdot \vec{S}$$

All these terms resume in a quadratic form of  $S_x, S_y, S_z$

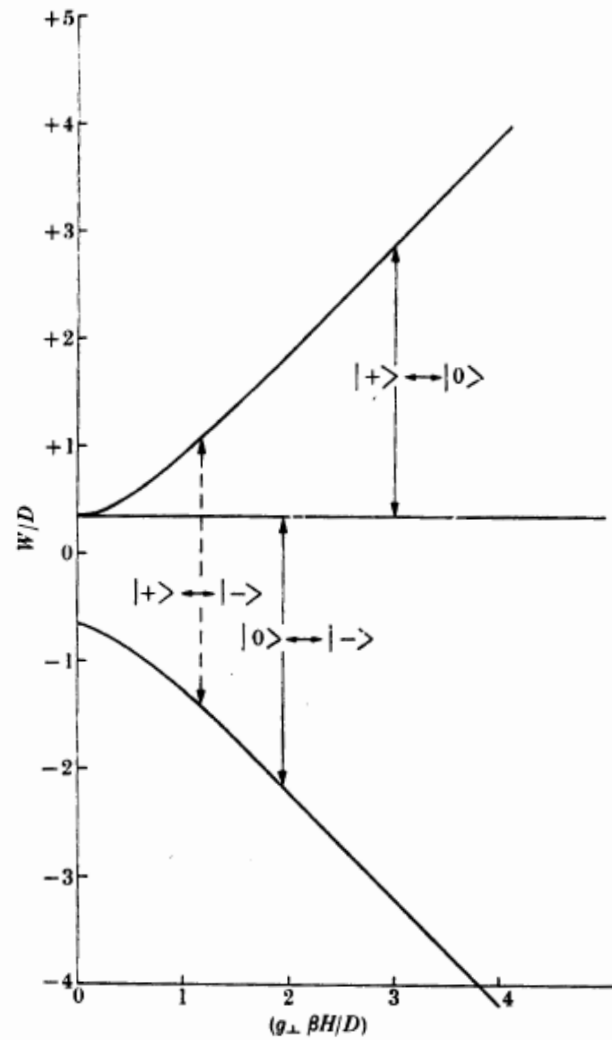
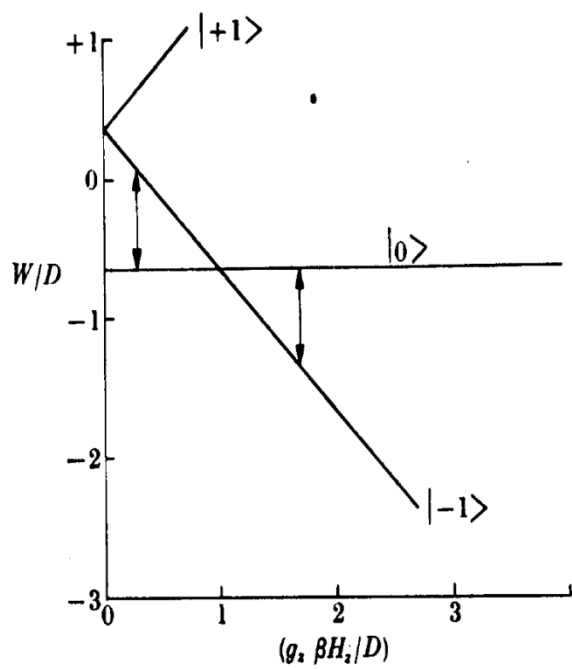
$$\begin{aligned} H_{ZFS} &= D_x S_x^2 + D_y S_y^2 + D_z S_z^2 = \\ &= D \left[ S_z^2 - \frac{1}{3} S(S+1) \right] + E (S_x^2 - S_y^2) \end{aligned}$$

- $S=1/2$ : no effect
- $S>1/2$ : example,  $S=1$ ;  
 $E=0$ : 3 states, singlet(1)  
and triplet (2)



$$(S > 2) \quad H_{ZFS} = \frac{a_{ZFS}}{6} \left[ S_x^4 + S_y^4 + S_z^4 - \frac{1}{5} S(S+1)(3S^2 + 3S - 1) \right]$$

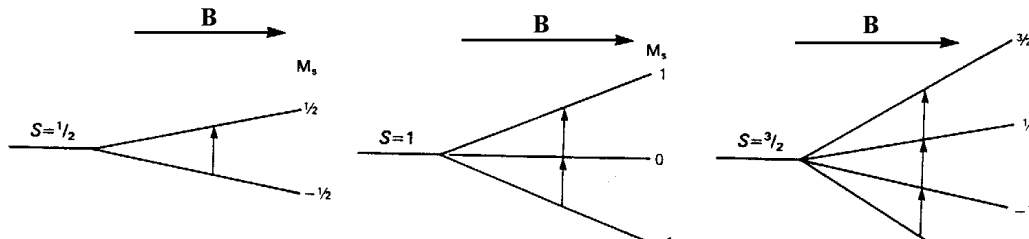
# Zero Field Splitting



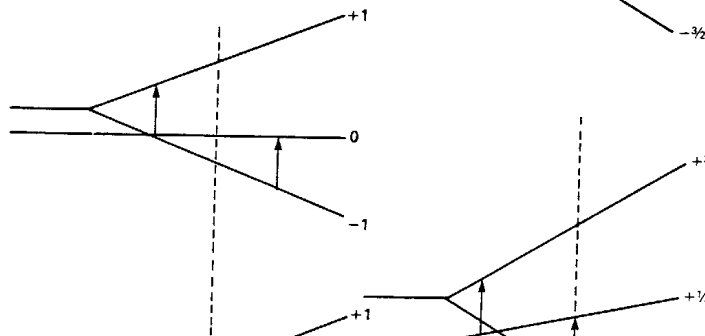
On a powder, broad line due to anisotropy

# Zero Field Splitting

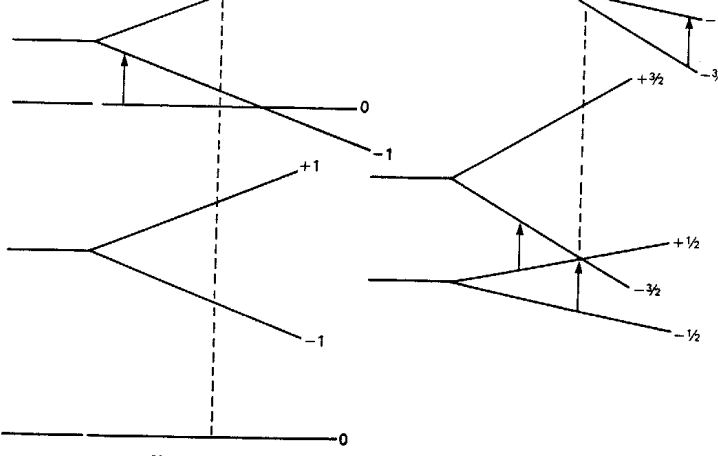
no zero-field splitting



with zero-field splitting



large zero-field splitting

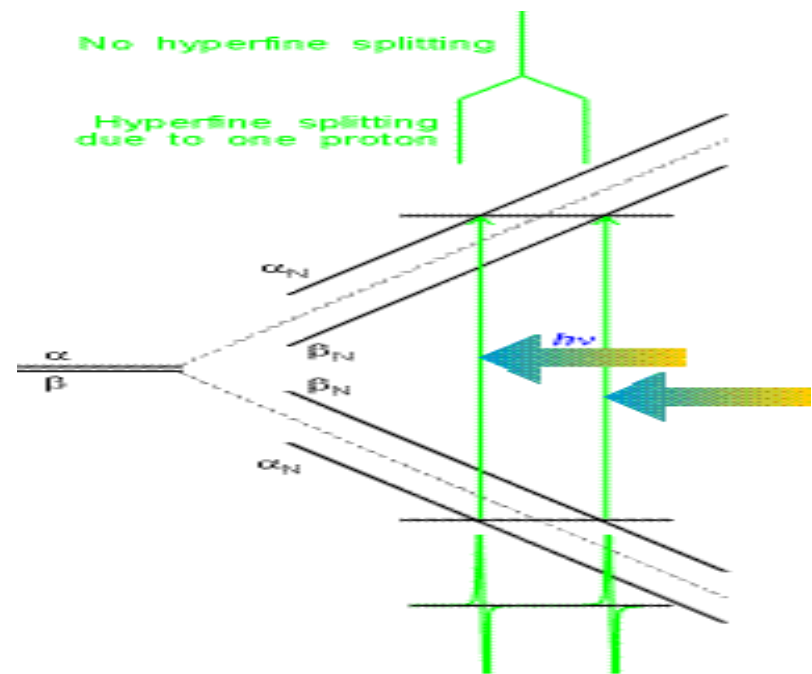
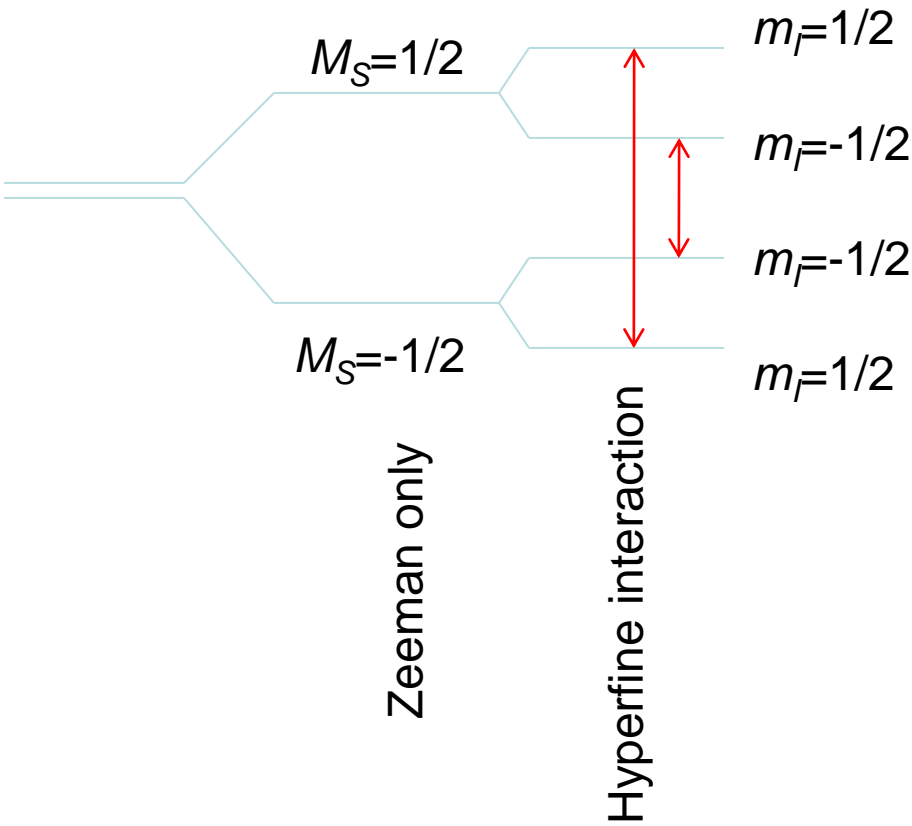


# Hyperfine Splitting

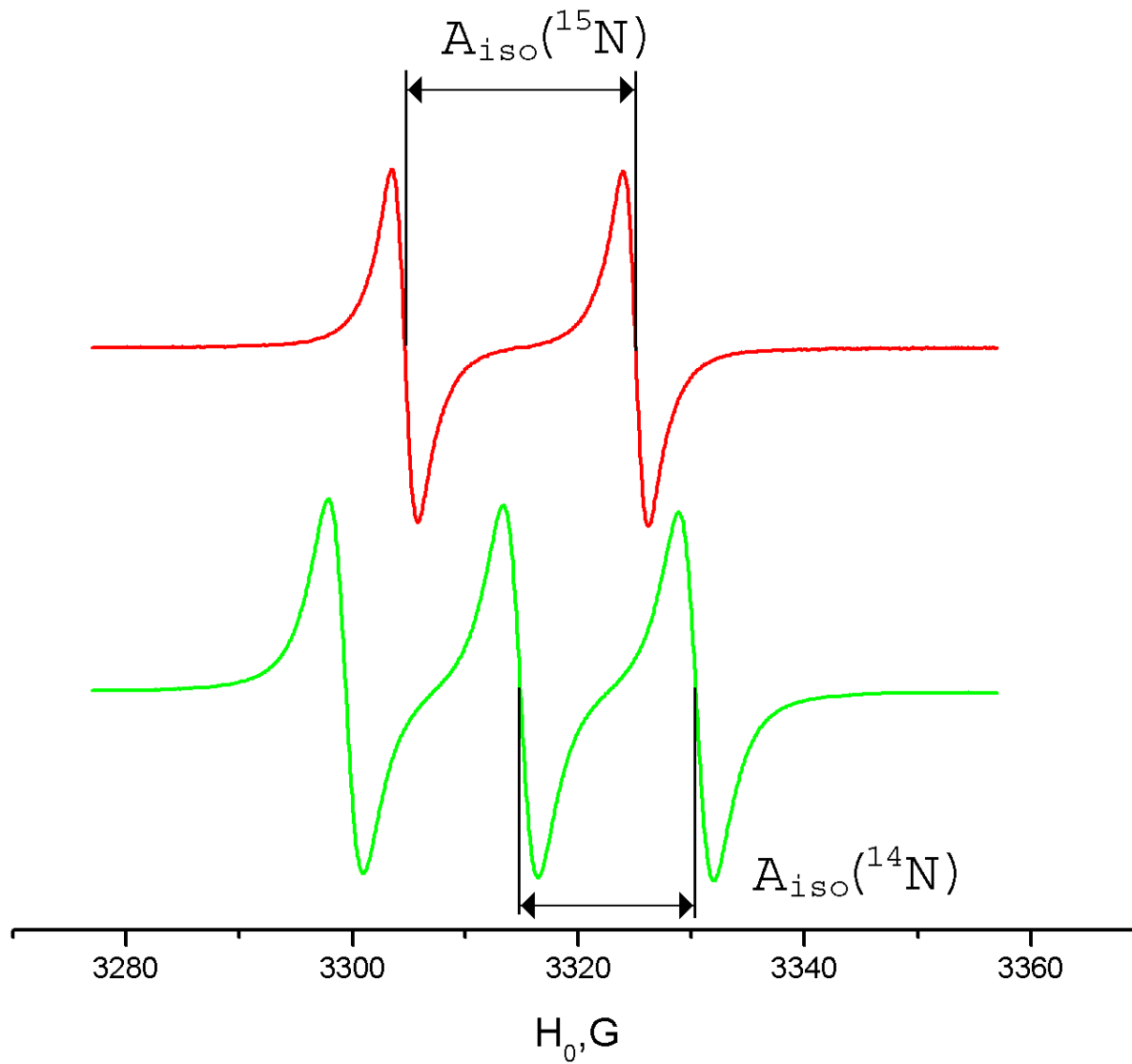
$$H_{e-n} = \vec{I} \cdot \underline{\underline{A}} \cdot \vec{S}$$

$$E = g\mu_B B_o M_S + aM_S m_I$$

Isotropic case

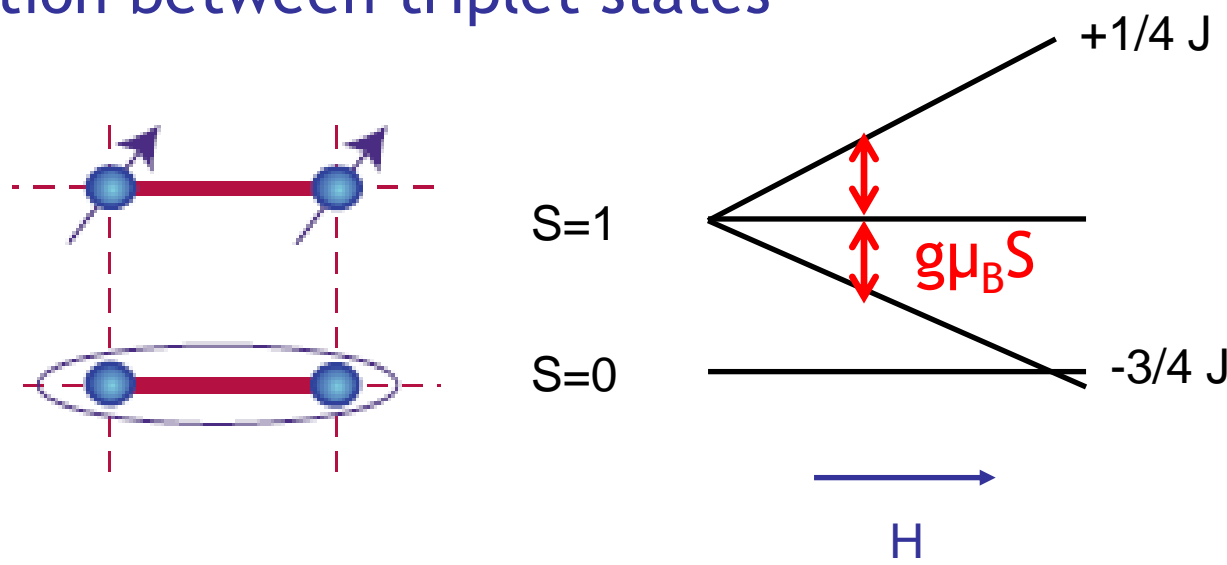


# Hyperfine Splitting: example



# Coupled spins: paramagnetic regime and exchange narrowing

- A toy-model: 2 identical spins. Isotropic coupling  $J\vec{S}_1\vec{S}_2$
- Only transition between triplet states



- More generally, the moment of order 2,  $M_2$  is invariant under isotropic coupling.
- $M_4$  increases with  $J$ . **Exchange narrowing**
- $\tau \sim h/J$ ,  $J \gg$  dip, DM, ...  $|(\mathcal{J}/h)| \gg (\langle \Delta\nu^2 \rangle)^{1/2} \rightarrow$  fast random precess

Only anisotropic part contributes to  $M_2$ - e.g. dipolar, DM

# Coupled spins: paramagnetic regime

$$\mathcal{H} = g\mu_B \mathbf{H} \cdot \sum_i \mathbf{S}_i + J \sum_i \mathbf{S}_i \cdot \mathbf{S}_{i+1} + \mathcal{H}'$$

Zeeman  
energy

isotropic  
exchange

additional  
interactions

e.g. crystal field  
anisotropic exchange  
dipole-dipole interaction  
hyperfine interaction

strong isotropic coupling

- averages local fields similar to fast movements of the spins
- “exchange narrowing” of the ESR signal

local inhomogeneous fields

- local, static resonance shift
- inhomogenous broadening of the ESR signal

$$\mathcal{H}' = \sum_{ij} \sum_{\alpha\beta} K_{ij}^{\alpha\beta} S_i^\alpha S_j^\beta$$

$$K_{ij}^{\alpha\beta}(\text{dip}) = \frac{1}{2} (g\mu_B)^2 \hbar^2 \frac{r_{ij}^2 \delta_{\alpha\beta} - 3r_{ij}^\alpha r_{ij}^\beta}{r_{ij}^5}$$

# Coupled spins: Kubo Tomita

$$\Delta H_{pp} = \frac{2\pi}{\sqrt{6g\mu_B}} \sqrt{\frac{M_2^3}{M_4}} \approx \frac{M_2}{J}$$

Uncoupled spins

$$\Delta H_{KT}(T) = \frac{\chi_0(T)}{\chi(T)} \Delta H_\infty$$

$$\Delta H_\infty \sim \frac{M_2}{J}$$

- ◆ anisotropies completely contained in the second Moment  $M_2$ :

$$M_2 = \frac{\langle [\mathcal{H}, S^+][\mathcal{H}, S^-] \rangle_\infty}{\hbar^2 \langle S^+ S^- \rangle}$$

- ◆ remaining task: calculate the second moment for the different contributions to the spin Hamiltonian, find the dominating line-broadening mechanism (and check for the anisotropy)

# Ordered phases: FMR

Similar to NMR with  $\mathbf{S}$  = total spin of ferromagnet.

Magnetic selection rule:  $\Delta m_S = \pm 1$ .

## Special features:

- Transverse  $\chi'$  &  $\chi''$  very large (  $\mathbf{M}$  large).
- Shape effect prominent (demagnetization field large).
- Exchange narrowing  
(dipolar contribution suppressed by strong exchange coupling).
- Easily saturated (Spin waves excited before rotation of  $\mathbf{S}$  ).

# FMR: shape effects

Consider an ellipsoid sample of cubic ferromagnetic insulator with principal axes aligned with the Cartesian axes.

$$\mathbf{B}^i = \mathbf{B}^0 - \mathbf{N} \cdot \mathbf{M}$$

$$N_{ij} = \delta_{ij} N_i$$

$\mathbf{B}^i$  = internal field .

$\mathbf{B}^0$  = external field.

$\mathbf{N}$  = demagnetization tensor

Lorenz field =  $(4\pi/3)\mathbf{M}$ .      ( don't contribute to torque)  
 Exchange field =  $\lambda \mathbf{M}$ .

Bloch equations:

$$\frac{d\mathbf{M}}{dt} = \gamma \mathbf{M} \times \mathbf{B}^i = \gamma \mathbf{M} \times (\mathbf{B}^0 - \mathbf{N} \cdot \mathbf{M})$$

$$\mathbf{B}^0 = B_0 \hat{\mathbf{z}}$$

$$M_z = M_0$$

$$\frac{dM_x}{dt} = \gamma \left[ B_0 + (N_y - N_z)M_0 \right] M_y$$

$$\frac{dM_y}{dt} = -\gamma \left[ B_0 + (N_x - N_z)M_0 \right] M_x$$

$$M_k = M_{k0} e^{-i\omega t}$$

$$\begin{pmatrix} i\omega & \gamma \left[ B_0 + (N_y - N_z)M_0 \right] \\ -\gamma \left[ B_0 + (N_x - N_z)M_0 \right] & i\omega \end{pmatrix} \begin{pmatrix} M_{x0} \\ M_{y0} \end{pmatrix} = 0$$

FMR frequency:

$$\boxed{\omega_0^2 = \gamma^2 \left[ B_0 + (N_y - N_z)M_0 \right] \left[ B_0 + (N_x - N_z)M_0 \right]}$$

uniform mode

$$\omega_0^2 = \gamma^2 \left[ B_0 + (N_y - N_z) M_0 \right] \left[ B_0 + (N_x - N_z) M_0 \right]$$

For a spherical sample,

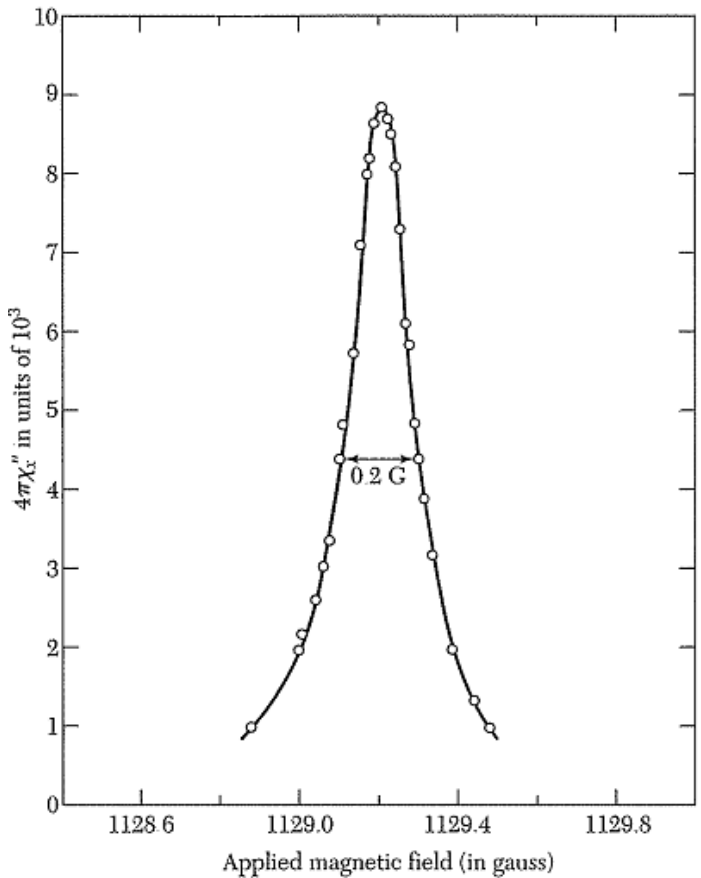
$$N_x = N_y = N_z \rightarrow \omega_0 = \gamma B_0$$

For a plate  $\perp B_0$ ,

$$N_x = N_y = 0, \quad N_z = 4\pi \rightarrow \omega_0 = \gamma (B_0 - 4\pi M_0)$$

For a plate  $\parallel B_0$ .

$$N_x = N_z = 0, \quad N_y = 4\pi \rightarrow \omega_0 = \gamma \sqrt{B_0 + 4\pi M_0}$$



Shape-effect experiments determine  $\gamma$  & hence  $g$ .

	Fe	Co	Ni
$g$	2.10	2.18	2.21

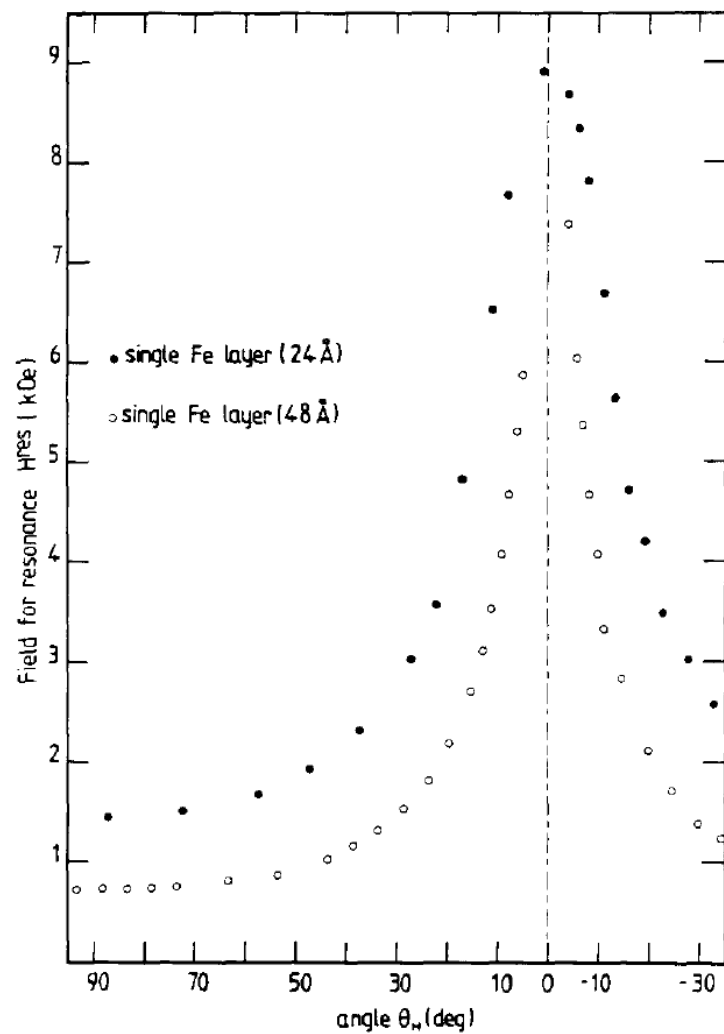
Polished sphere of YIG at 3.33GHz & 300K for  $B_0 \parallel [111]$

# FMR: anisotropy in thin films Fe/Ag

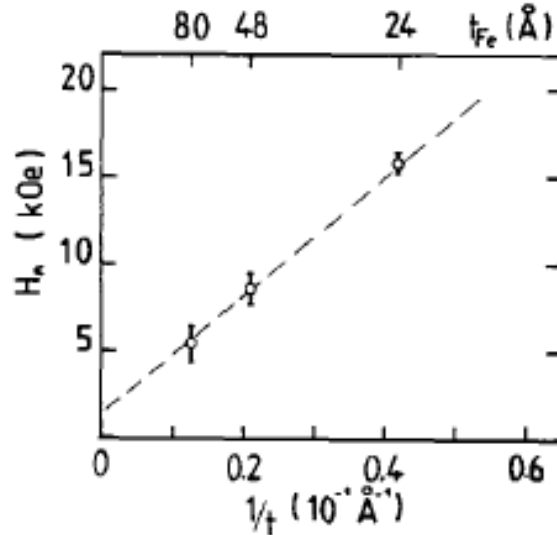
$$E = -\mathbf{M} \cdot \mathbf{H} + 2\pi M^2 \cos^2 \theta - K \cos^2 \theta - (AM/M^2) \cdot \nabla^2 \mathbf{M}, \quad (1)$$

where  $\mathbf{H}$  is the applied dc field,  $\mathbf{M}$  the saturated magnetization whose orientation is given by  $\theta = (\hat{N}, \hat{M})$ . The first term represents the Zeeman energy, the second the demagnetization energy, the fourth one the non-uniform exchange energy (with  $A$  the exchange stiffness constant). The

$$\begin{aligned} &(\omega/\gamma)^2 \\ &= [H \cos(\theta_0 - \theta_H) - (4\pi M - H_A) \cos^2 \theta_0] \\ &\times [H \cos(\theta_0 - \theta_H) - (4\pi M - H_A) \cos 2\theta_0] \end{aligned}$$



# FMR: anisotropy in thin films Fe/Ag



$$K = K_{vol} + (1/t_{Fe}) 2 K_S$$

(H. Hurdequint)

# AF ordered phases: AFMR

VOLUME 79, NUMBER 14

PHYSICAL REVIEW LETTERS

6 OCTOBER 1997

## Antiferromagnetic Resonance in the Linear Chain Conducting Polymers $\text{RbC}_{60}$ and $\text{CsC}_{60}$

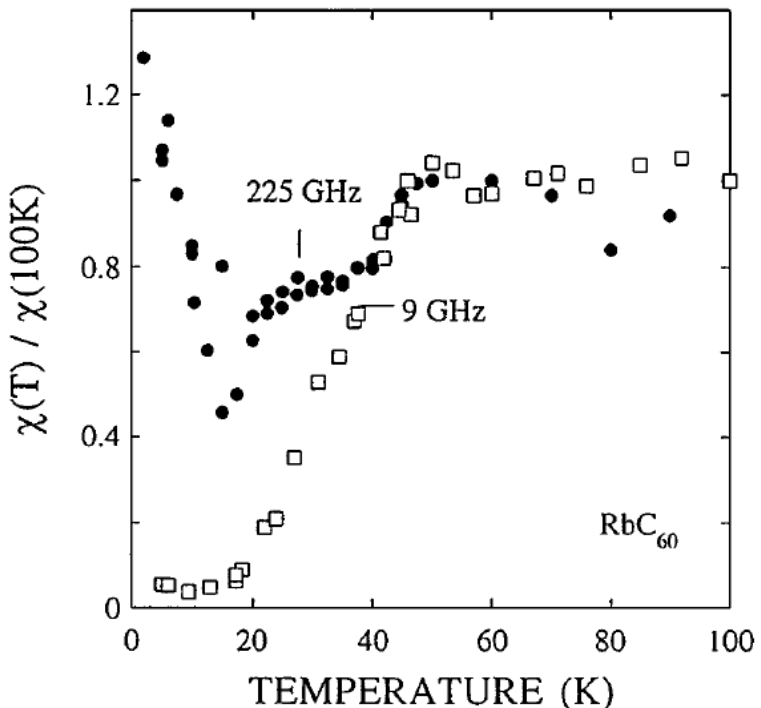
A. Jánossy,<sup>1</sup> N. Nemes,<sup>1</sup> T. Fehér,<sup>1</sup> G. Oszlányi,<sup>2</sup> G. Baumgartner,<sup>3</sup> and L. Forró<sup>3</sup>

<sup>1</sup>*Institute of Physics, Technical University Budapest, H-1521 Budapest, Hungary*

<sup>2</sup>*Research Institute for Solid State Physics, H-1525 Budapest, POB. 49, Hungary*

<sup>3</sup>*Département de Physique, Ecole Polytechnique Fédérale de Lausanne, 1015 Lausanne, Switzerland*

(Received 28 April 1997)



# AF ordered phases: AFMR

VOLUME 79, NUMBER 14

PHYSICAL REVIEW LETTERS

6 OCTOBER 1997

## Antiferromagnetic Resonance in the Linear Chain Conducting Polymers $\text{RbC}_{60}$ and $\text{CsC}_{60}$

A. Jánossy,<sup>1</sup> N. Nemes,<sup>1</sup> T. Fehér,<sup>1</sup> G. Oszlányi,<sup>2</sup> G. Baumgartner,<sup>3</sup> and L. Forró<sup>3</sup>

<sup>1</sup>*Institute of Physics, Technical University Budapest, H-1521 Budapest, Hungary*

<sup>2</sup>*Research Institute for Solid State Physics, H-1525 Budapest, POB. 49, Hungary*

<sup>3</sup>*Département de Physique, Ecole Polytechnique Fédérale de Lausanne, 1015 Lausanne, Switzerland*

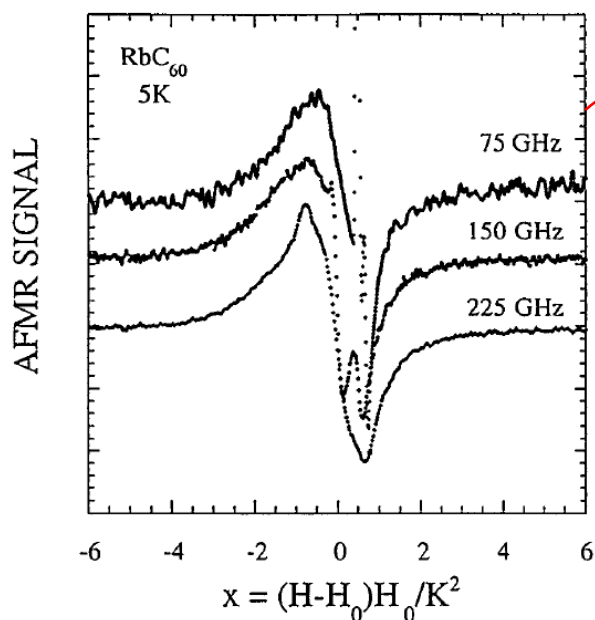


FIG. 3. The antiferromagnetic resonance line shape scales with the inverse of the resonance field  $H_0$ . The scaling constant  $K = 0.2$  T is the spin-flop field reduced by coupling between differently oriented domains. The impurity lines near  $x = 0.5$  are more visible at lower frequencies.

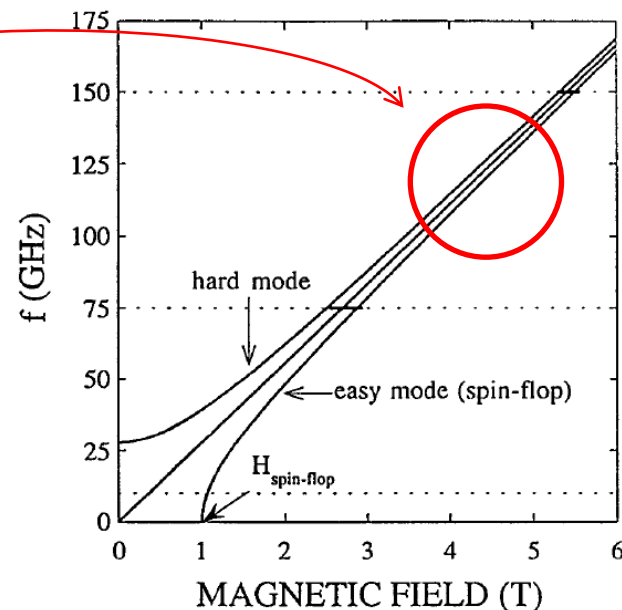


FIG. 4. Resonance modes of a uniaxial antiferromagnet for magnetic fields along and perpendicular to the easy magnetization direction. Only modes relevant to the experiment are shown. At high frequencies, the linewidth of the AFMR of a powder (heavy lines) is inversely proportional to the frequency.

# ESR and NMR comparison!

	<i>electron</i>	<i>proton</i>	<i>ratio</i>
Rest mass	$m_e = 9.1094 \times 10^{-28} \text{ g}$	$m_p = 1.6726 \times 10^{-24} \text{ g}$	$5.446 \times 10^{-4}$
Magnetic dipole moment	$\mu_S = -g_e \mu_e \mathbf{S}$ $g_e = 2.002322$ $\mu_e = e\hbar / 4\pi m_e c =$ $9.274 \times 10^{-21} \text{ erg/G}$	$\mu_S = -g_N \mu_N \mathbf{S}$ $g_N = 5.5856$ $\mu_N = e\hbar / 4\pi m_N c =$ $5.0504 \times 10^{-24} \text{ erg/G}$	1836.12

**Frequency:** Factor 1000 larger in EPR ! (*GHz instead of MHz*)

**Dipolar coupling:** Factor 1 000 000 larger in EPR ! (*MHz instead of Hz*)

**Relaxation Times:** Factor 1000 000 smaller in EPR ! (*ns instead of ms*)

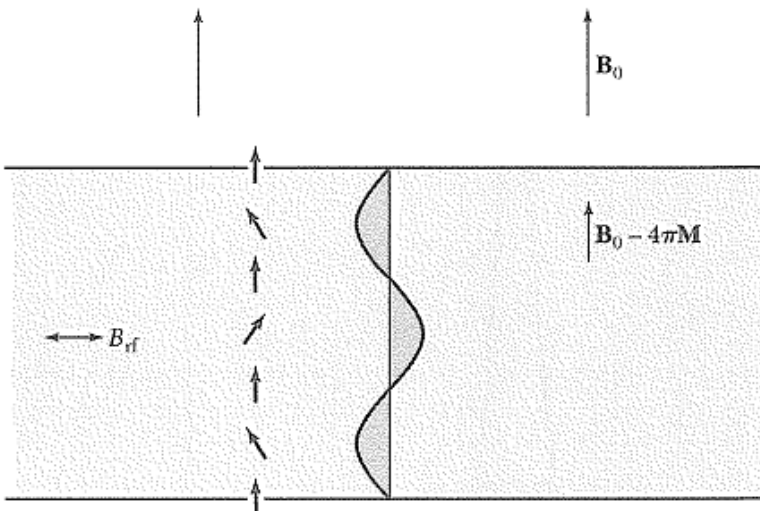
= much higher technical requirements, but unique sensitivity to molecular motion

**Sensitivity :** Factor 1 000 000 better than in NMR !! (*1nM instead of 1mM* )

*An ideal case, though*

**Very powerful, quite involved treatment, if detected:**  
single crystals needed  $\oplus$  other information  $\oplus$  modeling

# FMR: Spin wave resonance



Spin waves of odd number of half-wavelengths can be excited in thin film by uniform  $B_{rf}$   
Condition for long wavelength SWR:

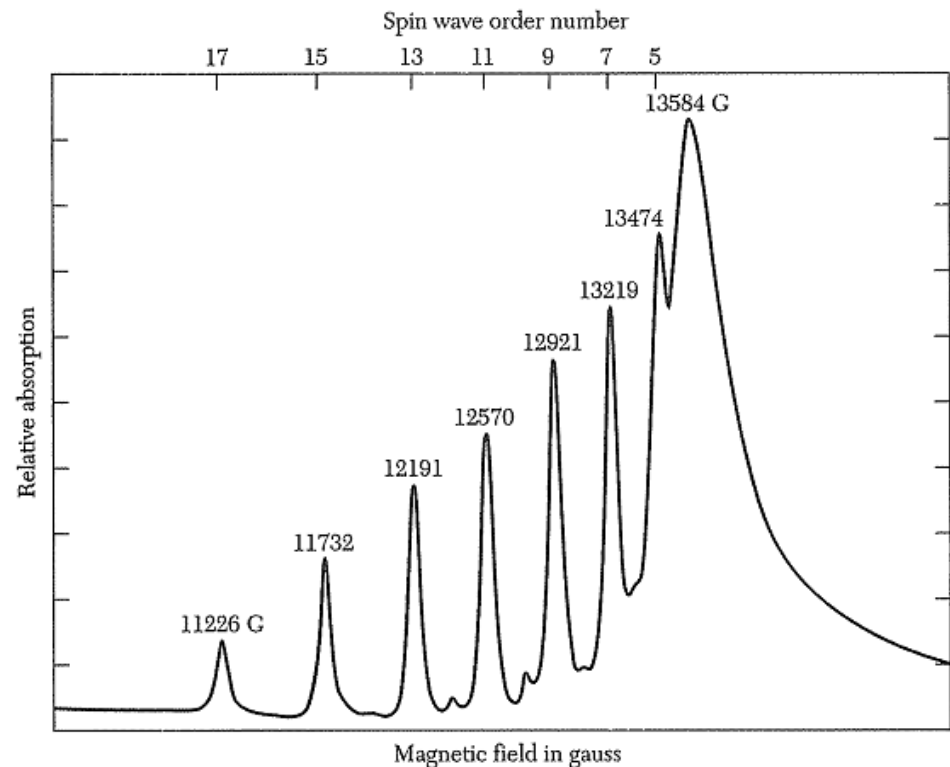
$$\omega_0 = \gamma (B_0 - 4\pi M_0) + Dk^2$$

$D$  = exchange constant

For wave of  $n$  half-lengths:

$$\omega_0 = \gamma (B_0 - 4\pi M_0) + D \left( \frac{n \pi}{L} \right)^2$$

Permalloy  
(80Ni20Fe)  
at 9GHz



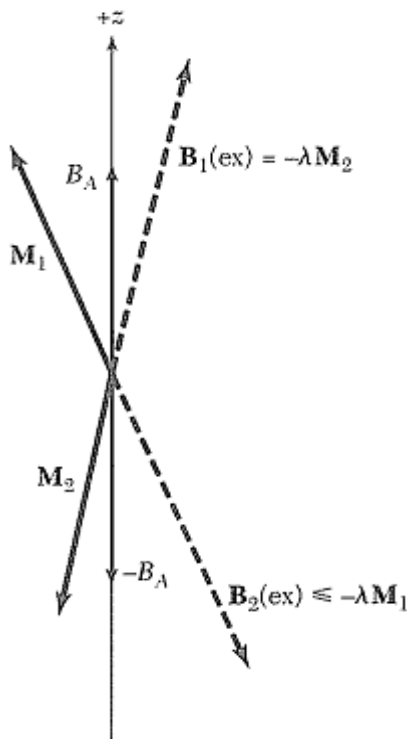
# AF ordered phases: AFMR

Consider a uniaxial antiferromagnet with spins on 2 sublattices 1 & 2.

Let  $\mathbf{M}_1 = B_A \hat{\mathbf{z}}$        $B_A$  = anisotropy field derived from  
 $\mathbf{M}_2 = -B_A \hat{\mathbf{z}}$        $\rightarrow B_A = \frac{2K}{M}$        $M = |\mathbf{B}_1| = |\mathbf{B}_2|$

$U_K = K \sin^2 \theta_1$   
 $\theta_1$  = angle between  $\mathbf{M}_1$  & z-axis.

Exchange fields:       $\mathbf{B}_1(ex) = -\lambda \mathbf{M}_2$        $\mathbf{B}_2(ex) = -\lambda \mathbf{M}_1$        $\lambda > 0$



For  $\mathbf{B}_a = \mathbf{0}$

$$\mathbf{B}_1 = -\lambda \mathbf{M}_2 + B_A \hat{\mathbf{z}}$$

$$\mathbf{B}_2 = -\lambda \mathbf{M}_1 - B_A \hat{\mathbf{z}}$$

# AF ordered phases: AFMR

With  $M_1^z = M = -M_2^z$  the linearized Bloch equations become:

$$\frac{dM_1^x}{dt} = \gamma \left[ M_1^y (\lambda M + B_A) - M (-\lambda M_2^y) \right] \quad \frac{dM_2^x}{dt} = \gamma \left[ M_2^y (-\lambda M - B_A) - (-M)(-\lambda M_1^y) \right]$$

$$\frac{dM_1^y}{dt} = \gamma \left[ M (-\lambda M_2^x) - M_1^x (\lambda M + B_A) \right] \quad \frac{dM_2^y}{dt} = \gamma \left[ (-M)(-\lambda M_1^x) - M_2^x (-\lambda M - B_A) \right]$$

$$M_j^+ = M_j^x + i M_j^y \propto e^{-i \omega t} \quad \rightarrow \quad \begin{aligned} -i\omega M_1^+ &= -i \gamma \left[ M_1^+ (\lambda M + B_A) + M_2^+ (\lambda M) \right] \\ -i\omega M_2^+ &= i \gamma \left[ M_2^+ (\lambda M + B_A) + M_1^+ (\lambda M) \right] \end{aligned}$$

$$\begin{pmatrix} \gamma(B_A + B_E) - \omega & \gamma B_E \\ \gamma B_E & \gamma(B_A + B_E) + \omega \end{pmatrix} \begin{pmatrix} M_1^+ \\ M_2^+ \end{pmatrix} = 0 \quad B_E = \lambda M \quad \text{exchange field}$$

$$\therefore \quad \omega_0^2 = \gamma^2 B_A (B_A + 2B_E) \quad \begin{array}{l} \text{AFMR} \\ \text{frequency} \end{array}$$

# References

- **NMR Textbooks :**
  - Abragam A., The Principles of Nuclear Magnetism, Clarendon Press, Oxford 1961
  - Slichter C.P., Principles of Magnetic Resonance, Springer Verlag, 1978
  - A.Narath: Hyperfine Interactions, ed. A. J. Freeman and R. B. Frankel (Academic Press, New York, 1967) Chap. 7
  - Understanding NMR Spectroscopy, J. Keeler, Wiley
- **Mössbauer Textbooks :**
  - GK Wertheim Mossbauer effect: principle and applications, Academic Press, 1965
  - P. Carretta, A Lascialfari NMR-MRI, muSR, and Mössbauer spectroscopies in molecular magnets, Springer, 2007
- **ESR Textbooks :**
  - Abragam A & Bleaney B. Electron paramagnetic resonance of transition ions. Oxford, England: Oxford University Press, 1970.
  - A. Bencini and D. Gatteschi "Book Review: EPR of Exchange Coupled Systems"